

HOMOLOGICAL MIRROR SYMMETRY FOR ORBIFOLD LOG CALABI-YAU SURFACES

BOGDAN SIMEONOV

ABSTRACT. We construct mirror abstract Lefschetz fibrations associated to a class of surfaces with cyclic quotient singularities which we call effective. These surfaces can be obtained by contracting disjoint chains of smooth rational curves inside the anticanonical cycle D of a smooth log Calabi-Yau surface (Y, D) with maximal boundary and considering the result as an orbifold. The Fukaya-Seidel categories of these abstract Lefschetz fibrations admit semiorthogonal decompositions akin to the ones described via the derived special McKay correspondence of Ishii and Ueda [IU15]. We apply this construction to establish an equivalence at the large volume limit between the derived category of an effective orbifold log Calabi-Yau surface with points of type $\frac{1}{k}(1, 1)$ and the Fukaya-Seidel category of its mirror Lefschetz fibration. We also compare the abstract construction to an explicit Landau-Ginzburg model defined by a Laurent polynomial associated to a toric degeneration in the case of the family of hypersurfaces $X_{k+1} \subset \mathbb{P}(1, 1, 1, k)$. The hypersurfaces X_{k+1} admit a non-trivial moduli of complex structures, which we compare with an open subset of the space of symplectic structures on the total space of the mirror Landau-Ginzburg model via a mirror map built out of intrinsic quantities in a non-exact Fukaya-Seidel category.

CONTENTS

0. Introduction	2
0.1. Main results	2
0.2. The derived category of an orbifold surface	4
0.3. The construction of the mirror abstract Lefschetz fibration	4
0.4. The case of log CY orbifold surfaces with singularities of type $\frac{1}{k}(1, 1)$	6
0.5. The family of del Pezzo surfaces X_{k+1}	7
0.6. Organization of the paper	11
0.7. Acknowledgements	11
1. The derived category of an orbifold surface with points of type $\frac{1}{k}(1, 1)$	11
1.1. The special McKay correspondence	11
1.2. The McKay algebra of a $\frac{1}{k}(1, 1)$ point	12
1.3. The gluing bimodule	13
1.4. A model of the gluing subcategory via the Auslander order over D	15
1.5. A description of $D^b(X_{k+1})$ via a quiver with relations	17
2. An abstract Lefschetz fibration construction and the proof of mirror symmetry at the large volume limit	19
2.1. HMS for smooth log Calabi-Yau surfaces: the work of Hacking and Keating	19
2.2. A collection of vanishing cycles on the Lekili-Polishchuk surfaces	20

2.3. The proof of homological mirror symmetry	21
3. The geometry of the LG model mirror to X_{k+1}	27
3.1. Toric degenerations and an explicit LG model	27
3.2. The total space of the Lefschetz fibration	29
3.3. Critical points and critical values	29
3.4. A collection of vanishing cycles	30
3.5. The manifold M^{in}	37
3.6. The vanishing cycles mirror to the alternative line bundle collection	37
4. Homological mirror symmetry for X_{k+1}	39
4.1. Grading and morphism spaces	40
4.2. The mirror to the algebra of the McKay quiver	41
4.3. The mirror to the derived category of Y	41
4.4. The gluing morphisms and their composition law	45
Appendix	48
5.5. Lemmata on the critical points and the dynamics of the branch points	48
5.6. The Palais-Smale condition	51
5.7. Special representations and modular arithmetic	52
References	53

0. INTRODUCTION

0.1. Main results. In this paper, we study homological mirror symmetry for log Calabi-Yau orbifold surfaces, building on earlier work of [HK23] pertaining to smooth log Calabi-Yau surfaces. The main objects of study are a class of log Calabi-Yau orbifold surfaces that we call *effective* (Definition 1.1). These are the surfaces which can be constructed by taking a smooth log Calabi-Yau pair (Y, D) with $D \in |-K_Y|$ a reduced nodal curve, contracting disjoint chains $\mathcal{E}_i = \bigcup E_{i,j}$ of rational curve components $\mathbb{P}^1 \simeq E_{i,j} \subset D$ satisfying $E_{i,j}^2 \leq -2$ and considering the resulting surface with cyclic quotient singularities as an orbifold. This produces a different compactification (\mathcal{X}, D^{orb}) of the same open Calabi-Yau variety $U = Y \setminus D = \mathcal{X} \setminus D^{orb}$.

Associated to such a log Calabi-Yau pair (\mathcal{X}, D^{orb}) we construct an abstract mirror Lefschetz fibration $w' : W' \rightarrow \mathbb{C}$ (Construction 2.2 in Section 2). This construction is applied to prove homological mirror symmetry in the case where each chain \mathcal{E}_i consists of a single curve E_i with $E_i \cdot E_i = -k_i < -2$.

Theorem 0.1 (Homological Mirror Symmetry at the large complex structure limit). *Suppose (\mathcal{X}, D^{orb}) is an effective log Calabi-Yau surface whose orbifold points $\{p_i\}_{i=1}^m$ are of type $\frac{1}{k_i}(1, 1)$, with $k_i > 2$. Assume that Y , the minimal resolution of the coarse space of \mathcal{X} , is equipped with the distinguished complex structure as in [HK23, Section 2.1.1]. Consider the Lefschetz fibration $w' : W' \rightarrow \mathbb{C}$ from construction 2.2 and the Hacking-Keating Lefschetz fibration $w : W \rightarrow \mathbb{C}$ from [HK23] which is mirror to (Y, D) . Then:*

- The exact Lefschetz fibration $w' : W' \rightarrow \mathbb{C}$ is equivalent to stabilizing $w : W \rightarrow \mathbb{C}$ along $\sum_{i=1}^m (k_i - 2)$ Lagrangian arcs in the reference fiber F of w .

- There is an equivalence of A_∞ categories $D^b(\mathcal{X}) \simeq D^b\mathcal{F}uk^\rightarrow(w')$ and a commutative diagram

$$\begin{array}{ccc} D^b(Y) & \xrightarrow{\simeq} & D^b\mathcal{F}uk^\rightarrow(w) \\ \Phi \downarrow & & \downarrow \\ D^b(\mathcal{X}) & \xrightarrow{\simeq} & D^b\mathcal{F}uk^\rightarrow(w') \end{array}$$

intertwining the fully faithful embedding Φ defined via a Fourier-Mukai kernel by Ishii-Ueda [IU15] and the fully faithful inclusion induced by Lefschetz stabilization.

The process of stabilizing a Lefschetz fibration¹ is described in [GP17], see also [Kea18, Section 2]. We will review it briefly in Section 0.5.4. Notably, stabilizing a Lefschetz fibration does not change the total space, up to Liouville deformation equivalence. This is consistent with the expectation that compactifying U by adding a divisor is mirror to equipping the SYZ mirror U^\vee with a function, with different divisors corresponding to different functions on the same space.

We will also consider an example which is not at the large complex structure limit, namely the family of quasismooth hypersurfaces with a single $\frac{1}{k}(1,1)$ point $X_{k+1} \subset \mathbb{P}(1,1,1,k)$. These are orbifold del Pezzo surfaces which can be geometrically realized by taking \mathbb{P}^2 , blowing up $k+1$ distinct points on a line (resulting in a smooth surface Y) and contracting the strict transform of the line. The mirror to X_{k+1} is an explicit Landau-Ginzburg model arising from a toric degeneration of X_{k+1} . We verify that the Lefschetz fibration induced by this Landau-Ginzburg model coincides, topologically, with the abstract one from Construction 2.2. However, unlike in the assumption of Theorem 0.1, Y does not come equipped with the distinguished complex structure since the points blown up on \mathbb{P}^2 are distinct: there is a nontrivial moduli of complex structures depending on the positions of these points. An explicit mirror map is constructed, identifying an open subset of this moduli of complex structures with a space of non-exact symplectic structures on the total space of the mirror Landau-Ginzburg model. This mirror map is defined by computing intrinsic quantities in a non-exact Fukaya-Seidel category, in a similar vein as [AKO06],[AKO08].

Theorem 0.2. (Theorem 4.16) *There is a symplectic manifold M^0 and a potential function $\mathbf{f}_s : M^0 \rightarrow \mathbb{C}$ such that, given any quasismooth del Pezzo surface \mathcal{X} in the family of hypersurfaces $X_{k+1} \subset \mathbb{P}(1,1,1,k)$, there is a complexified Kahler class $[B + i\omega] \in H^2(M^0; \mathbb{C})$ and an equivalence of A_∞ categories*

$$D^b(\mathcal{X}) \simeq D^b\mathcal{F}uk^\rightarrow(\mathbf{f}_s; B + i\omega)$$

In both theorems, the directed Fukaya-Seidel category refers to the category whose objects are an ordered collection of vanishing cycles with A_∞ operations defined on a fiber of the Lefschetz fibration, as in Definition 0.6.

Remark 0.3. In this paper, we restrict ourselves to work with orbifolds with points of type $\frac{1}{k}(1,1)$. However, we believe that Construction 2.2 can be used to prove homological mirror symmetry in higher generality using the same idea as in the proof of Theorem 0.1. One technical reason to restrict to this case is that we rely on a computation of the left adjoint Ψ of Φ from [GR23], which has a particularly simple description when applied to the exceptional collection of [IU15] in the $\frac{1}{k}(1,1)$ case. The author hopes to extend the results of this paper to arbitrary cyclic quotient singularities in the future.

¹This should not be confused with the stabilization operation in [GPS23, Section 8.4] which multiplies a Liouville sector with T^*I .

0.1.1. *Context: mirror symmetry and orbifold del Pezzo surfaces.* Mirror symmetry has been applied in other forms in an attempt to classify orbifold del Pezzo surfaces. While the smooth del Pezzo surfaces fall into exactly 10 deformation families, an analogous classification for del Pezzo surfaces admitting at most cyclic quotient singularities remains an open problem. A promising approach using mirror symmetry was laid out in [Akh+15], which describes a conjectural correspondence between \mathbb{Q} -Gorenstein deformation classes of orbifold del Pezzo surfaces which admit toric degenerations and mutation-equivalence classes of Fano polygons. Additionally, under this conjectural correspondence, the classical periods of maximally-mutable Laurent polynomials whose Newton polytope produces a Fano polygon should recover the regularized quantum period of the mirror orbifold del Pezzo surface.

A notable example of a class of orbifold del Pezzo surfaces which do not admit toric degenerations arise from the anticanonical quasismooth wellformed log del Pezzo surfaces in weighted projective 3-spaces which were classified by Johnson and Kollar in [JK01]. A series of such anticanonical log del Pezzo surfaces were studied extensively from the viewpoint of mirror symmetry in [CG21] and their derived categories were described in [GR23]. Unfortunately, our setup does not apply to these surfaces, since the effective log Calabi-Yau orbifold surfaces by definition have an effective anticanonical cycle. Proving homological mirror symmetry for the Johnson-Kollar surfaces is an interesting open problem, currently out of reach.

0.2. **The derived category of an orbifold surface.** When \mathcal{X} is a surface with m orbifold points p_i admitting local charts of the form $[\mathbb{C}^2/G_i]$ with $G_i \subset GL_2(\mathbb{C})$ a small finite subgroup, it was proved by Ishii and Ueda [IU15, Theorem 1.4] (see also [GR23], [Ish02], [Ito02]) that there is a semiorthogonal decomposition of the form

$$D^b(\mathcal{X}) = \langle \mathbf{e}_{p_1}, \dots, \mathbf{e}_{p_m}, \Phi D^b(Y) \rangle$$

This decomposition has a component which is the fully faithful image under a Fourier-Mukai functor Φ of the derived category of a smooth surface Y , the minimal resolution of the coarse space X of \mathcal{X} . Moreover, for each orbifold point $p_i \in \mathcal{X}$, there is a component \mathbf{e}_{p_i} admitting a full exceptional collection $N_j^{p_i}$ of sheaves² with support at the orbifold point which are indexed by the non-special representations of G_i (the notion of special representations was introduced in [Wun88], where it is shown that the nontrivial special representations correspond to the exceptional curves of the minimal resolution of the quotient singularity). In the case where p_i is a $\frac{1}{k_i}(1,1)$ point, there are exceptional collections $\mathbf{e}_{p_i} = \langle N_2^{p_i}, \dots, N_{k_i-1}^{p_i} \rangle$ with each $N_j^{p_i} = \mathcal{O}_{p_i} \otimes \rho_j$ being an equivariant skyscraper sheaf supported at p_i (this is not necessarily true for other types of cyclic quotient singularities). We will use the notation $e_j^{p_i} := \mathcal{O}_{p_i} \otimes \rho_j$, as in [GR23].

0.3. **The construction of the mirror abstract Lefschetz fibration.** Mirror symmetry heuristics suggest that the general fiber F' of $w' : W' \rightarrow \mathbb{C}$ should be mirror to the nodal stacky cycle D^{orb} . This is constructed in [LP18] (see also [Hab25]) by attaching handles to a disjoint union of cylinders, one for each irreducible component of D^{orb} . More precisely, for each $\frac{1}{n}(1,q)$ singularity of \mathcal{X} appearing as a node on D^{orb} where two orbifold rational curves \mathbf{E}, \mathbf{E}' meet³, Lekili and Polishchuk attach n handles to the two cylinders C, C' associated to \mathbf{E}, \mathbf{E}' . Identifying the circles $\partial_+ C$ and $\partial_- C'$ with \mathbb{R}/\mathbb{Z} , the handle attachment is constructed so as to join together the point $\frac{a}{n} \in \partial_+ C$ with the point $\frac{-q^{-1}a}{n} \in \partial_- C$, where q^{-1} denotes the residue modulo n .

Now consider the set of weights $\{i_1 = q, i_2, \dots, i_{r+1} = 0\}$ of special representations associated to a $\frac{1}{n}(1,q)$ singularity, as in [GR23, Definition 2.5]. We make the following elementary but crucial observation:

Observation 0.4. (Proposition 5.26) *The map $\{i_1, i_2, \dots, i_{r+1}\} \rightarrow \{0, 1, \dots, n-1\}$ defined by $i_j \mapsto -i_j q^{-1} \bmod n$ is order-preserving.*

²We use the notation N_j instead of the notation E_j which appears in [IU15, Proposition 8.1] so as to not confuse these with the exceptional curves in the resolution Y .

³These could be the same, in the case that D^{orb} is a reduced nodal orbifold curve with one component.

Hence, during the construction of the Lekili-Polishchuk mirror to D^{orb} , if one only attaches handles associated to the special representations instead of all of $\{0, 1, \dots, n-1\}$ for each $\frac{1}{n}(1, q)$ point of \mathcal{X} , the handles will not overlap and the resulting surface will be (after completion) a punctured torus. This punctured torus is exactly the mirror to the anticanonical boundary D of Y . If we denote this Riemann surface by $F_I \subset F'$, there is a natural identification between F_I and F , the fiber of the Hacking-Keating mirror $w : W \rightarrow \mathbb{C}$ to (Y, D) . This can be visualized by rotating the punctures of F to be distributed vertically instead of horizontally. Under this identification, the meridian which is mirror to a skyscraper sheaf on $E \subset \mathcal{E} \subset D$ passes through exactly one of the handles. This is the handle associated to the special representation which corresponds to the exceptional curve E under Wunram's correspondence [Wun88, Theorem 1.2]. In Construction 2.2, using intuition from a B-side projective resolution, for each orbifold point $p \in \mathcal{X}$ of type $\frac{1}{n}(1, q)$ we create a collection of Lagrangian S^1 's indexed by the non-special representations: $\mathfrak{N}_p := \{\tilde{L}_d^p\}_{d \in \{0, 1, \dots, n\} \setminus I(n, q)}$, ordered in increasing order. The abstract Weinstein Lefschetz fibration $w' : W' \rightarrow \mathbb{C}$ is determined by the data

$$\{F', (\mathfrak{N}_{p_1}, \dots, \mathfrak{N}_{p_m}, \mathcal{V}_1, \mathcal{V}_2, \dots, \mathcal{V}_n)\}$$

where the \mathcal{V}_i are Lagrangian vanishing cycles contained in $F_I \subset F'$ determined by the Hacking-Keating construction.

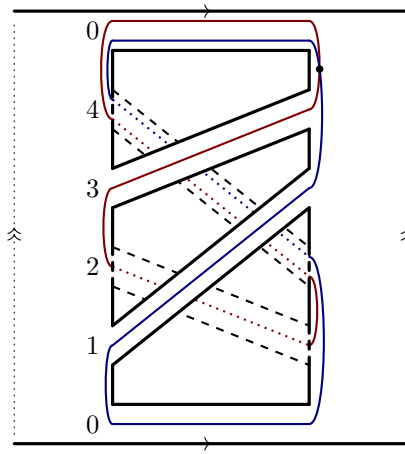


FIGURE 1. The general fiber of the Lefschetz fibration associated to a surface with a $\frac{1}{5}(1, 3)$ orbifold point. The non-special handles are drawn with a dash. The blue curve describes the Lagrangian \tilde{L}_2 and the red one describes \tilde{L}_4 .

0.3.1. *Example.* Consider \mathbb{P}^2 with its toric boundary. Then, blow up the point $[0 : 1 : -1]$ three times in a row and the point $[1 : 0 : -1]$ four times in a row. The result is a log Calabi-Yau surface (Y, D) such that $D = D_1 \cup D_2 \cup D_3$, $D_1^2 = 1$, $D_2^2 = -2$, $D_3^2 = -3$. The chain $D_2 \cup D_3$ can be contracted to a $\frac{1}{5}(1, 3)$ singularity, producing an orbifold surface (\mathcal{X}, D^{orb}) .

Associated to this singularity are the special representations ρ_0, ρ_1, ρ_3 and the non-special representations ρ_2, ρ_4 . There is a semiorthogonal decomposition

$$D^b(\mathcal{X}) = \langle \underbrace{N_2, N_4}_{\mathbf{e}_p}, \Phi D^b(Y) \rangle$$

The construction 2.2 produces a Lefschetz fibration whose general fiber is a genus three Riemann surface F' with one boundary component, which can be thought of as a torus with three boundary components $F_I \simeq F$ to which two handles have been attached, as in Figure 1.

Remark 0.5. In this case, to realize $w' : W' \rightarrow \mathbb{C}$ as a stabilization of $w : W \rightarrow \mathbb{C}$, one needs to consider the Lagrangian vanishing cycles corresponding to the mutated subcollection $\langle N_4, \mathbb{R}_{N_4} N_2 \rangle$.

0.4. The case of log CY orbifold surfaces with singularities of type $\frac{1}{k}(1, 1)$. The construction of the Lefschetz fibration from the previous section will be used to prove homological mirror symmetry for the effective log Calabi-Yau orbifold surfaces with points of type $\frac{1}{k}(1, 1)$. These orbifold surfaces \mathcal{X} are obtained by taking a smooth log Calabi-Yau surface (Y, D) with maximal boundary (i.e. D is either an irreducible nodal rational curve, or a cycle of at least 2 rational curves) and contracting a collection of m disjoint rational curves $\mathbb{P}^1 \simeq E_i \subset D$, with $E_i^2 < -2$. We will require the mirror symplectic manifold to have the exact symplectic structure, which in turn requires picking the special complex structure on (Y, D) as in [HK23, Section 2.1.1]. The pair (\mathcal{X}, D^{orb}) has an associated exact abstract Lefschetz fibration $w' : W' \rightarrow \mathbb{C}$ with reference fiber F' from Construction 2.2, whereas the pair (Y, D) has an associated Hacking-Keating mirror $w : W \rightarrow \mathbb{C}$ with reference fiber F .

The definition of the Fukaya-Seidel category of a Lefschetz fibration that we will use is given below.

Definition 0.6. The directed category of Lagrangian vanishing cycles $\mathcal{F}uk^\rightarrow(\mathbf{f}, \gamma; \omega)$ is defined to be the \mathbb{Z} -graded A_∞ category whose objects are the Lagrangian vanishing cycles Γ_i of $\mathbf{f} : M^0 \rightarrow \mathbb{C}$ corresponding to an ordered collection of vanishing paths γ , together with morphisms spaces and A_∞ operations defined in the compact Fukaya category of a reference fiber Σ^0 :

$$\text{Hom}_{\mathcal{F}uk^\rightarrow}^\bullet(\Gamma_i, \Gamma_j) := \begin{cases} CF_{\mathcal{F}(\Sigma^0)}^\bullet(\Gamma_i, \Gamma_j), & i < j \\ \mathbb{C}\langle \text{id} \rangle, & i = j \\ 0, & i > j \end{cases}$$

Note that while $\mathcal{F}uk^\rightarrow(\mathbf{f}, \gamma)$ depends on the choice of vanishing paths γ , the derived category of twisted complexes $D^b\mathcal{F}uk^\rightarrow(\mathbf{f})$ does not, by [Sei08, Theorem 18.24].

Remark 0.7. There are various alternative definitions of the Fukaya-Seidel category in the exact setting, including the partially wrapped Fukaya categories of Sylvan [Syl19] and Ganatra-Pardon-Shende [GPS20]. In the case of an exact Lefschetz fibration, these categories are known to be generated by the Lefschetz thimbles (see [GPS23, Corollary 1.17]).

0.4.1. Strategy of the proof of Theorem 0.1. One might attempt to mimic the proof in [HK23] by restricting the collection of exceptional sheaves on $D^b(\mathcal{X})$ to the boundary D^{orb} and apply homological mirror symmetry for nodal stacky curves as in [LP18]. However, this is not completely straightforward due to the fact that the functor Φ does not necessarily send line bundles to line bundles. We will use a different method of proof which relies crucially on the use of the partially wrapped Fukaya category of a torus $\mathcal{W}(F; \Lambda)$ and its mirror, the derived category $D^b(\mathcal{A}_D - \text{mod})$ of modules over the Auslander order of a cycle of rational curves D .

The first step in the proof of Theorem 0.1 in Section 2 is to describe the categories via semiorthogonal decompositions:

$$\begin{aligned} D^b(\mathcal{X}) &= \langle \mathbf{e}_{p_1}, \dots, \mathbf{e}_{p_m}, \Phi D^b(Y) \rangle \\ D^b\mathcal{F}uk^\rightarrow(w') &= \langle \mathfrak{N}_{p_1}, \dots, \mathfrak{N}_{p_m}, D^b\mathcal{F}uk^\rightarrow(w) \rangle \end{aligned}$$

The categories $\mathbf{e}_{p_i}, \mathbf{e}_{p_j}$ and $\mathfrak{N}_{p_i}, \mathfrak{N}_{p_j}$ are completely orthogonal for $i \neq j$. By direct computation, we show that $\mathbf{e}_{p_i} \simeq \mathfrak{N}_{p_i}$. Furthermore, the main result in [HK23] proves that $D^b(Y) \simeq D^b\mathcal{F}uk^\rightarrow(w)$.

To complete the equivalence, one needs to match the gluing morphism spaces from \mathbf{e}_i to $\Phi D^b(Y)$ with the gluing morphism spaces from \mathfrak{N}_{p_i} to $D^b\mathcal{F}uk^\rightarrow(w)$, as well as their A_∞ structures.

0.4.2. *Describing the gluing structure on the B-side by restricting to a categorical resolution of $\text{Perf}(D)$.* In each component $\mathbf{e}_{p_i} = \langle e_2^{p_i}, \dots, e_{k_i-1}^{p_i} \rangle$, there are only two objects $e_{k_i-2}^{p_i}, e_{k_i-1}^{p_i}$ with nontrivial morphisms to $\Phi D^b(Y)$. Hence, the gluing bimodule of morphisms is seen entirely in the morphism spaces of the subcategory $\mathcal{B} \subset D^b(\mathcal{X})$ generated by $e_{k_i-2}^{p_i}, e_{k_i-1}^{p_i}, i = 1, \dots, m$ and $\Phi D^b(Y)$. Using the computation of the left adjoint Ψ to Φ from [GR23], as well as [HK23, Lemma 4.2], in Corollary 1.5 we describe natural isomorphisms relating the morphism spaces in \mathcal{B} to ones on D :

$$\begin{aligned} \text{Ext}_{\mathcal{X}}^{\bullet}(e_{k_i-1}^{p_i}[-1], \Phi \mathcal{L}) &\simeq \text{Ext}_D^{\bullet}(\mathcal{O}_{E_i}(-1), \iota_D^* \mathcal{L}), & \text{Ext}_{\mathcal{X}}^{\bullet}(e_{k_i-2}^{p_i}[-2], \Phi \mathcal{L}) &\simeq \text{Ext}_D^{\bullet}(\mathcal{O}_{E_i}(-2), \iota_D^* \mathcal{L}), \\ \text{Ext}_{\mathcal{X}}^{\bullet}(e_{k_i-2}^{p_i}[-2], e_{k_i-1}^{p_i}[-1]) &\simeq \text{Ext}_D^0(\mathcal{O}_{E_i}(-2), \mathcal{O}_{E_i}(-1)), & \text{Ext}_{\mathcal{X}}^{\bullet}(\Phi \mathcal{L}, \Phi \mathcal{L}') &\simeq \text{Ext}_D^{\bullet}(\iota_D^* \mathcal{L}, \iota_D^* \mathcal{L}') \end{aligned}$$

where $\mathcal{L}, \mathcal{L}'$ are exceptional sheaves on Y . This identification is slightly awkward, since one has to pick out the degree 0 part of the infinite-dimensional group $\text{Ext}_D^{\bullet}(\mathcal{O}_{E_i}(-2), \mathcal{O}_{E_i}(-1))$. Instead, it is better to work with a certain categorical resolution of singularities of $\text{Perf}(D)$ given by the derived category of modules over the Auslander order of D , which was defined in [BD11]. There is a fully faithful functor $\pi^* : \text{Perf}(D) \rightarrow D^b(\mathcal{A}_D - \text{mod})$, which has a right (and also left) adjoint $\pi_* : D^b(\mathcal{A}_D - \text{mod}) \rightarrow D^b(D)$ (in the sense of [KL12]).

In Corollary 1.7, we show that \mathcal{B} admits a model \mathcal{B}_{dg} which is a directed subcategory of $D^b(\mathcal{A}_D - \text{mod})$, replacing $e_{k_i-2}^{p_i}[-2]$ with $\mathcal{P}_{E_i}(-2)$, $e_{k_i-1}^{p_i}[-1]$ with $\mathcal{P}_{E_i}(-1)$ and $\iota_D^* \mathcal{L}_i$ with $\pi^* \iota_D^* \mathcal{L}_i$, where $\mathcal{P}_{E_i}(j)$ are exceptional objects defined in [BD11, Section 5] (see also [LP18, Section 1]) satisfying $\pi_* \mathcal{P}_{E_i}(j) = \mathcal{O}_{E_i}(j) \in D^b(D)$.

0.4.3. *Describing the gluing structure on the A-side by restricting to a partially wrapped Fukaya category of a torus.* On the A-side, we define analogously a category $\mathcal{C} \subset D^b \mathcal{F}\text{uk}^{\rightarrow}(w')$ generated by $\tilde{L}_{k_i-2}^{p_i}, \tilde{L}_{k_i-1}^{p_i}, i = 1, 2, \dots, m$ and $D^b \mathcal{F}\text{uk}^{\rightarrow}(w)$. In Corollary 2.8 we show that all holomorphic disks u in F' which appear in the A_{∞} products of \mathcal{C} are contained within the bordered torus $F \simeq F_I \subset F'$. Restricting to this torus, the Lagrangian S^1 s $\mathcal{V}_1, \dots, \mathcal{V}_n$ remain unaffected, but the Lagrangians $\tilde{L}_{k_i-2}^{p_i}, \tilde{L}_{k_i-1}^{p_i}$ get replaced by Lagrangian arcs $\mathring{\tilde{L}}_{k_i-2}^{p_i}, \mathring{\tilde{L}}_{k_i-1}^{p_i}$. As such, in the full wrapped Fukaya category, the morphism space $HW_{\mathcal{W}(F)}^{\bullet}(\mathring{\tilde{L}}_{k_i-2}^{p_i}, \mathring{\tilde{L}}_{k_i-1}^{p_i})$ is infinite-dimensional, due to the presence of infinitely many Reeb chords traversing the boundary components of F . We will equip F with stops precluding this from occurring. In Proposition 2.10 we describe a model \mathcal{C}' of \mathcal{C} sitting inside the wrapped Fukaya category $\mathcal{W}(F; \Lambda)$ where Λ consists of two marked points on each boundary circle of F serving as stops.

The proof of Theorem 0.1 is completed by matching \mathcal{B}_{dg} with \mathcal{C}' using the equivalence $D^b(\mathcal{A}_D - \text{mod}) \simeq \mathcal{W}(F; \Lambda)$ from [LP18].

0.5. **The family of del Pezzo surfaces X_{k+1} .** We will also prove, by different means, homological mirror symmetry for the family X_{k+1} of orbifold del Pezzo surfaces with a single $\frac{1}{k}(1, 1)$ point, with k assumed to be odd⁴. For this family, there is an explicit Landau-Ginzburg model defined using a Laurent polynomial associated to a toric degeneration of X_{k+1} . The resulting Lefschetz fibration will be shown to coincide, topologically, with the abstract one constructed in 2.2. Symplectically, the total space of this Landau-Ginzburg model must be equipped with a non-exact symplectic structure in order to match the complex structure of a quasismooth del Pezzo surface.

Remark 0.8. The orbifold del Pezzo surfaces with a single $\frac{1}{k}(1, 1)$ point have been classified completely by [CP20]: all but one exceptional case are given by blowing up a collection of points on $\mathbb{P}(1, 1, k)$. In the notation of [CP20], the exceptional case consists of a family denoted $B_k^{(k)}$ which coincides with the family of hypersurfaces X_{k+1} .

⁴This is a simplifying assumption: the mirror Laurent polynomial when k is even has one more term, but we prefer to keep things uniform.

0.5.1. *The derived category of X_{k+1} .* By applying Ishii and Ueda's theorem [IU15] to a member \mathcal{X} of the family of hypersurfaces X_{k+1} , we obtain a semiorthogonal decomposition of $D^b(\mathcal{X})$ into torsion sheaves supported at the orbifold point, each of which corresponds to a non-special representation of the subgroup $\{\begin{pmatrix} \chi & 0 \\ 0 & \chi \end{pmatrix}, \chi^k = 1\} \subset GL(2, \mathbb{C})$, as well as the fully faithful image under a Fourier-Mukai functor Φ of the derived category of the smooth surface Y which is the minimal resolution of the coarse space of \mathcal{X} :

$$D^b(\mathcal{X}) = \langle \underbrace{e_2, \dots, e_{k-1}}_{\mathbf{e}_p}, \Phi D^b(Y) \rangle$$

0.5.2. *The mirror LG model.* The task now is to produce an analogous semiorthogonal decomposition on the Fukaya-Seidel category of the mirror LG model.

The mirror manifold M^0 is defined to be, topologically, the total space of the manifold defined by the algebraic equation

$$\{zx = P(y)\} \subset \mathbb{C}_x \times \mathbb{C}_z \times \mathbb{C}_y^\times$$

where $P(y) = \prod_{i=1}^{k+1} (y + \mathbf{q}_i)$ is a polynomial of degree $k+1$. We will take $P = (1+y)^{k+1} + \epsilon$ for a small constant ϵ . We will remark later on the significance of the parameters \mathbf{q}_i . In other words, M^0 is diffeomorphic to the complement of a cylinder in the A_k Milnor fiber. As a symplectic manifold, M^0 will come equipped with a symplectic form of the following type:

$$\omega^\varepsilon := \underbrace{dx \wedge d\bar{x} + d \log y \wedge d \log \bar{y} + dz \wedge d\bar{z}}_{\omega^{ex}} + \sum_{i=1}^k \varepsilon_i \eta_i, \quad \varepsilon_i \neq 0 \quad (0.9)$$

where η_i are Thom forms supported near a chain of -2 spheres in M^0 . There is a function $\mathbf{f} : M^0 \rightarrow \mathbb{C}$ which in the coordinates x, y, z is written as

$$\mathbf{f} = \frac{\prod_{i=1}^{k+1} (y + \mathbf{q}_i)}{xy} + x + (\tau_1 y + \dots + \tau_{\frac{k-1}{2}} y^{\frac{k-1}{2}}) = \frac{z}{y} + x + (\tau_1 y + \dots + \tau_{\frac{k-1}{2}} y^{\frac{k-1}{2}})$$

This function defines a fibration whose general fiber is a twice-punctured Riemann surface of genus $\frac{k+1}{2}$.

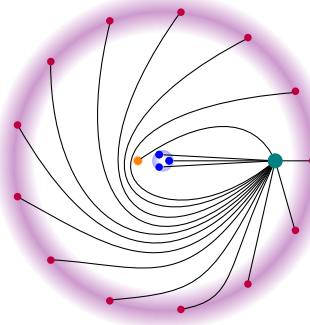


FIGURE 2. A reference fiber (green), $k - 2$ critical values which go to infinity as $s \rightarrow 0$ (purple), three critical values close to 0 in blue, as well as a critical value at -1 (orange) with multiplicity $k + 1$, in the case $k = 15, \mathbf{q}_i = 1, \tau_1 = 1, \tau_j = 0, j > 1$.

The parameters \mathbf{q}_i and τ_i have a precise interpretation in terms of holomorphic curve invariants of \mathcal{X} , namely the disk potential and the quantum orbifold cohomology: \mathbf{q}_i is a Novikov parameter associated to a class in $H^2(\mathcal{X})$, whereas the τ_i correspond to twisted sectors in the Chen-Ruan cohomology of \mathcal{X} . As

such, they depend on the symplectic structure of \mathcal{X} which in turn determines the complex structure of M^0 . However, our main goal is to study instead the symplectic structure of M^0 so these values will not be of particular importance. In particular, there exists a deformation $\mathbf{f}_s := \frac{\prod(y+\mathbf{q}_i)}{xy} + sx + (\tau_1 y + \dots + \tau_{\frac{k-1}{2}} y^{\frac{k-1}{2}})$ which, for s very small, $\tau_1 = 1, \tau_j = 0, j > 1$ and \mathbf{q}_i all equal to 1, has critical values distributed as in Figure 2. There are $k-2$ critical values which shoot off to infinity as $s \rightarrow 0$, three critical values near 0 (in blue) and a degenerate $k+1$ -fold critical value at -1 . After perturbing P from $(1+y)^{k+1}$ to $(1+y)^{k+1} + \epsilon$, the degenerate critical value splits off into $k+1$ non-degenerate ones (alternatively, one can resolve the degenerate critical point, obtaining a tower of rational curves within a single singular fiber with multiple nodes). It is crucial to take s very small, otherwise the distribution of critical values will be quite different than the one depicted in Figure 2.

The total space of the Landau-Ginzburg model is a non-exact symplectic manifold. Following Auroux-Katzarkov-Orlov in [AKO08], we will define our non-exact Fukaya-Seidel category to be generated by the vanishing cycles as in 0.6 with the various pseudoholomorphic polygons weighted by their symplectic area, as well as the holonomy associated to a B-field (this, as well as the grading data and spin structure, is explained in more detail in Section 4).

0.5.3. *Homological mirror symmetry for X_{k+1} .* A natural collection of vanishing paths (like the ones depicted in Figure 2, after perturbing P) produces a collection of Lagrangian vanishing cycles that we denote by:

$$\mathbf{L}_{k-1}, \mathbf{L}_{k-2}, \dots, \mathbf{L}_2, \mathbf{P}_{-1}, \mathbf{P}_0, \mathbf{P}_1, \mathbf{B}_1, \dots, \mathbf{B}_{k+1}$$

To compare this to the semiorthogonal decomposition on the B-side, a further step is required, mutating the subcollection $\langle L_{k-1}, \dots, L_2 \rangle$ into its left dual $\langle \tilde{L}_2, \dots, \tilde{L}_{k-1} \rangle$. After this is done⁵, one obtains Lagrangian vanishing cycles which can be graded so that all morphism spaces are concentrated in degree 0, provided that all $\varepsilon_i \neq 0$ in 0.9. As such, the only non-trivial A_∞ operation is the product μ^2 . We compute the endomorphism algebra of this exceptional collection and match it with the algebra of a full, strong exceptional collection on the B-side, proving Theorem 4.16.

0.5.4. *Contracting a $-k$ curve and a Lefschetz stabilization procedure.* On the B-side, the special McKay correspondence produces a fully faithful embedding $\Phi : D^b(Y) \rightarrow D^b(\mathcal{X})$. Moreover, contracting the $-k$ curve on Y enlarges the derived category by adding a residual component supported at the orbifold point consisting of $k-2$ exceptional sheaves. We explain here how this manifests on the A-side.

As $s \rightarrow 0$, there are $k-2$ critical values of \mathbf{f}_s going to infinity. Furthermore, under the y -projection, the general fiber Σ^0 becomes a branched double cover of \mathbb{C}^\times with a total of $k+1$ branch points (two extra branch points appear at 0 and ∞ if one compactifies Σ^0 to a compact genus $\frac{k+1}{2}$ Riemann surface). An equidistributed collection of $k-2$ branch points move towards infinity as $s \rightarrow 0$ (this is explained in Proposition 3.8). In Section 3.5, we construct a codimension 0 submanifold $M^{in} \subset M^0$ which, roughly speaking, does not see the $k-2$ critical values and $k-2$ branch points which move towards infinity. The general fiber of \mathbf{f}_s when restricted to M^{in} is a torus with three boundary components, as in Figure 3.

⁵And also mutating P_{-1} past P_0

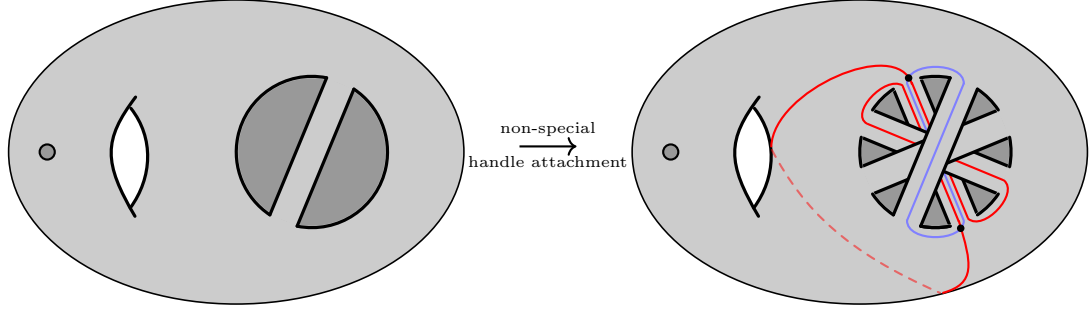


FIGURE 3. The case $k = 5$: a surface of genus 3 with two boundary components, which can be viewed as a torus with three boundary components and $k - 2 = 3$ handles attached. The blue curve describes the vanishing cycle \tilde{L}_{k-1} mirror to $e_{k-1} = e_4$ and the red one describes the mirror \tilde{L}_{k-2} to $e_{k-2} = e_3$. There is also another Lagrangian vanishing cycle \tilde{L}_2 that is not depicted.

Now recall the Lefschetz stabilization procedure (see [GP17], also [Kea18, Section 2]), which turns a Lagrangian arc in the fiber of a Lefschetz fibration into a vanishing cycle of an extended Lefschetz fibration. Begin with an exact Lefschetz fibration on an exact symplectic 4-manifold $(W, d\theta)$ with fiber F and a set of vanishing paths determining a collection of vanishing cycles. Given an arc $\gamma \subset F$ with $\partial\gamma \subset \partial F, [\theta] = 0 \in H^1(\gamma, \partial\gamma)$, one can construct a new Lefschetz fibration W' with fiber F' given by attaching a Weinstein handle to F along $\partial\gamma$. This process adds a new critical point with associated vanishing cycle given by gluing the core of the Weinstein handle to $\partial\gamma$. The total space of W' is deformation equivalent to W .

Equipping M^0 and M^{in} with the exact symplectic structure ω^{ex} respectively $\omega^{ex}|_{M^{in}}$, the Lefschetz stabilization procedure can be applied to $\mathbf{f}_s|_{M^{in}} : M^{in} \rightarrow \mathbb{C}$. The Lagrangians L_i , $2 \leq i \leq k - 1$ in the reference fiber Σ^0 of M^0 intersect the reference fiber Σ^{in} of M^{in} in arcs L_i^0 , with ∂L_i^0 consisting of two points which meet two of the boundary components of $\mathbf{f}|_{M^{in}}^{-1}(\ast)$. After successively stabilizing along the arcs $L_2^0, L_3^0, \dots, L_{k-1}^0$, we arrive back at the original Lefschetz fibration (M^0, \mathbf{f}_s) .

Theorem 0.10. (Proposition 3.16 and Corollary 4.9) *The Lefschetz fibration defined by \mathbf{f}_s on (M^0, ω^{ex}) is equivalent to a stabilization of the Lefschetz fibration defined by $\mathbf{f}_s|_{M^{in}}$ on $(M^{in}, \omega^{ex}|_{M^{in}})$ along $k - 2$ Lagrangian arcs L_i^0 . After stabilization, the arcs L_i^0 extend to Lagrangian vanishing cycles L_i which form a subcategory $\langle L_{k-1}, \dots, L_2 \rangle \subset D^b\mathcal{F}\text{uk}^\rightarrow(\mathbf{f})$ equivalent to the category of orbifold skyscraper sheaves $\langle e_2, \dots, e_{k-1} \rangle \subset D^b(\mathcal{X})$.*

Moreover, for \mathcal{X} in the family X_{k+1} with an associated smooth surface Y which is the minimal resolution of its coarse space, there is a complexified Kahler class $[B + i\omega]$ as in Theorem 0.2 and a commutative diagram:

$$\begin{array}{ccc} D^b(Y) & \xrightarrow{\cong} & D^b\mathcal{F}\text{uk}^\rightarrow(\mathbf{f}_s|_{M^{in}}; (B + i\omega)|_{M^{in}}) \\ \downarrow & & \downarrow \\ D^b(\mathcal{X}) & \xrightarrow{\sim} & D^b\mathcal{F}\text{uk}^\rightarrow(\mathbf{f}_s; B + i\omega) \end{array}$$

where the horizontal arrows are equivalences and the vertical arrows are fully faithful inclusions.

Remark 0.11. One could have instead stabilized along the Lagrangians \tilde{L}_i in the opposite order, achieving the same result. The Lagrangians \tilde{L}_i are the ones mapped under the mirror symmetry equivalence to the sheaves e_i .

0.6. **Organization of the paper.** The structure of the paper is divided as follows:

- In Section 1, we study the derived categories of orbifold surfaces. The main tool is the special McKay correspondence, as well as the computation of the left adjoint Ψ to Φ from [GR23].
- In Section 2, we construct the mirror abstract Lefschetz fibration associated to an arbitrary effective log Calabi-Yau orbifold surface (\mathcal{X}, D^{orb}) and prove Theorem 0.1 for surfaces with $\frac{1}{k}(1, 1)$ points.
- In Section 3, we introduce the mirror Landau-Ginzburg model to X_{k+1} , which is constructed using a toric degeneration. The critical values and a collection of vanishing cycles are described and the submanifold M^{in} is constructed.
- In Section 4, we compute the A_∞ structure on the category of vanishing cycles associated to the Landau-Ginzburg model mirror to X_{k+1} . This is done by showing there is grading data with all intersection points in degree 0, after which we compute the μ^2 product. The disks are enumerated using a bifibration method, realizing the general fiber as a branched double cover. This results in the proof of Theorem 4.16.

0.7. **Acknowledgements.** The author would like to thank his supervisor Yankı Lekili for suggesting this project and for numerous invaluable discussions. Moreover, the author would like to thank Matthew Habermann for reading an early draft of this paper and for his many helpful suggestions, as well as Calum Crossley for his insights on derived categories. The author is funded by a London School of Geometry and Number Theory–Imperial College London PhD studentship, which is supported by the Engineering and Physical Sciences Research Council [EP/S021590/1].

1. THE DERIVED CATEGORY OF AN ORBIFOLD SURFACE WITH POINTS OF TYPE $\frac{1}{k}(1, 1)$

In this section, we study the derived categories of orbifold surfaces with $\frac{1}{k}(1, 1)$ points. We use the special McKay correspondence of Ishii and Ueda [IU15] to describe full exceptional collections on them. Moreover, for the class of effective orbifold log Calabi-Yau surfaces, we describe the gluing subcategory \mathcal{B} from the introduction as a subcategory of the derived category of modules over the Auslander order of the cycle of smooth rational curves D . We first describe this favourable class of effective surfaces.

Definition 1.1. An effective log Calabi-Yau orbifold surface (\mathcal{X}, D^{orb}) is defined to be any surface which can be constructed by the following construction:

- Start with a smooth log Calabi-Yau surface (Y, D) with maximal boundary. This means that $D \in |-K_Y|$ is either an irreducible nodal rational curve, or a cycle of at least 2 rational curves.
- Contract a (possibly empty) collection $\mathcal{C} = \{\mathcal{E}_1, \dots, \mathcal{E}_m\}$, $\mathcal{E}_i = E_{i,1} \cup \dots \cup E_{i,r_i}$ of chains of rational curves $E_{i,j} \simeq \mathbb{P}^1$, $E_{i,j} \cdot E_{i,j} \leq -2$ contained in D which are pairwise disjoint: $E_{i,j} \cdot E_{i',j'} = 0$ whenever $i \neq i'$. The contraction map $(Y, D) \rightarrow (X, D^{orb})$ sends D to a cycle $D^{orb} \subset X$. The result upon considering X as an orbifold is the effective log Calabi-Yau orbifold pair (\mathcal{X}, D^{orb}) .

Contractibility of the chains \mathcal{E}_i is guaranteed by Artin's theorem [Art62]. The cycle D^{orb} is a nodal stacky curve in the sense of [LP18].

1.1. **The special McKay correspondence.** The special McKay correspondence is a generalization of the derived McKay correspondence to non-Gorenstein quotient singularities. It was proved in Ishii-Ueda [IU15].

Briefly, given \mathcal{X} an orbifold surface with quotient singularities of the form \mathbb{C}^2/G with $G \subset GL_2(\mathbb{C})$ a small finite subgroup whose underlying singular coarse space X admits a minimal resolution Y , one can

consider the correspondence

$$\begin{array}{ccc} \mathcal{Z} & \xrightarrow{\mu} & Y \\ \nu \downarrow & & \downarrow f \\ \mathcal{X} & \xrightarrow{s} & X \end{array}$$

Here, \mathcal{Z} is the stack $(\mathcal{X} \times_X Y)_{red}$. It can be thought of as Y with a root stack structure along the exceptional curves of the resolution. This correspondence induces a fully faithful Fourier-Mukai functor

$$\Phi : D^b(Y) \rightarrow D^b(\mathcal{X})$$

by pulling back along μ and pushing down along ν . Furthermore, there is a semiorthogonal decomposition

$$D^b(\mathcal{X}) = \langle \mathbf{e}_{p_1}, \dots, \mathbf{e}_{p_m}, \Phi D^b(Y) \rangle$$

where the \mathbf{e}_{p_j} are themselves generated by sheaves with support at the orbifold points of \mathcal{X} .

The special case we are interested in is when \mathcal{X} has orbifold points of type $\frac{1}{k}(1,1)$. In this case, each component \mathbf{e}_{p_i} admits a full exceptional collection $\mathbf{e}_{p_i} = \langle e_2^{p_i}, \dots, e_{k_i-1}^{p_i} \rangle$ where the $e_j^{p_i}$ are sheaves supported only at the orbifold point. We begin by understanding the endomorphism algebra of this subcategory.

1.2. The McKay algebra of a $\frac{1}{k}(1,1)$ point. The material in this subsection is to a large extent borrowed from [GR23, Section 2.3]. We only discuss the case of $\frac{1}{k}(1,1)$ orbifold points. The algebra of the local orbifold piece is governed by the McKay graph, see Figure 4. Since the sheaves are supported only at the orbifold point, the Ext-algebra can be computed locally on the stack $[\mathbb{C}^2/\frac{1}{k}(1,1)]$. Coherent sheaves on this stack are equivalent to G -equivariant sheaves on \mathbb{C}^2 , where $G \subset GL(2, \mathbb{C})$ is the cyclic group generated by the matrices $\begin{pmatrix} \chi^i & 0 \\ 0 & \chi^i \end{pmatrix}$ with $\chi^k = 1$ a primitive root of unity. For each $i = 0, 1, \dots, k-1$ define ρ_i to be the irreducible weight i representation of G . The structure sheaf of the origin admits the equivariant Koszul resolution

$$[\mathcal{O} \otimes \rho_2 \xrightarrow{(y, -x)^T} \mathcal{O} \otimes \rho_1^{\oplus 2} \xrightarrow{(x, y)} \mathcal{O}] \rightarrow \mathcal{O}_0$$

where $\rho_2 = \rho_{det}$ is the determinant representation and $\mathcal{O}^{\oplus 2} \otimes \rho_1$ is the natural representation induced by $G \subset GL(2, \mathbb{C})$. The sheaf $\mathcal{O} \otimes \rho_i$ is the sheaf associated to the G -equivariant $\mathbb{C}[u, v]$ -module which is $\mathbb{C}[u, v]$ equipped with the action $f(u, v) \mapsto \chi^i f(\chi u, \chi v)$. The Koszul resolution yields a resolution of the sheaves $e_i := \mathcal{O}_0 \otimes \rho_i$:

$$[\mathcal{O} \otimes \rho_{i+2} \xrightarrow{(y, -x)^T} \mathcal{O}^{\oplus 2} \otimes \rho_{i+1} \xrightarrow{(x, y)} \mathcal{O} \otimes \rho_i] \rightarrow \mathcal{O}_0 \otimes \rho_i$$

As such, we have generators $p_{1,i}, p_{2,i} \in \text{Ext}^1(e_i, e_{i+1}) = \mathbb{C}^2$ represented by the following maps of complexes:

$$\begin{array}{ccccc} \mathcal{O} \otimes \rho_{i+2} & \longrightarrow & \mathcal{O}^{\oplus 2} \otimes \rho_{i+1} & \longrightarrow & \mathcal{O} \otimes \rho_i \\ \downarrow (-1)^j \iota_j & & \downarrow \pi_j & & \\ \mathcal{O} \otimes \rho_{i+3} & \longrightarrow & \mathcal{O}^{\oplus 2} \otimes \rho_{i+2} & \longrightarrow & \mathcal{O} \otimes \rho_{i+1} \end{array}$$

Here, $\pi_j, j = 1, 2$ denotes the projection to the first respectively second factor, and ι_j denotes the inclusions $f \mapsto (0, f)$ respectively $f \mapsto (f, 0)$. There are the following relations:

$$p_{1,i+1} \circ p_{1,i} = -p_{2,i+1} \circ p_{2,i}, \quad p_{1,i+1} \circ p_{2,i} = p_{2,i+1} \circ p_{1,i} = 0$$

with $p_{1,i+1} \circ p_{1,i}$ a generator of $\text{Ext}^2(e_i, e_{i+2}) = \mathbb{C}$. After replacing e_i by $e_i[i-k]$, all the Ext groups become concentrated in degree zero, completing the description of the dg algebra associated to the orbifold skyscrapers.

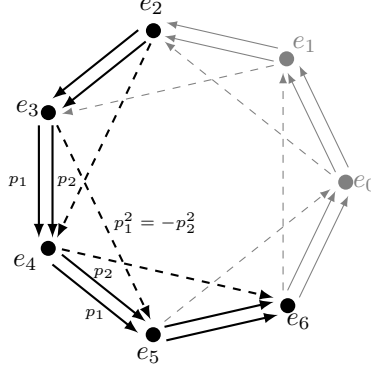


FIGURE 4. The case $\frac{1}{7}(1,1)$. Thick arrows are degree 1 and dashed ones are degree 2.

Remark 1.2. The sheaves e_0, e_1 do not appear in the component $\langle e_2, \dots, e_{k-1} \rangle$. They correspond to ρ_0, ρ_1 , the special representations of the group G : ρ_0 is the trivial representation and ρ_1 corresponds to the unique rational curve in the minimal resolution of $\mathbb{C}^2/\frac{1}{k}(1,1)$ (see [Wun88, Theorem 1.2]).

1.3. The gluing bimodule. The category $D^b(\mathcal{X})$ is obtained by gluing $D^b(Y)$ and $\langle \mathbf{e}_{p_1}, \dots, \mathbf{e}_{p_m} \rangle$. This is most efficiently described by the left adjoint Ψ to the fully faithful $\Phi : D^b(Y) \rightarrow D^b(\mathcal{X})$, which is computed in [GR23, Theorem 3.1], and in particular, the case of $\frac{1}{k}(1,1)$ points in [GR23, Example 3.5]. If $e_j^{p_i}$ is the orbifold skyscraper sheaf $\mathcal{O}_{p_i} \otimes \rho_j$, then

$$\Psi e_j^{p_i} = \begin{cases} 0, & i = 0, \dots, k_i - 3 \\ \mathcal{O}_{E_i}(-k_i)[1], & j = k_i - 2 \\ \mathcal{O}_{E_i}(-k_i + 1), & j = k_i - 1 \end{cases}$$

where E_i is the $-k_i$ curve in the minimal resolution of the $\frac{1}{k_i}(1,1)$ singularity. We denote by $\iota_{E_i} : E_i \rightarrow Y$ and $\iota_D : D \rightarrow Y$ (in the case when \mathcal{X} is effective) the inclusions.

Proposition 1.3. *The functors Ψ and ι_{E_i*} induce isomorphisms:*

$$\text{Ext}_{\mathcal{X}}^0(e_{k_i-2}^{p_i}[-2], e_{k_i-1}^{p_2}[-1]) \xrightarrow{\Psi} \text{Ext}_Y^0(\mathcal{O}_{E_i}(-k_i), \mathcal{O}_{E_i}(-k_i + 1)) \xleftarrow{\iota_{E_i*}} \text{Ext}_{E_i}^0(\mathcal{O}(-k_i), \mathcal{O}(-k_i + 1))$$

Moreover, if \mathcal{X} is effective, this group is also isomorphic to $\text{Ext}_D^0(\mathcal{O}_{E_i}(-k_i), \mathcal{O}_{E_i}(-k_i + 1))$.

Proof. We first prove the claims about ι_{E_i*} and ι_{D*} . The map ι_{E_i*} is the same as the composition of the counit with an adjunction isomorphism:

$$\text{Ext}_{E_i}^0(\mathcal{O}(-k_i), \mathcal{O}(-k_i + 1)) \rightarrow \text{Ext}_{E_i}^0(\iota_{E_i}^* \iota_{E_i*} \mathcal{O}(-k_i), \mathcal{O}(-k_i + 1)) \xrightarrow{\simeq} \text{Ext}_Y^0(\iota_{E_i*} \mathcal{O}(-k_i), \iota_{E_i*} \mathcal{O}(-k_i + 1)) \quad (1.4)$$

By [Huy06, Corollary 11.4], since $\mathcal{O}(-k_i) = \iota_{E_i}^* \mathcal{O}(E_i)$, the distinguished triangle for the counit

$$\mathcal{O}[1] \rightarrow \iota_{E_i}^* \iota_{E_i*} \iota_{E_i}^* \mathcal{O}(E_i) \rightarrow \iota_{E_i}^* \mathcal{O}(E_i)$$

splits, so that $\iota_{E_i}^* \iota_{E_i*} \mathcal{O}(-k_i) = \mathcal{O}(-k_i) \oplus \mathcal{O}[1]$ and the counit morphism is just projection to the first factor, inducing an isomorphism on Ext^0 in 1.4.

Now, assuming that \mathcal{X} is effective (meaning that it is obtained from a smooth log Calabi-Yau surface (Y, D) with maximal boundary by contracting a disjoint set of $-k_i$ curves $E_i \subset D$), the inclusion ι_{E_i} factors through D . Moreover, $\text{Ext}_D^0(\mathcal{O}_{E_i}(-k_i), \mathcal{O}_{E_i}(-k_i + 1)) = \mathbb{C}^2$, consisting of the underived sheaf homomorphisms. The composition

$$\text{Ext}_{E_i}^0(\mathcal{O}_{E_i}(-k_i), \mathcal{O}_{E_i}(-k_i + 1)) \rightarrow \text{Ext}_D^0(\mathcal{O}_{E_i}(-k_i), \mathcal{O}_{E_i}(-k_i + 1)) \xrightarrow{\iota_{D*}} \text{Ext}_Y^0(\mathcal{O}_{E_i}(-k_i), \mathcal{O}_{E_i}(-k_i + 1))$$

is given by ι_{E_i*} which is an isomorphism, and all the groups are \mathbb{C}^2 , which shows that ι_{D*} also induces an isomorphism on Ext^0 .

We proceed to show the analogous claim for the functor Ψ . Since it is a purely local statement around the orbifold point p_i , we will from now on assume $\mathcal{X} = [\mathbb{C}^2/\frac{1}{k_i}(1,1)]$, $Y = \text{Tot } \mathcal{O}(-k_i)$.

As a first step, note that there are two decompositions

$$D^b[\mathbb{C}^2/\frac{1}{k_i}(1,1)] = \langle \underbrace{\ker \Theta}_{e_2^{p_i}, \dots, e_{k_i-1}^{p_i}}, \Phi D^b(\text{Tot } \mathcal{O}(-k_i)) \rangle = \langle \Phi D^b(\text{Tot } \mathcal{O}(-k_i)), \underbrace{\ker \Psi}_{e_0^{p_i}, \dots, e_{k_i-3}^{p_i}} \rangle$$

where Θ is the right adjoint to Φ as in [GR23]. Next, we will right mutate $e_{k_i-2}^{p_i}, e_{k_i-1}^{p_i}$ through $\Phi D^b(Y)$: this mutation will be denoted by \mathbb{R} .

The counit of the adjunction produces canonical exact triangles $\text{id} \rightarrow \Phi\Psi \rightarrow \mathbb{R}[1]$ which induces a long exact sequence

$$\dots \rightarrow \text{Ext}_{\mathcal{X}}^{\bullet}(e_{k_i-2}^{p_i}[-2], e_{k_i-1}^{p_i}[-1]) \rightarrow \text{Ext}_{\mathcal{X}}^{\bullet}(e_{k_i-2}^{p_i}[-2], \Phi\Psi e_{k_i-1}^{p_i}[-1]) \rightarrow \text{Ext}_{\mathcal{X}}^{\bullet}(e_{k_i-2}^{p_i}[-2], \mathbb{R}e_{k_i-1}^{p_i}) \rightarrow \dots$$

The first term in this long exact sequence is $\mathbb{C}^2[0]$, whereas the second, by adjunction, is the morphism space $\text{Ext}_{\mathcal{X}}^0(\Psi e_{k_i-2}^{p_i}[-2], \Psi e_{k_i-1}^{p_i}[-1])$. By naturality of adjunction, the map

$$\text{Ext}_{\mathcal{X}}^{\bullet}(e_{k_i-2}^{p_i}[-2], e_{k_i-1}^{p_i}[-1]) \rightarrow \text{Ext}_{\mathcal{X}}^{\bullet}(e_{k_i-2}^{p_i}[-2], \Phi\Psi e_{k_i-1}^{p_i}[-1]) \xrightarrow{\simeq} \text{Ext}_{\mathcal{X}}^{\bullet}(\Psi e_{k_i-2}^{p_i}[-2], \Psi e_{k_i-1}^{p_i}[-1])$$

is given by the functor Ψ on morphisms.

To complete the proof of the lemma, we need to show that $\text{Ext}_{\mathcal{X}}^{\leq 0}(e_{k_i-2}^{p_i}[-2], \mathbb{R}e_{k_i-1}^{p_i}) = 0$.

$$\begin{aligned} \text{Ext}_{\mathcal{X}}^{\bullet}(e_{k_i-2}^{p_i}[-2], \mathbb{R}e_{k_i-1}^{p_i}) &\simeq \text{Ext}_{\mathcal{X}}^{-\bullet}(\mathbb{R}e_{k_i-1}^{p_i}, e_0^{p_i})^{\vee} \simeq \text{Ext}_{\mathcal{X}}^{-\bullet}(\mathbb{R}e_{k_i-1}^{p_i}, [\mathcal{O} \otimes \rho_2 \rightarrow \underbrace{\mathcal{O}^{\oplus 2} \otimes \rho_1 \rightarrow \mathcal{O} \otimes \rho_0}_{\in \text{im } \Phi}])^{\vee} \simeq \\ &\simeq \text{Ext}_{\mathcal{X}}^{-\bullet}(\mathbb{R}e_{k_i-1}^{p_i}, \mathcal{O} \otimes \rho_2[2])^{\vee} \simeq \text{Ext}_{\mathcal{X}}^{\bullet}(\mathcal{O}, \mathbb{R}e_{k_i-1}^{p_i}) \simeq \text{Ext}_{\mathcal{X}}^{\bullet}(\mathcal{O}, [e_{k_i-1}^{p_i} \rightarrow \Phi\Psi e_{k_i-1}^{p_i}]) \simeq \\ &\simeq \text{Ext}_{\mathcal{X}}^{\bullet-1}(\mathcal{O}, \Phi\Psi e_{k_i-1}^{p_i}) \underbrace{\simeq}_{\Phi^{-1}} \text{Ext}_{\mathcal{Y}}^{\bullet-1}(\mathcal{O}, \Psi e_{k_i-1}^{p_i}) \simeq \text{Ext}_{\mathcal{Y}}^{\bullet-1}(\mathcal{O}, \mathcal{O}_{E_i}(-k_i + 1)) \simeq \\ &\simeq \text{Ext}_{E_i}^{\bullet-1}(\mathcal{O}, \mathcal{O}(-k_i + 1)) \begin{cases} \mathbb{C}^{k_i-2}, \bullet = 2 \\ 0, \text{ otherwise} \end{cases} \end{aligned}$$

We are using Serre duality, the Koszul sequence, the fact that $\mathbb{R}e_{k_i-1}^{p_i} \in \Phi D^b(Y)^{\perp}$ and the fact that $e_{k_i-1}^{p_i} \in {}^{\perp} \Phi D^b(Y)$. Moreover, we use the fact that the sheaves $\mathcal{O} \otimes \rho_0, \mathcal{O} \otimes \rho_1$ lie in the essential image of Φ . This follows from [IU15, Proposition 1.1] since ρ_0, ρ_1 are special representations.

□

Corollary 1.5. *If $\mathcal{L}, \mathcal{L}' \in D^b(Y)$ are exceptional, then the compositions on $D^b(\mathcal{X})$ involving the sheaves $e_{k_i-2}^{p_i}[-2], e_{k_i-1}^{p_i}[-1]$ and $\Phi\mathcal{L}, \Phi\mathcal{L}'$ can be computed via the compositions involving $\mathcal{O}, \mathcal{O}(1), \iota_{E_i}^*\mathcal{L}, \iota_{E_i}^*\mathcal{L}'$ in $D^b(E_i)$ and similarly compositions involving $\mathcal{O}_{E_i}(-2), \mathcal{O}_{E_i}(-1), \iota_D^*\mathcal{L}, \iota_D^*\mathcal{L}'$ in $D^b(D)$ in the case that \mathcal{X} is effective.*

Proof. The claims follow by naturality of adjunction and a big commutative diagram:

$$\begin{array}{ccc}
\mathrm{Ext}_{\mathcal{X}}^{\bullet}(e_{k_i-1}^{p_i}[-1], \Phi \mathcal{L}) \otimes \mathrm{Ext}_{\mathcal{X}}^0(e_{k_i-2}^{p_i}[-2], e_{k_i-1}^{p_i}[-1]) & \xrightarrow{\mu^2} & \mathrm{Ext}_{\mathcal{X}}^{\bullet}(e_{k_i-2}^{p_i}[-2], \Phi \mathcal{L}) \\
\downarrow (\Psi \dashv \Phi) \otimes \Psi & & \downarrow \Psi \dashv \Phi \\
\mathrm{Ext}_Y^{\bullet}(\mathcal{O}_{E_i}(-k_i+1)[-1], \mathcal{L}) \otimes \mathrm{Ext}_Y^0(\mathcal{O}_{E_i}(-k_i), \mathcal{O}_{E_i}(-k_i+1)) & \xrightarrow{\mu^2} & \mathrm{Ext}_Y^{\bullet}(\mathcal{O}_{E_i}(-k_i)[-1], \mathcal{L}) \\
\uparrow (\iota_{D*} \dashv \iota_D^!) \otimes \iota_{D*} & & \uparrow \iota_{D*} \dashv \iota_D^! \\
\mathrm{Ext}_D^{\bullet}(\mathcal{O}_{E_i}(-k_i+1)[-1], \iota_D^! \mathcal{L}) \otimes \mathrm{Ext}_D^0(\mathcal{O}_{E_i}(-k_i), \mathcal{O}_{E_i}(-k_i+1)) & \xrightarrow{\mu^2} & \mathrm{Ext}_D^{\bullet}(\mathcal{O}_{E_i}(-k_i)[-1], \iota_D^! \mathcal{L}) \\
\uparrow & & \uparrow \\
\mathrm{Ext}_D^{\bullet}(\mathcal{O}_{E_i}(-1), \iota_{E_i*}^* \mathcal{L}) \otimes \mathrm{Ext}_D^0(\mathcal{O}_{E_i}(-2), \mathcal{O}_{E_i}(-1)) & \xrightarrow{\mu^2} & \mathrm{Ext}_D^{\bullet}(\mathcal{O}_{E_i}(-2), \iota_{E_i*}^* \mathcal{L}) \\
\uparrow (\iota_{E_i*} \dashv \iota_{E_i}^!) \otimes \iota_{E_i*} & & \uparrow \iota_{E_i*} \dashv \iota_{E_i}^! \\
\mathrm{Ext}_{E_i}^{\bullet}(\mathcal{O}(-1), \iota_{E_i/D}^* \iota_D^* \mathcal{L}) \otimes \mathrm{Ext}_{E_i}^0(\mathcal{O}(-2), \mathcal{O}(-1)) & \xrightarrow{\mu^2} & \mathrm{Ext}_{E_i}^{\bullet}(\mathcal{O}(-2), \iota_{E_i/D}^* \iota_D^* \mathcal{L}) \\
\uparrow & & \uparrow \\
\mathrm{Ext}_{E_i}^{\bullet}(\mathcal{O}(1), \iota_{E_i}^* \mathcal{L}) \otimes \mathrm{Ext}_{E_i}^0(\mathcal{O}, \mathcal{O}(1)) & \xrightarrow{\mu^2} & \mathrm{Ext}_{E_i}^{\bullet}(\mathcal{O}, \iota_{E_i}^* \mathcal{L})
\end{array}$$

The unlabelled vertical morphisms are given by tensoring by $\mathcal{O}(D)|_D$, respectively $\mathcal{O}(2)$, using the fact that $\iota_D^! = \iota_D^* \otimes \omega_D \otimes \omega_Y^{-1}|_D[-1] = \iota^* \otimes \mathcal{O}(D)|_D[-1]$ and $D \cdot E_i = 2 - k_i$, as well as $\iota_{E_i}^! = \iota_{E_i}^* \otimes \omega_{E_i} \otimes \omega_D^{-1}|_{E_i} = \iota_{E_i}^* \otimes \mathcal{O}(-2)$. All the vertical morphisms are isomorphisms, by Proposition 1.3. There is an analogous diagram, involving compositions between one of $e_{k_i-2}^{p_i}[-2]$ and $e_{k_i-1}^{p_i}[-1]$ and two objects of $D^b(Y)$ (using [HK23, Lemma 4.2] which shows that restricting exceptional pairs in $D^b(Y)$ to $\mathrm{Perf}(D)$ induces isomorphisms on Ext groups). \square

1.4. A model of the gluing subcategory via the Auslander order over D . As we saw in the previous section, the gluing data of the subcategories $\langle \mathbf{e}_{p_1}, \dots, \mathbf{e}_{p_m} \rangle$ and $D^b(Y)$ can be understood by restricting to each of the exceptional curves E_i . It is more uniform, in the case that \mathcal{X} is effective, to instead compute on the anticanonical cycle D of Y , which contains all of the curves E_i . However, in the derived category of D , there is an infinite-dimensional hom space $\mathrm{Ext}^{\bullet}(\mathcal{O}_{E_i}(-2), \mathcal{O}_{E_i}(-1))$, whereas we would like to extract only the degree 0 part of it. To achieve this, we will replace $D^b(D)$ with the derived category of modules over the Auslander order over D .

1.4.1. The Auslander order over a cycle of rational curves. Let $D = \bigcup_{j=1}^l D_j$ be the nodal anticanonical boundary cycle of Y , \mathcal{O}_D denote the structure sheaf of D , \mathcal{I} the ideal sheaf of the singular locus of D and $\tilde{\mathcal{O}}$ denote the structure sheaf of the normalization \tilde{D} of D , which is a disjoint union of rational curves. Moreover, let $\mathcal{F} := \mathcal{I} \oplus \mathcal{O}_D$. Burban and Drozd [BD11] define the Auslander sheaf of D as

$$\mathcal{A}_D := \mathrm{End}_D(\mathcal{I} \oplus \mathcal{O}_D) \simeq \begin{pmatrix} \tilde{\mathcal{O}} & \mathcal{I} \\ \tilde{\mathcal{O}} & \mathcal{O}_D \end{pmatrix}$$

A left \mathcal{A}_D -module $\mathcal{M} = \alpha_1 \mathcal{M} \oplus \alpha_2 \mathcal{M}$ consists of an underlying $\tilde{\mathcal{O}}$ -module $\alpha_1 \mathcal{M}$ and an underlying \mathcal{O}_D -module $\alpha_2 \mathcal{M}$, where $\alpha_1 = \begin{pmatrix} 1 & 0 \\ 0 & 0 \end{pmatrix}$, $\alpha_2 = \begin{pmatrix} 1 & 0 \\ 0 & 0 \end{pmatrix}$ are two idempotents $\alpha_1 + \alpha_2 = 1$. Moreover, it comes equipped with off-diagonal structure maps $\mathcal{I} \otimes \alpha_2 \mathcal{M} \rightarrow \alpha_1 \mathcal{M}$ and $\alpha_1 \mathcal{M} \rightarrow \alpha_2 \mathcal{M}$, thought of as \mathcal{O}_D -modules. There is a functor $\pi : \mathcal{A}_D - \mathrm{mod} \rightarrow \mathcal{O}_D - \mathrm{mod}$ sending $\mathcal{M} \mapsto \alpha_2 \mathcal{M}$.

Moreover, on the level of derived categories, it is shown in [BD11, Theorem 2.6, Corollary 3.5] that there are functors

$$\begin{array}{ccc}
D^b(\mathcal{A}_D - \text{mod}) & \xleftarrow{\pi^*} & \text{Perf } D \\
\pi_* \downarrow & \nearrow & \\
D^b(D) & &
\end{array}$$

such that π^* is both left and right adjoint to π_* and $\pi_* \circ \pi^* \simeq \text{id}$ - in other words, $D^b(\mathcal{A}_D - \text{mod})$ is a categorical resolution of singularities of $\text{Perf}(D)$, in the sense of [KL12] (see also [Cro25, Section 2]). In [BD11] it is also shown that $D^b(\mathcal{A}_D - \text{mod})$ has a strong exceptional collection of generators

$$\{\mathcal{P}_{D_j}(-1), \mathcal{P}_{D_j}\}_{j=1, \dots, l}, \{\mathcal{S}_q[-1] \mid q \text{ is a node}\}$$

where $\alpha_1 \mathcal{P}_i = \tilde{\mathcal{O}}_{D_i}$, $\alpha_2 \mathcal{P}_i = \mathcal{O}_{D_i}$ and $\alpha_1 \mathcal{S}_q = 0$, $\alpha_2 \mathcal{S}_q = \mathcal{O}_q$.

1.4.2. A gluing subcategory.

Proposition 1.6. *Let \mathcal{X} be an effective log Calabi-Yau orbifold with orbifold points of type $\frac{1}{k}(1, 1)$. Let $\mathcal{L}, \mathcal{L}'$ be two line bundles on Y . Then there are natural identifications*

$$\begin{aligned}
\text{Ext}_{\mathcal{X}}^{\bullet}(e_{k_i-2}^{p_i}[-2], e_{k_i-1}^{p_i}[-1]) &\simeq \text{Ext}_{\mathcal{A}_D}^{\bullet}(\mathcal{P}_{E_i}(-2), \mathcal{P}_{E_i}(-1)), & \text{Ext}_{\mathcal{X}}^{\bullet}(\Phi \mathcal{L}, \Phi \mathcal{L}') &\simeq \text{Ext}_{\mathcal{A}_D}^{\bullet}(\pi^* \iota_D^* \mathcal{L}, \pi^* \iota_D^* \mathcal{L}') \\
\text{Ext}_{\mathcal{X}}^{\bullet}(e_{k_i-2}^{p_i}[-2], \Phi \mathcal{L}) &\simeq \text{Ext}_{\mathcal{A}_D}^{\bullet}(\mathcal{P}_{E_i}(-2), \pi^* \iota_D^* \mathcal{L}), & \text{Ext}_{\mathcal{X}}^{\bullet}(e_{k_i-2}^{p_i}[-2], \Phi \mathcal{L}) &\simeq \text{Ext}_{\mathcal{A}_D}^{\bullet}(\mathcal{P}_{E_i}(-2), \pi^* \iota_D^* \mathcal{L})
\end{aligned}$$

compatible with compositions.

Proof. All arrows

$$\text{Ext}_{\mathcal{X}}^{\bullet}(\Phi \mathcal{L}, \Phi \mathcal{L}') \xleftarrow{\Phi} \text{Ext}_Y^{\bullet}(\mathcal{L}, \mathcal{L}') \xrightarrow{\iota_D^*} \text{Ext}_D^{\bullet}(\iota_D^* \mathcal{L}, \iota_D^* \mathcal{L}') \xrightarrow{\pi^*} \text{Ext}_{\mathcal{A}_D}^{\bullet}(\pi^* \iota_D^* \mathcal{L}, \pi^* \iota_D^* \mathcal{L}')$$

are isomorphisms: Φ and π^* are fully faithful, whereas ι_D^* is an isomorphism by [HK23, Lemma 4.2]

The rest of the proposition follows from Corollary 1.5, using the fact that $\pi_* \mathcal{P}_{E_i}(-j) = \mathcal{O}_{E_i}(-j)$ and the adjunction $\pi_* \dashv \pi^*$. Note that

$$\text{Ext}_D^0(\mathcal{O}_{E_i}(-k_i), \mathcal{O}_{E_i}(-k_i + 1)) \xleftarrow{\pi^*} \text{Ext}_{\mathcal{A}_D}^{\bullet}(\mathcal{P}_{E_i}(-2), \mathcal{P}_{E_i}(-1))$$

is an isomorphism. This is because $\text{Ext}^{\bullet}(\mathcal{P}_{E_i}(-2), \mathcal{P}_{E_i}(-1)) = \mathbb{C}^2[0]$ is concentrated in degree 0 (as in [BD11, Proposition 5.14]), and under the map π , the (underived) homomorphisms of sheaves

$$\text{Hom}_{\mathcal{A}_D}(\mathcal{P}_{E_i}(-2), \mathcal{P}_{E_i}(-1)) \simeq \text{Hom}_{\mathbb{P}^1}(\mathcal{O}(-2), \mathcal{O}(-1))$$

get sent to the respective homomorphisms of sheaves in $\text{Ext}_D^0(\mathcal{O}_{E_i}(-k_i), \mathcal{O}_{E_i}(-k_i + 1))$. \square

We proceed to pick a dg-enhancement of $D^b(\mathcal{A}_D - \text{mod})$, for example by considering the dg-category of complexes of projective \mathcal{A}_D -modules. Up to quasi-equivalence, this choice is unique, by [LO10].

Corollary 1.7. *Let $\mathcal{B} \subset D^b(\mathcal{X})$ be the subcategory generated by $\{e_{k_i-2}^{p_i}[-2], e_{k_i-1}^{p_i}[-1]\}_{i=1}^m$ and $\Phi D^b(Y)$. Then there is a dg model \mathcal{B}_{dg} of \mathcal{B} which sits inside $D_{dg}^b(\mathcal{A}_D - \text{mod})$ as a directed subcategory.*

Proof. Consider a full exceptional collection $\mathcal{L}_1, \dots, \mathcal{L}_n$ on Y , which exists by [HK23, Section 2.3]. Let \mathcal{B}_{dg} be the subcategory of $D_{dg}^b(\mathcal{A}_D - \text{mod})$ with objects

$$\{\mathcal{P}_{E_i}(-2), \mathcal{P}_{E_i}(-1)\}_{i=1}^m, \{\pi^* \iota_D^* \mathcal{L}_1, \dots, \pi^* \iota_D^* \mathcal{L}_n\}$$

imposing directedness on morphisms so that any morphism in \mathcal{B}_{dg} goes from left to right, under the ordering above (this includes the identity morphism). Applying Proposition 1.6 it follows that $\mathcal{B} \simeq H^0(\text{perf } \mathcal{B}_{dg})$. \square

1.5. A description of $D^b(X_{k+1})$ via a quiver with relations. The model using the Auslander order of D is useful when proving homological mirror symmetry at the large complex structure limit - then, the restrictions of the line bundles \mathcal{L} on Y to D are determined by the collection of degrees $\{\mathcal{L} \cdot D_i\}_{i=1}^l$. However, this is not the case when Y is not equipped with the special complex structure, as is the case of \mathbb{P}^2 blown up at $k+1$ distinct points, all lying on a line. This is the minimal resolution of the underlying coarse space of an orbifold \mathcal{X} belonging to the family X_{k+1} . In this section, we describe $D^b(\mathcal{X})$ for this family of orbifold del Pezzos using a quiver with relations model.

The surface \mathcal{X} has exactly one orbifold point and thus there is a semiorthogonal decomposition

$$D^b(\mathcal{X}) = \langle e_2, \dots, e_{k-1}, \Phi D^b(Y) \rangle$$

1.5.1. The derived category of the resolution. An application of Orlov's blowup formula, as in [AKO06, Theorem 2.5], yields a full exceptional collection:

$$D^b(Y) = \langle \mathcal{O}, \mathcal{T}(-H), \mathcal{O}(H), \begin{array}{c} \mathcal{O}_{B_1} \\ \mathcal{O}_{B_2} \\ \vdots \\ \mathcal{O}_{B_{k+1}} \end{array} \rangle$$

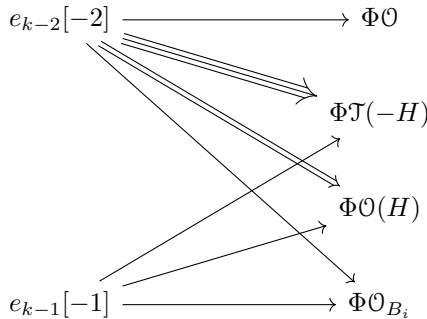
The assumption on the points being distinct ensures that \mathcal{O}_{B_i} is completely orthogonal to \mathcal{O}_{B_j} for $i \neq j$. The most important feature of the composition law is that the compositions $\mathcal{T}(-H) \rightarrow \mathcal{O}(H) \rightarrow \mathcal{O}_{B_i}$ induce a surjective map from the three-dimensional vector space $\mathbb{C}^3 = \text{Hom}(\mathcal{T}(-H), \mathcal{O}(H))$ to the two-dimensional space $\text{Hom}(\mathcal{T}(-H), \mathcal{O}_{B_i})$. The kernel is a line in \mathbb{C}^3 which determines the point in \mathbb{P}^2 associated to the exceptional curve B_i .

1.5.2. The gluing morphism spaces.

Proposition 1.8. *The morphism spaces between e_{k-2}, e_{k-1} and $\Phi D^b(Y)$ are all concentrated in 0 and are given by*

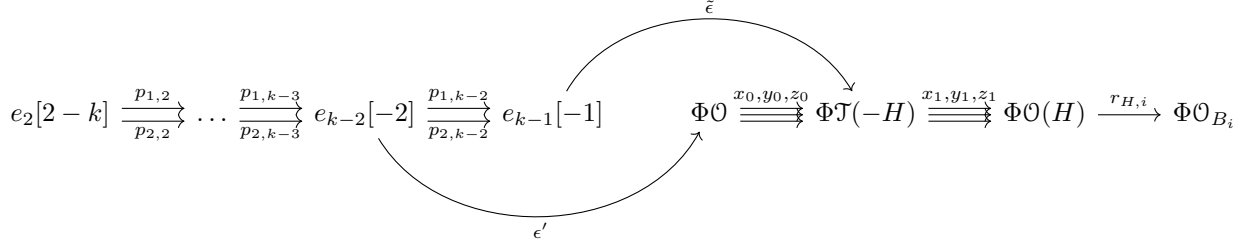
$$\begin{aligned} \text{Ext}_Y^\bullet(e_{k-2}[-2], \Phi\mathcal{O}) &= \mathbb{C}, & \text{Ext}_Y^\bullet(e_{k-2}[-2], \Phi\mathcal{T}(-H)) &\simeq \mathbb{C}^3 \\ \text{Ext}_Y^\bullet(e_{k-2}[-2], \Phi\mathcal{O}(H)) &\simeq \mathbb{C}^2, & \text{Ext}_Y^\bullet(e_{k-2}[-2], \Phi\mathcal{O}_{B_i}) &\simeq \mathbb{C} \\ \text{Ext}_Y^\bullet(e_{k-1}[-1], \Phi\mathcal{T}(-H)) &\simeq \mathbb{C}, & \text{Ext}_Y^\bullet(e_{k-1}[-1], \Phi\mathcal{O}(H)) &\simeq \mathbb{C} \\ \text{Ext}_Y^\bullet(e_{k-1}[-1], \Phi\mathcal{O}_{B_i}) &\simeq \mathbb{C}, & \text{Ext}_Y^\bullet(e_{k-1}[-1], \Phi\mathcal{O}) &= 0 \end{aligned}$$

They are summarized in the quiver, with the thickness of the arrow indicating the rank of the morphism vector space:



Proof. Corollary 1.5 shows that $\text{Ext}^\bullet(e_{k-2}[-2], \mathcal{L}) \simeq \text{Ext}^\bullet(\mathcal{O}, \iota_E^*\mathcal{L})$, $\text{Ext}^\bullet(e_{k-1}[-1], \mathcal{L}) \simeq \text{Ext}^\bullet(\mathcal{O}(1), \iota_E^*\mathcal{L})$. The rest of the computation is straightforward, using the Euler sequence $\mathcal{O}(-H) \rightarrow \mathcal{O}^{\oplus 3} \rightarrow \mathcal{T}(-H)$ and the fact that $\iota_E^*\mathcal{O}_{B_i} = \mathcal{O}_{pt_i}$ where pt_i is one of the $k+1$ points on the $-k$ curve $E \subset D$. \square

We now choose a set of generators in order to describe the directed quiver with relations for the exceptional collection. We pick these so that $\{z = 0\}$ defines the line on \mathbb{P}^2 which is blown up $k + 1$ times, and moreover so that $\Psi p_{1,k-2}, \Psi_{2,k-2}$ are identified with $\iota_E^* x, \iota_E^* y$ under the isomorphism $\text{Ext}_E^0(\mathcal{O}, \mathcal{O}(1)) \simeq \text{Ext}_Y^0(\mathcal{O}_E(-k), \mathcal{O}_E(-k+1))$.



Proposition 1.9. *The endomorphism algebra of the exceptional collection above can be described as the algebra of the quiver with relations*

$$\begin{aligned}
 p_{1,i+1} \circ p_{1,i} &= -p_{2,i+1} \circ p_{2,i}, & p_{1,i+1} \circ p_{2,i} &= p_{2,i+1} \circ p_{1,i} = 0, & \epsilon' \circ p_{1,k-3} &= \epsilon' \circ p_{2,k-3} = 0 \\
 y_1 \circ x_0 &= -x_1 \circ y_0 = -z \\
 z_1 \circ x_0 &= -x_1 \circ z_0 = y \\
 z_1 \circ y_0 &= -y_1 \circ z_0 = -x \\
 x_1 \circ x_0 &= y_1 \circ y_0 = z_1 \circ z_0 = 0 \\
 r_{H,i} \circ (a_i x_1 + b_i y_1) &= 0
 \end{aligned}$$

where the coefficients a_i, b_i define the point $[a_i : b_i : 0] \in \mathbb{P}^2$ which is blown up corresponding to the exceptional divisor B_i . There are also relations for the gluing maps $\epsilon', \tilde{\epsilon}$:

$$x_1 \circ \tilde{\epsilon} = y_1 \circ \tilde{\epsilon} = 0, \quad x_0 \circ \epsilon' = \tilde{\epsilon} \circ p_{2,k-2}, \quad y_0 \circ \epsilon' = \tilde{\epsilon} \circ p_{1,k-2}$$

Proof. The relations for $p_{1,i}, p_{2,i}$ were described in Section 1.2. For the rest of the relations, under the Euler sequence isomorphism $[\mathcal{O}(-H) \rightarrow \mathcal{O}^3] \simeq \mathcal{T}(-H)$, the maps x_0, y_0, z_0 are represented by the morphisms of chain complexes which are the three inclusions of \mathcal{O} into \mathcal{O}^3 . On the other hand, x_1, y_1, z_1 are represented by the morphisms of chain complexes which are given in vector form $(0, z, -y)^T, (-z, 0, x)^T, (y, -x, 0)^T$ as maps from $\mathcal{O}^3 \rightarrow \mathcal{O}$. From this, the first set of relations readily follow.

For the gluing compositions, by Corollary 1.5 we can compute by restricting to E . We have the splitting $\iota^* \mathcal{T}(-H) = \mathcal{O} \oplus \mathcal{O}(1)$, under which we can identify $\tilde{\epsilon}$ as $(0, 1) \in \text{Hom}_E(\mathcal{O}(1), \mathcal{O} \oplus \mathcal{O}(1))$, $\iota^* z_0$ with $(1, 0) \in \text{Hom}_E(\mathcal{O}, \mathcal{O} \oplus \mathcal{O}(1))$ and $\iota^* z_1$ with $(0, 1)^T \in \text{Hom}(\mathcal{O} \oplus \mathcal{O}(1), \mathcal{O}(1))$. Furthermore, $\iota^* x_0$ can be identified with $(0, \iota^* y)$ and $\iota^* y_0$ with $(0, \iota^* x)$, and similarly $\iota^* x_1$ with $(\iota^* y, 0)^T$ and $\iota^* y_1$ with $(\iota^* x, 0)^T$. The compositions $x_1 \circ \tilde{\epsilon}, y_1 \circ \tilde{\epsilon}$ are then immediately seen to be 0 in the composition

$$\text{Hom}_E(\mathcal{O} \oplus \mathcal{O}(1), \mathcal{O}(1)) \otimes \text{Hom}_E(\mathcal{O}(1), \mathcal{O} \oplus \mathcal{O}(1)) \rightarrow \text{Hom}_E(\mathcal{O}(1), \mathcal{O}(1))$$

Finally, the composition $x_0 \circ \epsilon', y_0 \circ \epsilon'$ are given by

$$\underbrace{\text{Hom}_E(\mathcal{O}, \mathcal{O} \oplus \mathcal{O}(1))}_{\iota^* x_1 = (0, \iota^* y), \iota^* y_1 = (0, \iota^* x)} \otimes \underbrace{\text{Hom}_E(\mathcal{O}, \mathcal{O})}_{\epsilon' = 1} \rightarrow \text{Hom}_E(\mathcal{O}, \mathcal{O} \oplus \mathcal{O}(1))$$

which are the same as the compositions

$$\underbrace{\text{Hom}_E(\mathcal{O}(1), \mathcal{O} \oplus \mathcal{O}(1))}_{\tilde{\epsilon} = (0, 1)} \otimes \underbrace{\text{Hom}_E(\mathcal{O}, \mathcal{O}(1))}_{\Psi p_{2,k-2} = y, \Psi p_{1,k-2} = x} \rightarrow \text{Hom}_E(\mathcal{O}, \mathcal{O} \oplus \mathcal{O}(1))$$

The fact that these morphisms generate the algebra is a simple consequence of Proposition 1.8. \square

1.5.3. *An alternative full strong exceptional collection of line bundles.* There is an alternative presentation of the derived category of \mathcal{X} which consists of a cyclic, full, strong, exceptional collection of orbifold line bundles. Moreover, this exceptional collection deforms from the standard one on $\mathbb{P}(1, k, k+1)$ under a toric degeneration. It can be described as follows:

$$D^b(\mathcal{X}) = \langle \mathcal{O}, \mathcal{O}(\mathbf{L}_1), \mathcal{O}(\mathbf{L}_1 + \mathbf{L}_2), \dots, \mathcal{O}(C), \mathcal{O}(C + \mathbf{L}_1), \dots, \mathcal{O}(C + \mathbf{L}_1 + \dots + \mathbf{L}_k) \rangle$$

where the orbifold lines \mathbf{L}_i are such that $C = \mathbf{L}_1 + \dots + \mathbf{L}_{k+1}$ is the hyperplane section given by $z = 0$, i.e. $\mathcal{O}(C) = \mathcal{O}_X(1)$. In other words, presenting X_{k+1} as given by $\mathbb{V}(p_{k+1}(x, y) + zw) \subset \mathbb{P}(1, 1, 1, k)$ for a polynomial p of degree $k+1$, the hyperplane section $z = 0$ intersects X_{k+1} in $k+1$ orbifold lines which correspond to the $k+1$ roots of p . One can realize X_{k+1} as a pencil of orbifold rational curves with two basepoints by taking the two sections $x, y \in H^0(\mathcal{O}_X(1))$. This pencil has $k+1$ nodal fibers of the form $\mathbf{L}_i \cup \mathbf{E}_i$.

The benefit of this exceptional collection is that it remains strong even when going to the boundary strata of the moduli stack of orbifold del Pezzo surfaces. More precisely, when two points $p_i, p_j \in E$ collide, a -2 curve is introduced on Y which leads to both degree 0 and 1 morphisms between \mathcal{O}_{B_i} and \mathcal{O}_{B_j} . This means that our previous collection does not remain strong, but is strong only on an open subset of the moduli stack. In contrast, the collection of line bundles remains strong everywhere.

The disadvantage of this sequence is that on the mirror A-side (which turns out to be non-exact), it is quite a lot more challenging to determine the weights associated to the symplectic areas of the holomorphic triangles appearing in the composition law. For this reason, in this paper, we focus on the open subset consisting of quasimooth del Pezzo surfaces. In Section 3, we provide a set of vanishing paths and Lagrangian vanishing cycles which we expect are mirror to the cyclically shifted collection

$$\langle \mathcal{O}(-2C + \mathbf{L}_{k+1}), \mathcal{O}(-2C + \mathbf{L}_{k+1} + \mathbf{L}_k), \dots, \mathcal{O} \rangle$$

2. AN ABSTRACT LEFSCHETZ FIBRATION CONSTRUCTION AND THE PROOF OF MIRROR SYMMETRY AT THE LARGE VOLUME LIMIT

In this section, we construct abstract Lefschetz fibrations associated to the effective log Calabi-Yau orbifold surfaces. We prove homological mirror symmetry at the large complex structure limit in the case that the orbifolds have points of type $\frac{1}{k}(1, 1)$.

2.1. HMS for smooth log Calabi-Yau surfaces: the work of Hacking and Keating. We will now briefly review homological mirror symmetry at the large complex structure limit for smooth log Calabi-Yau surfaces (Y, D) as developed in [HK23]. This will be the first step in constructing the mirror to (\mathcal{X}, D^{orb}) . Note that Y is the minimal resolution of the coarse space of \mathcal{X} .

Given a log Calabi-Yau pair (Y, D) with maximal boundary and a toric model such that all interior blowups on $(\overline{Y}, \overline{D})$ occur at the points identified with $-1 \in \mathbb{C}^\times \subset \overline{D}_i$ ⁶ in the components of \overline{D} , the mirror is constructed as an exact symplectic manifold W which is the total space of a Lefschetz fibration $w : W \rightarrow \mathbb{C}$ whose general fiber F is a punctured torus. The number of punctures on this torus coincides with the number of nodes on D . Associated to a full exceptional collection of line bundles $D^b(Y) = \langle \mathcal{L}_1, \dots, \mathcal{L}_n \rangle$ are a collection of vanishing cycles defined by the restrictions of \mathcal{L}_j to the boundary divisor D which is mirror to the punctured torus F , due to [LP17]. This can be chosen so that the mirror to the structure sheaf \mathcal{O} is identified with a reference longitude \mathcal{V}_0 , whereas the mirror to a skyscraper sheaf on D_i is identified with a meridian W_i . The mirror to a line bundle \mathcal{L} is constructed by Dehn twisting the longitude along this collection of meridians: $\mathcal{V}_i := \prod \tau_{W_j}^{\mathcal{L} \cdot D_j} \mathcal{V}_0$. With this data, Hacking and Keating show there is an A_∞ equivalence

$$D^b(Y) \simeq D^b \mathcal{F}uk^\rightarrow(w)$$

⁶This assumption picks out a special complex structure on Y which is mirror to the exact symplectic structure. It can be relaxed if the mirror is allowed to be non-exact

between the derived category of Y and the derived Fukaya-Seidel category of w .

2.2. A collection of vanishing cycles on the Lekili-Polishchuk surfaces. Consider now (\mathcal{X}, D^{orb}) . As explained in the introduction, we will set the general fiber of the mirror $w' : W' \rightarrow \mathbb{C}$ to be the Lekili-Polishchuk mirror F' to D^{orb} . In Observation 0.4 (proved in Proposition 5.26), it was explained that F' contains a torus $F_I \subset F'$ mirror to the boundary divisor D of Y , which is obtained from F' by ignoring the handles associated to the non-special representations. As such, we can identify F_I (after completion) with the reference fiber F of the Hacking-Keating mirror $w : W \rightarrow \mathbb{C}$ to (Y, D) . Using this identification, we can define a Lefschetz fibration with general fiber F' and a collection of vanishing cycles of two types. The first type are defined by taking a full exceptional collection $\langle \mathcal{L}_1, \dots, \mathcal{L}_n \rangle = D^b(Y)$ and using the Hacking-Keating construction to produce a collection of vanishing cycles $(\mathcal{V}_1, \dots, \mathcal{V}_n)$ with $\mathcal{V}_i \subset F$ and passing through the identification $F \simeq F_I \subset F'$. The second type are the mirrors to the exceptional sheaves of Ishii and Ueda which correspond to the non-special representations.

To motivate the construction of the vanishing cycles mirror to these sheaves, we consider the local picture on the B-side near a $\frac{1}{n}(1, q)$ point. The exceptional sheaf N_d corresponding to a non-special representation ρ_d with $i_{t-1} > d > i_t$ has a resolution on $[\mathbb{C}^2/\frac{1}{n}(1, q)]$ given as in [IU15, Proposition 3.5]⁷:

$$[\mathcal{O} \otimes \rho_{1+d+q} \xrightarrow{\begin{pmatrix} y^{j_t} \\ -x \end{pmatrix}} \mathcal{O} \otimes \rho_{1+d+q-j_t q} \oplus \mathcal{O} \otimes \rho_{d+q} \xrightarrow{\begin{pmatrix} x & y^{j_t} \end{pmatrix}} \mathcal{O} \otimes \rho_{d+q-j_t q}] \simeq N_d$$

Here, j_t denotes the dual sequence to the I -series i_t (as in [IU15, Section 3]), defined by the recursion $j_1 = 1$, $j_t = b_{t-1}j_{t-1} - j_{t-2}$ with $-b_i$ being the collection of self-intersection numbers of the exceptional curves in the resolution of $\mathbb{C}^2/\frac{1}{n}(1, q)$.

On the Lekili-Polishchuk surface F' , we will perform a surgery mirror to the projective resolution of N_d . Denote the i -th handle associated to a $\frac{1}{n}(1, q)$ point p on D^{orb} by H_i^p and its core by c_i^p . Moreover, denote the negative end of this core by $c_i^{p,-}$ and its positive end by $c_i^{p,+}$.

Definition 2.1. The Lagrangian $\tilde{L}_d^p \subset F'$ is defined as follows: consider the cores $c_{1+d+q}^p, c_{1+d+q-j_t q}^p, c_{d+q}^p$ and $c_{d+q-j_t q}^p$. If there are any duplicates, take disjoint parallel translates so that c_{1+d+q}^p is above c_{d+q}^p , which in turn is above $c_{1+d+q-j_t q}^p$ which finally sits above $c_{d+q-j_t q}^p$. These are then joined together by:

- An arc going from $c_{1+d+q}^{p,-}$ down to $c_{d+q}^{p,-}$
- An arc going from $c_{1+d+q}^{p,+}$ up to $c_{1+d+q-j_t q}^{p,+}$
- An arc going from $c_{1+d+q-j_t q}^{p,-}$ down to $c_{d+q-j_t q}^{p,-}$
- An arc going from $c_{d+q}^{p,+}$ up to $c_{d+q-j_t q}^{p,+}$

These Lagrangian S^1 s are depicted the case $n = 5, q = 3$ in Figure 1 and in the case $n = 5, q = 1$ in Figure 5 below.

⁷In some cases, for example when $q = 1$ or when $n = 2q + 1$, the sheaves N_d are just $\mathcal{O}_0 \otimes \rho_d$.

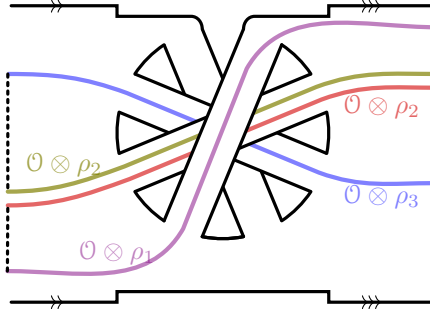


FIGURE 5. The mirror to two $[\mathbb{A}^1/\mu_n]$'s glued at a $\frac{1}{n}(1,1)$ point is given by two cylinders glued together with n handles. The picture above depicts the Lagrangian \tilde{L}_1 mirror to the Koszul resolution of $\mathcal{O}_0 \otimes \rho_1$ in the case $n = 5$.

Now, following [GP17, Definition 1.9] and inspired by [HK23, Definition 3.2] we can construct an abstract Lefschetz fibration.

Construction 2.2. The Lefschetz fibration $w' : W' \rightarrow \mathbb{C}$ associated to an effective log Calabi-Yau orbifold (\mathcal{X}, D^{orb}) is defined to be the exact Lefschetz fibration associated to the following data:

- A bordered Riemann surface F' , which is the Lekili-Polishchuk mirror to D^{orb} . This is the reference fiber of $w' : W' \rightarrow \mathbb{C}$.
- A collection of Lagrangian S^1 's $(\mathcal{V}_1, \dots, \mathcal{V}_n)$ which are the Hacking-Keating mirrors to a full exceptional collection of line bundles $\langle \mathcal{L}_1, \dots, \mathcal{L}_n \rangle = D^b(Y)$. These Lagrangians are constructed using the identification $F \simeq F_I \subset F'$, where F is the reference fiber of the Hacking-Keating mirror $w : W \rightarrow \mathbb{C}$ to (Y, D) .
- For each orbifold point $p \in \mathcal{X}$ of type $\frac{1}{n}(1, q)$, a collection of Lagrangian S^1 's indexed by the non-special representations: $\mathfrak{N}_p := \{\tilde{L}_d^p\}_{d \in \{0, 1, \dots, n\} \setminus I(n, q)}$. These are ordered in increasing order.
- The abstract Weinstein Lefschetz fibration $w' : W' \rightarrow \mathbb{C}$ is determined by the data

$$\{F', (\mathfrak{N}_{p_1}, \dots, \mathfrak{N}_{p_m}, \mathcal{V}_1, \mathcal{V}_2, \dots, \mathcal{V}_n)\}$$

2.3. The proof of homological mirror symmetry. In this section, we set out to prove Theorem 0.1. The assumptions of the Theorem are that (Y, D) is a smooth log Calabi-Yau surface with maximal boundary equipped with the special complex structure. The effective orbifold surface \mathcal{X} constructed from Y by contracting a set of disjoint curves E_1, \dots, E_m with $E_i \subset D, E_i^2 = -k_i, k_i > 2$ and considering the result as an orbifold. As such, there is a semiorthogonal decomposition

$$D^b(\mathcal{X}) = \langle \mathbf{e}_{p_1}, \dots, \mathbf{e}_{p_m}, \Phi D^b(Y) \rangle$$

with $\mathbf{e}_{p_i} = \langle e_2^{p_i}, \dots, e_{k_i-1}^{p_i} \rangle$.

We will show that the Fukaya-Seidel category of the mirror Lefschetz fibration associated to (\mathcal{X}, D^{orb}) using Construction 2.2 is derived equivalent to $D^b(\mathcal{X})$. First, we define the grading data on the Fukaya-Seidel category.

2.3.1. Grading data, spin structures, sign conventions. We equip the Lagrangian vanishing cycles with the unique non-trivial spin structure. The sign $v(u)$ of a holomorphic disk u can be computed using the same sign convention as in [AKO06, Section 4] by picking a marked point on each Lagrangian vanishing cycle which is distinct from the intersection points.

The grading data for F' , as well as the Lagrangians and the intersection points between them, depends on the choice of a line field, in other words a section of $\mathbb{P}T_{F'}$. We choose the horizontal line field in the planar description of the surface F' , as in Figure 5.

Definition 2.3. We define preliminary grading data α^{pre} as the collection of lifts of phase functions satisfying:

- $\alpha_{\tilde{L}_i^p}^{pre} : \tilde{L}_i^p \rightarrow \mathbb{R}$ such that $\alpha_{\tilde{L}_i^p} \equiv 2$ at the start and end of the i -th handle H_i^p , $\alpha_{\tilde{L}_i^p} \equiv 1$ at the start and end of the $i+1$ -st handle H_{i+1}^p , and $\alpha_{\tilde{L}_i^p} \equiv 0$ at the start and end of the $i+2$ -th handle H_{i+2}^p .
- $\alpha_{\mathcal{V}_i}^{pre} : \mathcal{V}_i \rightarrow \mathbb{R}$ to be the unique lift of the phase function which is 0 on the portion of the Lagrangian \mathcal{V}_i which is horizontal.

Recall that the grading of the intersection point between two Lagrangians $c \in CF(\Lambda_1, \Lambda_2)$, as shown by Seidel in [Sei08, Example 11.20], is given by

$$[\alpha_{\Lambda_2}(c) - \alpha_{\Lambda_1}(c)] + 1 \quad (2.4)$$

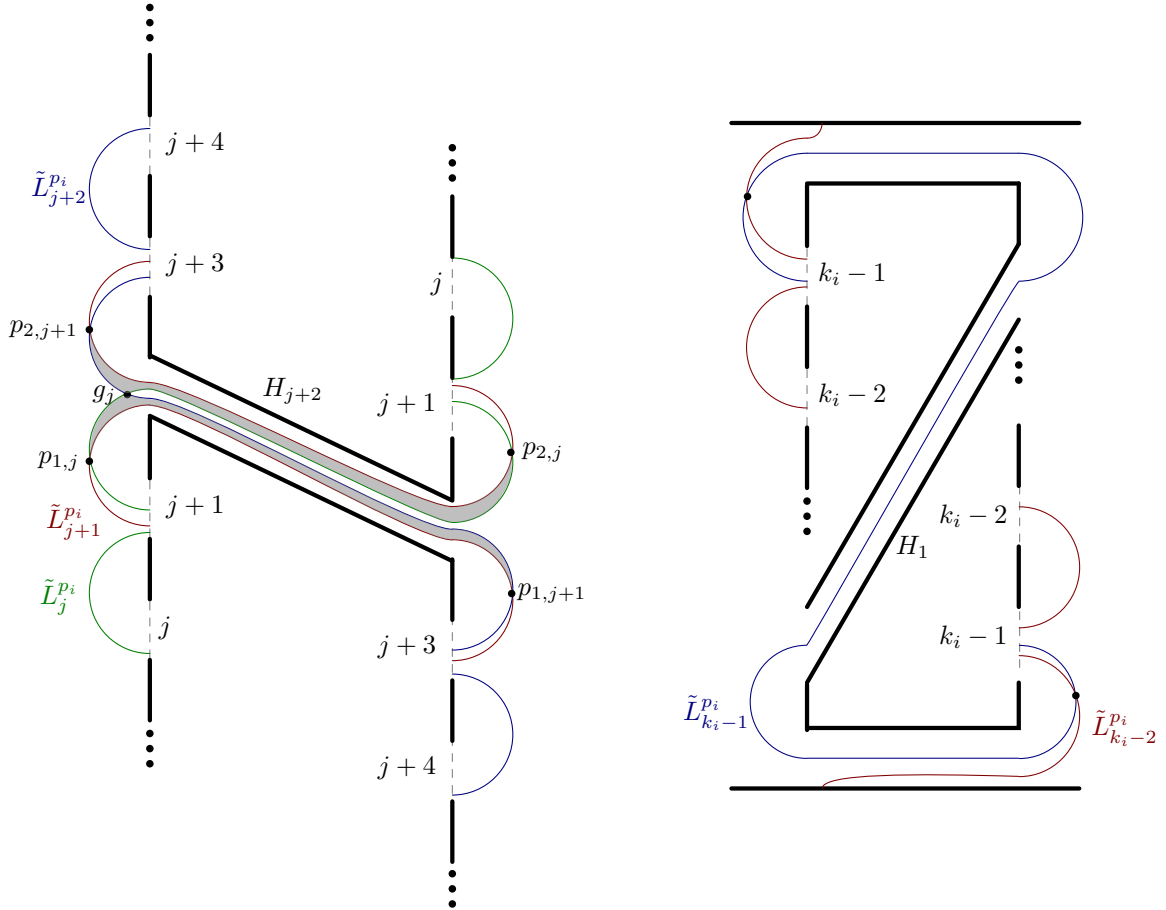


FIGURE 6. Left: the Lagrangians $\tilde{L}_j^{p_i}, \tilde{L}_{j+1}^{p_i}, \tilde{L}_{j+2}^{p_i}$ and two shaded holomorphic disks, with only the handle H_{j+2} drawn. Right: the Lagrangians $\tilde{L}_{k_i-2}^{p_i}, \tilde{L}_{k_i-1}^{p_i}$ with only the handles H_0, H_1 drawn.

Proposition 2.5. *With the preliminary grading data α^{pre} of 2.3, the Floer groups $CF(\tilde{L}_j^{p_i}, \tilde{L}_{j+1}^{p_i}) = \mathbb{C}p_{1,j}^i \oplus \mathbb{C}p_{2,j}^i$, $2 \leq j \leq k_i - 2$ are concentrated in degree 1 and the Floer group $CF(\tilde{L}_j^{p_i}, \tilde{L}_{j+2}^{p_i}) = \mathbb{C}g_j^i$, $2 \leq j \leq k_i - 3$ is concentrated in degree 2. Applying a shift of $[j - k_i]$ to $\tilde{L}_j^{p_i}$ makes these groups concentrated in degree 0.*

Proof. The intersection points can be adjusted to happen inside the torus $F_I \subset F'$ as in Figure 6. An application of Seidel's formula 2.4 leads to the conclusion. \square

We will denote the modified grading data, incorporating the shifts $[j - k_i]$, by α .

2.3.2. Matching the separate components.

Lemma 2.6. *There is a semiorthogonal decomposition*

$$D^b\mathcal{F}uk^\rightarrow(w') = \langle \mathfrak{N}_{p_1}, \dots, \mathfrak{N}_{p_m}, D^b\mathcal{F}uk^\rightarrow(w) \rangle$$

and A_∞ equivalences

$$\begin{aligned} \mathbf{e}_{p_i} &\simeq \mathfrak{N}_{p_i} \\ D^b\mathcal{F}uk^\rightarrow(w) &\simeq D^b(Y) \end{aligned}$$

Moreover, the components \mathfrak{N}_{p_i} and \mathfrak{N}_{p_j} are completely orthogonal to each other for $i \neq j$ and the only Lagrangians in \mathfrak{N}_{p_i} which have nontrivial morphisms to $D^b\mathcal{F}uk^\rightarrow(w)$ are $\tilde{L}_{k_i-2}^{p_i}$ and $\tilde{L}_{k_i-1}^{p_i}$.

Proof. Any disk with boundary on a union $\mathcal{V}_{j_1} \cup \dots \cup \mathcal{V}_{j_s} \subset F \subset F'$ must actually be contained in F , by an application of [Sei08, Lemma 7.5]. Hence, the component of $D^b\mathcal{F}uk^\rightarrow(w')$ generated by the vanishing cycles $\mathcal{V}_1, \dots, \mathcal{V}_n$ is isomorphic to $D^b\mathcal{F}uk^\rightarrow(w)$ which in turn is equivalent to $D^b(Y)$ by [HK23].

By the previous proposition 2.5, in the Floer algebra of the Lagrangians in \mathfrak{N}_{p_i} only the μ^2 product matters. We apply [Sei08, Lemma 7.5]: the Lagrangians $\tilde{L}_d^{p_i}$, $2 \leq d \leq k_i - 1$ are disjoint from the handles $H_s^{p_j}$, $j \neq i$. As such, any holomorphic disk with boundary on $\cup_j \tilde{L}_j^{p_i}$ will be contained within a surface $F_{p_i} \subset F'$ which is the result upon removing all of the handles $H_s^{p_j}$, $j \neq i$. In particular, this surface is constructed by taking two cylinders C, C' and adding k_i handles identifying $\frac{a}{k_i} \in \mathbb{R}/\mathbb{Z} \simeq \partial_+ C$ with $-\frac{a}{k_i} \in \mathbb{R}/\mathbb{Z} \simeq \partial_- C'$, as in Figure 5. We claim that there are exactly two disks, contributing with opposite signs (which can be seen visualized in 6). The surface F_{p_i} has a model⁸ given by a branched double cover of \mathbb{C}^\times with k_i branch points (each branch point corresponds to a handle). The Lagrangian vanishing cycles project to arcs connecting two branch points, as in 7.

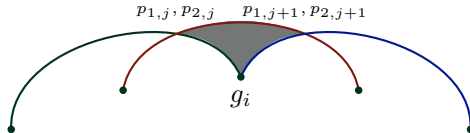


FIGURE 7. Projection of the Lagrangians $\tilde{L}_j^{p_i}, \tilde{L}_{j+1}^{p_i}, \tilde{L}_{j+2}^{p_i}$ under the branched double covering.

Since a disk in F_{p_i} projects to a disk in \mathbb{C}^\times with the projected boundary conditions, we see that it must necessarily be a lift of the shaded triangle in Figure 7. There are exactly two lifts of this triangle. Moreover, by picking a reference marker point which is a lift of the mid point in the projection of $\tilde{L}_j^{p_i}$ (resp. $\tilde{L}_{j+1}^{p_i}, \tilde{L}_{j+2}^{p_i}$), we see that the two disks contributing to $\mu^2(p_{1,j}^i, p_{1,j+1}^i)$ and $\mu^2(p_{2,j}^i, p_{2,j+1}^i)$ have opposite signs. This matches exactly the algebra of the McKay quiver, as described in Section 1.

The last two claims follow directly by construction 2.2. \square

⁸This is motivated by the explicit LG model for the mirror to X_{k+1} .

To complete the proof of homological mirror symmetry, it is thus enough to match the subcategory $\mathcal{C} \subset D^b\mathcal{F}\text{uk}^\rightarrow(w')$ generated by $\{\tilde{L}_{k_i-2}^{p_i}, \tilde{L}_{k_i-1}^{p_i}\}_{i=1}^m$ and $D^b\mathcal{F}\text{uk}^\rightarrow(w)$ with the subcategory \mathcal{B} constructed in Corollary 1.7. Recall that this subcategory had a dg model inside of $D_{dg}^b(\mathcal{A}_D - \text{mod})$. We will show that \mathcal{C} admits a model inside of a mirror partially wrapped Fukaya category.

2.3.3. Restricting to the torus F_I . On the A-side, we show that all the disks relevant to the A_∞ operations in \mathcal{C} sit inside the torus $F \subset F'$. First, we describe an elementary but handy lemma.

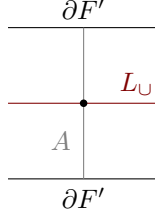


FIGURE 8. Depiction of an obstruction arc A

Lemma 2.7 (Obstructing arcs). *Suppose F' is a bordered Riemann surface and $u : (D, \partial D) \rightarrow (F', L_U)$ is a non-constant holomorphic disk with boundary on a union L_U of Lagrangians inside the interior of F' . Suppose that there exists an arc $A \subset F'$ avoiding the critical points of u such that $\partial A \subset \partial F'$ and A intersects L_U transversely at a single point p . Then, there is no point $\tilde{p} \in \partial D$ which is mapped under u to p .*

Proof. Suppose for the sake of contradiction that $u(\tilde{p}) = p$. By the maximum principle, u does not meet the boundary of F' so it is completely contained in the interior of F' . In particular, it avoids ∂A . By assumption of the regularity of \tilde{p} and non-constancy of u , there is a chart $\mathbb{H} = \mathbb{R} \times \mathbb{R}_{\geq 0}$ near \tilde{p} which maps diffeomorphically onto its image, with $\mathbb{R} \times \{0\}$ being sent to L_U .

Consider $\tilde{A} := u^{-1}(A) \subset D$, which is compact by properness of u . In particular, $\tilde{u} : \tilde{A} \rightarrow A$ has compact (and hence closed) image. The connected component of p in $\text{im } \tilde{u}$ contains $u(\mathbb{H}) \cap A$ and is therefore a compact interval. This interval must have an endpoint $q \neq p$. This point, by assumption, is not on L_U and cannot be on $\partial F'$ since u is contained in the interior of F' . In particular, $\emptyset \neq u^{-1}(q) \subset \tilde{D}$. By the regularity assumption, if $u(\tilde{q}) = q$, then there is a neighbourhood of \tilde{q} mapped diffeomorphically onto a neighbourhood of q , which is impossible if q is an endpoint of an interval. This contradiction proves the claim. \square

We proceed to apply this lemma to \mathcal{C} .

Corollary 2.8. *Any holomorphic disk with boundary on $L_U^{p_i} := \tilde{L}_{k_i-2}^{p_i} \cup \tilde{L}_{k_i-1}^{p_i} \cup \mathcal{V}_1 \cup \dots \cup \mathcal{V}_n$ is contained entirely within $F \simeq F_I \subset F'$.*

Proof. Suppose u is such a disk. If u is constant, the claim follows as all intersection points sit inside of F_I . If u is non-constant, we apply Lemma 2.7. Consider the union of cocores for the handle $H_{k_i-2}^{p_i}$, which by definition meet $\tilde{L}_{k_i-2}^{p_i}$ transversely at a single point, and no other Lagrangians in L_U . By [Laz00, Theorem 3.5], there are finitely many critical points of u on $c_{k_i-2}^{p_i} \subset \tilde{L}_{k_i-2}^{p_i}$, hence outside of this locus, we can apply Lemma 2.7 with the cocores serving the role of the obstructing arcs A . This shows that ∂u avoids the handle $H_{k_i-2}^{p_i}$.

A similar application of Lemma 2.7 shows that ∂u avoids the handle $H_{k_i-1}^{p_i}$, by using the obstruction arcs A_1, A_2, A_3 as in Figure 9, implying that $\partial u \subset F$. By an application of [Sei08, Lemma 7.5], the whole disk u is contained in F . \square

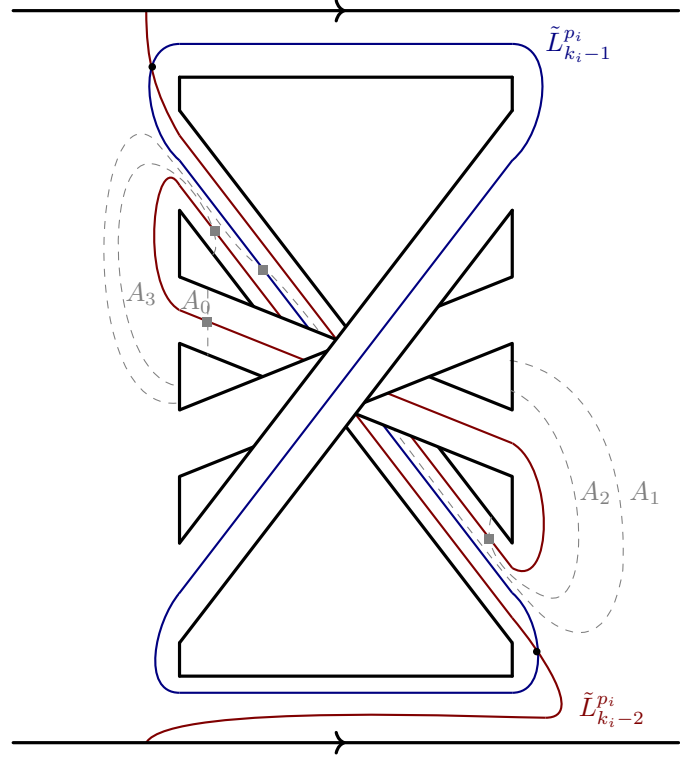


FIGURE 9. Cocore A_0 on $H_{k_i-2}^{p_i}$ obstructing holomorphic disks with boundary on L_{\cup} from having boundary somewhere on H_{k_i-2} . A collection of obstruction arcs A_1, A_2, A_3 on $H_{k_i-1}^{p_i}$ precluding holomorphic disks from having boundary somewhere on $H_{k_i-1}^{p_i}$. Depicted is the case $k_i = 5$.

Now, we define non-compact Lagrangians in F which are morally the Viterbo restrictions of $\tilde{L}_{k_i-2}^{p_i}, \tilde{L}_{k_i-1}^{p_i}$ from F' to F .

Definition 2.9. Define a Lagrangian arc $\mathring{\tilde{L}}_{k_i-1}^{p_i} := \tilde{L}_{k_i-1}^{p_i} \cap F$. Moreover, define a Lagrangian arc $\mathring{\tilde{L}}_{k_i-2}^{p_i}$ by taking the connected component of $\tilde{L}_{k_i-2}^{p_i} \cap F$ which traverses the handle $H_{k_i-1}^{p_i}$.

Note that the other connected component is a semi-circle with boundary on ∂F and it does not have any intersection points with either $\tilde{L}_{k_i-1}^{p_i}$ or any \mathcal{V}_j , so it is irrelevant when it comes to computing the disks contributing to the A_{∞} operations of \mathcal{C} .

2.3.4. A subcategory of the partially wrapped Fukaya category. In the previous section, we concluded that all of the holomorphic disks relevant to the computation of the directed A_{∞} algebra associated to the Lagrangian vanishing cycles $\tilde{L}_{k_i-2}^{p_i}, \tilde{L}_{k_i-1}^{p_i}, \mathcal{V}_1, \dots, \mathcal{V}_n$ are contained within the torus $F \subset F'$. In this torus, the vanishing cycles \mathcal{V}_i remain the same. However, the Lagrangians $\tilde{L}_{k_i-2}^{p_i}$ and $\tilde{L}_{k_i-1}^{p_i}$ get replaced with Lagrangian arcs, as in Definition 2.9. In the wrapped Fukaya category $\mathcal{W}(F)$, these Lagrangian arcs have infinite-dimensional hom spaces, which are accounted for by the Reeb chords along the boundary components of F . In contrast, no such phenomenon occurs in $D^b\mathcal{F}uk^{\rightarrow}(w')$, where all hom spaces are finite-dimensional. To remedy this, we will consider instead the partially wrapped Fukaya category $\mathcal{W}(F; \Lambda)$, where the stop Λ consists of two points on each boundary component of F .

Various models for the partially wrapped Fukaya category exist in the literature, most notably [Syl19] and [GPS20]. For our purposes, we will take the strictly unital, combinatorial model from [HKK17], which describes the partially wrapped Fukaya category of a Riemann surface equipped with a collection of marked points on the boundary serving as stops. The morphisms in this category are intersection points, as well as Reeb chords traversing the boundary of the Riemann surface whose intersection number with the stops is 0.

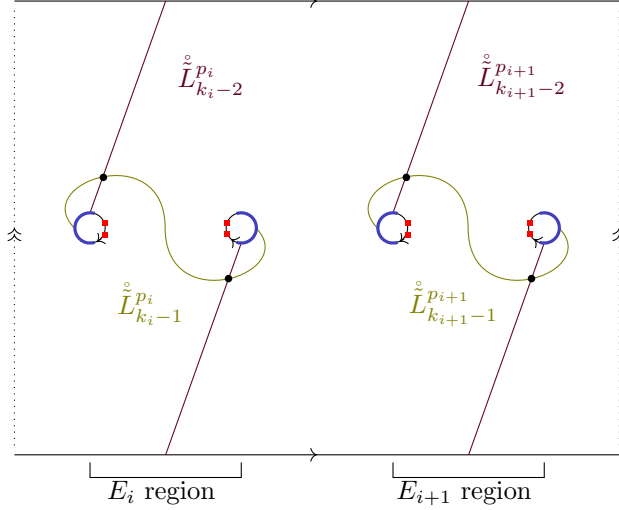


FIGURE 10. Description of the Riemann surface F which is a bordered torus, with the Lagrangian arcs depicted. The blue half-circle at the punctures denotes the region where the handles $H_{k_i-1}^{p_i}$ and $H_{k_{i+1}-1}^{p_{i+1}}$ are to be attached. The arrows signify the wrapping direction and the red squares designate the stops.

Proposition 2.10. *The category \mathcal{C} has an A_∞ model \mathcal{C}' sitting inside the partially wrapped Fukaya category $\mathcal{W}(F; \Lambda)$.*

Proof. Consider the torus F with two stops on each boundary component, as in Figure 10. Define the subcategory \mathcal{C}' of $\mathcal{W}(F; \Lambda)$ to be the A_∞ category with objects

$$\{\overset{\circ}{L}_{k_i-2}^{p_i}, \overset{\circ}{L}_{k_i-1}^{p_i}\}_{i=1}^m \cup \{\mathcal{V}_1, \dots, \mathcal{V}_n\}$$

by imposing directedness: the morphisms in \mathcal{C} go from left to right, including the identity element.

Then, by Corollary 2.8, we conclude that $\mathcal{C} \simeq H^0(\text{perf } \mathcal{C}')$. \square

2.3.5. The proof of homological mirror symmetry. Our proof crucially relies on an application of [LP17, Theorem 3.7.2].

Theorem 2.11 (Lekili-Polishchuk). *There is an A_∞ functor $\varphi : D_{dg}^b(\mathcal{A}_D - \text{mod}) \rightarrow \mathcal{W}(F; \Lambda)$ inducing an equivalence on derived categories. After composing with an autoequivalence of $D_{dg}^b(\mathcal{A}_D - \text{mod})$, the resulting functor φ' sends the object $\mathcal{P}_{E_i}(-1)$ to $\overset{\circ}{L}_{k_i-1}^{p_i}$, the object $\mathcal{P}_{E_i}(-2)$ to $\overset{\circ}{L}_{k_i-2}^{p_i}$ and the objects $\pi^* \iota_D^* \mathcal{L}_i$ to \mathcal{V}_i .*

A few remarks are in order: first of all, Lekili and Polishchuk only describe the effect of the functor on the generators, which on the B-side are the sheaves $\{\mathcal{P}_{D_j}(-1), \mathcal{P}_{D_j}\}_{j=1}^l$, together with the skyscraper

sheaves at the nodes \mathcal{S}_q . The mirror to a skyscraper sheaf at a smooth point can be recovered by using the exact sequence $[\mathcal{P}_{D_j}(-1) \rightarrow \mathcal{P}_{D_j}] \simeq \pi^* \mathcal{O}_{pt}$ which on the A-side, using the surgery exact triangle from [Sei08, Section 17j], is just a meridian circle. To describe the effect of the functor φ on $\pi^* \mathcal{O}_D = \mathcal{F}$, one uses the exact sequence

$$[\bigoplus_{q \text{ a node of } D} \mathcal{S}_q[-1] \rightarrow \bigoplus_{j=1}^l \mathcal{P}_{D_j}(-2)] \xrightarrow{\simeq} \mathcal{F}$$

from [BD11, Theorem 5.10]. This is enough to determine the effect of φ on $\pi^* \iota_D^* \mathcal{L}_i$.

The outcome of this is that the structure sheaf $\pi^* \mathcal{O}_D$ gets sent not to the horizontal reference longitude that we have been using, but rather one that differs from it by a Dehn twist along a meridian on each cylinder mirror to $\mathbb{C}^\times \subset D_j$. Moreover, the functor φ sends \mathcal{P}_{E_i} to $\mathring{L}_{k_i-1}^{p_i}$ (which is denoted P_{i,r_i}^\pm with $r_i = 1$ in the notation of [LP18]) and $\mathcal{P}_{E_i}(-1)$ to $\mathring{L}_{k_i-2}^{p_i}$ (denoted $P_{i,0}^\pm$ in [LP18]). After precomposing with the autoequivalence given by the tensor product with $\pi^* \mathcal{K}$, where \mathcal{K} is a line bundle having degree 1 on each component of D_i , the claim about the modified functor φ' follows. Finally, note that the grading in [LP18] is the same as our modified grading data α , which ensures that the intersection points between $\mathring{L}_{k_i-2}^{p_i}$ and $\mathring{L}_{k_i-1}^{p_i}$ have degree 0.

Proposition 2.12 (Identifying the gluing subcategories). *The functor φ' induces a quasi-equivalence:*

$$\varphi'|_{\mathcal{C}'} : \mathcal{C}' \simeq \mathcal{B}_{dg}$$

which in turn leads to a quasi-equivalence of triangulated categories

$$\mathcal{C} \simeq H^0(\text{perf } \mathcal{C}') \simeq H^0(\text{perf } \mathcal{B}_{dg}) \simeq \mathcal{B}$$

Proof. This is a direct consequence of 2.11 and the construction of the categories \mathcal{C}' and \mathcal{B}_{dg} . □

Finally, combining Lemma 2.6 together with Proposition 2.12 completes the proof of Homological Mirror Symmetry in Theorem 0.1. The claim about Lefschetz stabilizations is straightforward from the Construction 2.2 and is completely local. We will verify it in the next section using an explicit LG model.

Remark 2.13 (Orbifolds with points of type $\frac{1}{2n+1}(1, n)$). Virtually the same type of argument could be used for effective log Calabi-Yau orbifold surfaces with points of type $\frac{1}{2n+1}(1, n)$. In that case, $N_d = \mathcal{O} \otimes \rho_d$ and the adjoint functor Ψ in [GR23, Example 3.6] can be used to relate the gluing morphism spaces between N_i and $\Phi \mathcal{L}$ to morphisms between $\mathcal{O}_{E_i}(-1)$ and $\mathcal{L}|_D$ on D . On the A-side, one could use a collection of obstruction arcs, like in 2.8, to show analogously that the holomorphic disks contributing to the A_∞ products involving the gluing morphism spaces are contained within the bordered torus F_I .

3. THE GEOMETRY OF THE LG MODEL MIRROR TO X_{k+1}

In this chapter, we study an explicit Landau-Ginzburg model mirror to the orbifold del Pezzo surfaces in the family X_{k+1} and compare it to the abstract Lefschetz fibration from the previous section. We will construct a collection of vanishing paths whose vanishing cycles will be used to prove homological mirror symmetry for the family X_{k+1} in Section 4.

3.1. Toric degenerations and an explicit LG model. The orbifold \mathcal{X} admits a toric degeneration to $\mathbb{P}(1, k, k+1)$. This is most easily seen by viewing $\mathbb{P}(1, k, k+1)$ as $\mathbb{V}(x^{k+1} + zw) \subset \mathbb{P}(1, 1, 1, k)$ (see e.g. [CP20, Section 4]).

Standard mirror constructions of toric degenerations yield the following process: we pass to the polar dual toric variety V of $\mathbb{P}(1, k, k+1)$ and produce a pencil of algebraic curves on it. The pencil arises from two sections of a line bundle: the first section corresponds to the origin lattice point in the Fano polygon, and

the other section corresponds to the boundary lattice points. In our case V is polarized by the line bundle associated to $D_V = V_0 + V_1 + kV_2$ and given by the convex hull of the points $(-1, -1), (-1, k), (1, 0)$:

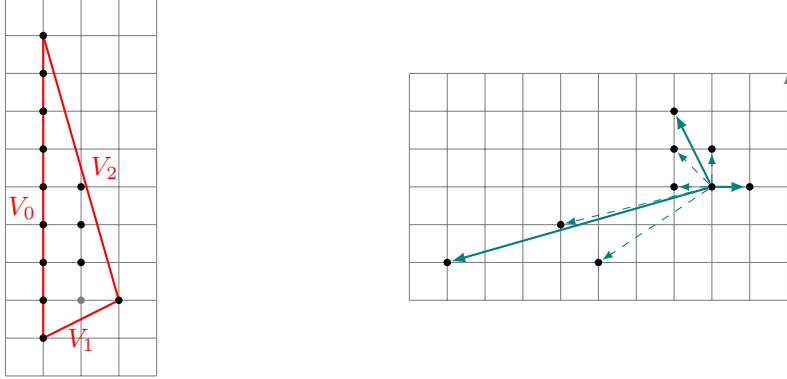


FIGURE 11. The polygon (left) and its fan (right) and also the resolution rays (dashed) in the case $k = 7$.

The resulting potential, for k odd, has the following form:

$$\mathbf{f}|_{(\mathbb{C}^\times)^2} = \frac{(y + \mathbf{q}_1) \dots (y + \mathbf{q}_{k+1})}{xy} + x + \tau_1 y + \dots \tau_{\frac{k-1}{2}} y^{\frac{k-1}{2}}$$

The first term comes from the left column of the polygon, the second from the lattice point $(1, 0)$ and the remaining terms arise from the interior lattice points. This Laurent polynomial appears in the case $k = 3$, $\mathbf{q}_i = 1$ in [OP18, Section 7.2].

Remark 3.1. When k is even, there is an extra boundary lattice point $(0, \frac{k}{2})$ and hence the potential will have a different form. We choose k to be odd purely for the sake of convenience.

The precise values of \mathbf{q}_i, τ_j , if generic, will not affect the symplectic geometry of this Landau-Ginzburg model. We will take $\mathbf{q}_i \approx 1$ but all distinct, $\tau_1 = 1, \tau_j = 0, j > 1$. This suffices for our purposes. Moreover, we introduce an auxiliary s -parameter in front of x and define:

$$\mathbf{f}_s = \frac{\prod_{i=1}^{k+1} (y + \mathbf{q}_i)}{xy} + sx + y$$

Remark 3.2. The Newton polytope of \mathbf{f} is exactly the Fano polygon described above, in other words it corresponds to a section of $\mathcal{O}(D_V)$. For \mathbf{f} to be non-degenerate (in the sense of [Kou76], see also [Sei10, Section 6]), the values of \mathbf{q}_i have to be generic i.e. $P(y) = \prod(y + \mathbf{q}_i)$ must not admit double roots, since the face polynomial on the left face V_0 of V is given by $P(y)/xy$. This non-degeneracy precludes the existence of critical points on the base locus of the pencil, which is related to the Palais-Smale condition.

Remark 3.3. The parameters \mathbf{q}_i are Novikov parameters associated to $H^2(\mathcal{X}) = \mathbb{Z}^{k+1}$, whereas the τ_j correspond to twisted sectors in the Chen-Ruan cohomology of \mathcal{X} . A piece of computer code made by the author which can compute the small quantum cohomology of \mathcal{X} can be found [here](#).

3.1.1. Homogeneous coordinates and the genus of the general fiber. The fan of V consists of the rays $(1, 0), (-1, 2), (-k, -2)$. It has two $\frac{1}{2}(1, 1)$ singularities where V_0 meets V_1, V_2 and also a $\frac{1}{2k+2}(1, k+2)$ singularity where V_1, V_2 meet. Moreover, $V_0^2 = \frac{k+1}{2}, V_1^2 = V_2^2 = \frac{1}{2k+2}, D_V^2 = 2k+2$. The homogeneous

coordinate ring has variables v_0, v_1, v_2 corresponding to the toric divisors and the lattice points correspond to the following monomials:

$$\begin{aligned} (0,0) &\leftrightarrow v_0 v_1 v_2^k \\ (1,0) &\leftrightarrow v_0^2 \\ (-1,i) &\leftrightarrow v_1^{2i+2} v_2^{2k-2i} = \{v_2^{2k+2}, v_2^{2k} v_1^2, \dots, v_1^{2k+2}\} \end{aligned}$$

A general section Σ of $\mathcal{O}(D_V)$ has Euler characteristic given by

$$\int_{\Sigma} c_1(\mathcal{T}_{\Sigma}) = \int_{\Sigma} c_1(\mathcal{T}_V) - c_1(\mathcal{O}(D_V)) = \int_{\Sigma} c_1(\mathcal{O}((1-k)V_2)) = (1-k) \Sigma \cdot V_2 = 1 - k$$

Hence its genus will be $\frac{k+1}{2}$, which is also the number of interior lattice points in the Newton polytope. Moreover, it satisfies $\Sigma \cdot V_0 = k+1$, $\Sigma \cdot V_1 = \Sigma \cdot V_2 = 1$.

Note that after resolving the A_1 singularity where V_0 meets V_1 , introducing an exceptional divisor V_3 , we can write \mathbf{f}_s in a chart $U_{0,3} \simeq \mathbb{C}^2$ as:

$$\mathbf{f}_s = P(v_3) + s v_0^2 v_3 + v_0 v_3^2, o = v_0 v_3 \quad (3.4)$$

where o is the monomial section of $\mathcal{O}(D_V)$ corresponding to the origin. These two functions define a pencil on \mathbb{C}^2 . We will be mostly working in this chart.

3.2. The total space of the Lefschetz fibration. So far, we have defined a pencil on a toric surface V . We explain how to turn this into a Lefschetz fibration.

The pencil on V has $k+1$ base points on V_0 and one base point each on V_1, V_2 . We blow these up, then remove the strict transform of the toric boundary, producing a manifold M . This admits a Lefschetz fibration whose general fiber is a compact genus $\frac{k+1}{2}$ Riemann surface. Since c_1 of this fiber is nonzero, this will preclude the possibility of a \mathbb{Z} -grading on the Fukaya-Seidel category to be defined later.

Instead, if we just worked in the chart $U_{0,3}$ and blew up the $k+1$ points on the axis corresponding to V_0 , then removed the strict transform of the coordinate lines, we will get a manifold that we denote by M^0 . This manifold admits a Lefschetz fibration induced by \mathbf{f} whose general fiber is a twice-punctured genus $\frac{k+1}{2}$ Riemann surface⁹. It is a partial compactification of $(\mathbb{C}^\times)^2$. By [Eva11, Section 7], the manifold M^0 is in fact diffeomorphic to the following manifold defined by an algebraic equation:

$$\{zx = P(y)\} \subset \mathbb{C}_{x,z}^2 \times \mathbb{C}_y^\times$$

The $(\mathbb{C}^\times)^2$ inside M^0 is given by the locus where $x \neq 0$. In other words, M^0 is diffeomorphic to the A_k Milnor fiber with a cylinder removed. As such, it has $H_2(M_0) = \mathbb{Z}^{k+1}$, with k of the factors coming from a chain of -2 spheres, and another one coming from the generator of $H_2((\mathbb{C}^\times)^2)$. We will equip M^0 with the non-exact symplectic form as in Equation 0.9.

3.3. Critical points and critical values. Now, we proceed to determine the critical points. These are all contained inside $(\mathbb{C}^\times)_{x,y}^2$ (provided that P does not admit double roots). We use the variable t to denote the value of \mathbf{f}_s .

Proposition 3.5. *As $s \rightarrow 0$ (setting $P(y) = (1+y)^{k+1} + \epsilon$ for a small ϵ), the critical values become distributed as follows:*

- I. $k-2$ of the critical values are distributed near the roots of $t^{k-2} - (\frac{k-2}{k})^{k-2} \frac{1}{s} = 0$.
- II. 3 of them will be arbitrarily close to 0
- III. Another $k+1$ critical points are equidistributed near -1 .

⁹The punctures correspond to the pencil's base points on V_1, V_2

Proof. We provide the proof in the appendix 5.5. The case when $\epsilon = 0$ is illustrated in Figure 2, where the $k + 1$ critical values of type III have all collided. \square

Remark 3.6. If we set $\mathbf{q}_i = 1$ there will be a single, $k + 1$ -fold degenerate critical point on the base locus on V_0 as in Figure 12 below. This can be thought of as the 'big' eigenvalue of the quantum multiplication by c_1 on $QH^\bullet(\mathcal{X})$ when \mathcal{X} is monotone. During the process of resolving the base locus, the point where the two branches meet at V_0 is replaced by a tower of k holomorphic spheres all living in this special fiber, so in the end, the fibration has the same number of vanishing cycles.

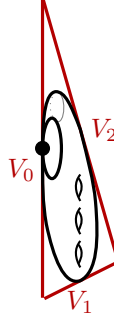


FIGURE 12. Sketch of the critical point at the base locus when all $\mathbf{q}_i = 1$. The base locus can be resolved after k consecutive blowups at the intersection of the branch of Σ_{-1} with intersection multiplicity k with V_0 .

We will from now on focus on this deformed LG model with s arbitrarily small and real. An animation of how the the critical values move as s goes from 1 to $s \approx 0$ can be found [here](#).

3.4. A collection of vanishing cycles. In this section, we determine the vanishing cycles topologically by using a bifibration method, looking at the branch points of some fixed reference fiber by projecting to the y -axis and observing how they collide when we reach a critical value. Initially, we will choose a reference fiber on the real line and follow vanishing paths similar to those of Figure 2. The diagram in Figure 2 depicts the case when all $\mathbf{q}_i = 1$, whereas (as in Proposition 3.5) we slightly deform the potential, in which case the orange critical value at -1 splits into $k + 1$ critical values nearby. We define the vanishing paths for these $k + 1$ points in a simple way: they start at the reference fiber, go slightly above the blue critical values and then go to the $k + 1$ points in a cyclic manner.

This gives us a collection of Lagrangian vanishing cycles which we label in clockwise order:

$$L_{k-1}, L_{k-2}, \dots, L_2, P_{-1}, P_0, P_1, B_1, \dots, B_{k+1}$$

We use the suggestive notation of B_i for the Lagrangian vanishing cycles in accordance with their putative mirror partner sheaves \mathcal{O}_{B_i} .

Remark 3.7. The vanishing cycles L_i are not the mirrors to the sheaves e_i on the B-side. Rather, to match them, one needs to apply a left dual mutation which we will describe later on in this section.

Throughout, we will pick a reference fiber whose value $\mathbf{f} = t_*$ is such that $|t_*|$ is smaller than the absolute values of the $k - 2$ critical values of type I as in Proposition 3.5.

3.4.1. *The general fiber as a branched double cover.* Let Σ_t^{torus} be a fiber $\mathbf{f}|_{(\mathbb{C}^\times)^2}^{-1}(t)$. Projecting to the y -axis realizes Σ^{torus} almost as a branched double cover of \mathbb{C}^\times , but with a certain caveat. Under the y projection, there are $k+1$ branch points. However, there are another $k+1$ points, the roots of $P(y)$ (these are *not* branch points), where the preimage under y consists of only one point, rather than the expected two. Once these are filled in (by partially compactifying $(\mathbb{C}^\times)^2$ to M^0), we get an honest branched double cover of \mathbb{C}^\times , which is what we now consider: the general fiber in the Lefschetz fibration of M^0 will be denoted Σ_t^0 . The $k+1$ punctures that are filled correspond to $k+1$ sections of the Lefschetz fibration arising from the $k+1$ points on the base locus on V_0 which are blown up.

Consider now the branch point equation for Σ_t^{torus} on the open torus: it is given by

$$\mathbf{f}_s = 0, \quad \partial_x \mathbf{f}_s = 0$$

From 5.5, this implies that

$$P(y) - \frac{1}{4s}y(t-y)^2 = 0$$

For $|t| \gg 0$ and with $|t|$ less than the absolute values of the critical values of type III (and with s sufficiently small), this has a root near 0 as well as two roots near t which we call the *twin branch points*¹⁰. Moreover, there are another $k-2$ equidistributed branch points y satisfying $|y^{k-2} - \frac{1}{4s}|^2 \approx 0$. We collect this into a proposition:

Proposition 3.8. *For s sufficiently small and $\frac{1}{s} \gg |t| \gg 0$ the branch points of the Riemann surface Σ_t^0 under the y -projection to \mathbb{C}^\times are distributed as follows:*

- I. $k-2$ are distributed close to the roots of $y^{k-2} = \frac{1}{4s}$.
- II. One is close to 0
- III. Two are close to t

Below is a schematic picture illustrating the branch points of a reference fiber Σ_t^0 for such a t .

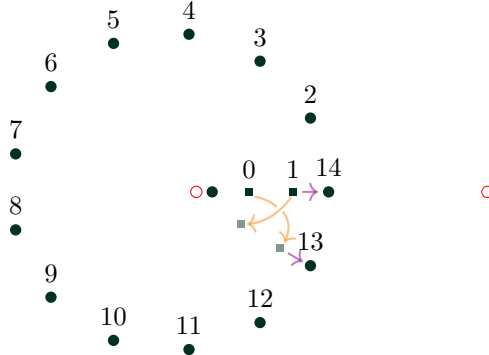


FIGURE 13. Branch points for Σ_t^0 when $k = 15$ and t is on the real line, with added numbered labels which will come in play later, with the 'twin' branch points labeled 0 and 1. The red branch points correspond to the two punctures of Σ_t^0 at $y = 0$ and $y = \infty$. Note that the one at $y = 0$ corresponds to the base point on V_1 and the one at ∞ to the base point on V_2

¹⁰One can reason as follows: consider the roots of the equation $4sP - y(t-y)^2 = 0$, once compactified to \mathbb{P}^1 . When $s = 0$, there is a root at 0, a double root at $y = t$ and a $k-2$ -fold root at ∞ . Then, perturbing s by a small amount deforms the positions of the roots continuously.

3.4.2. *The vanishing cycles for the critical values of type I.* Starting from the reference t_* , we consider the effect on the branch points by following the vanishing paths in Figure 2 that go to the $k - 2$ critical values of type I. These are isotopic to a combination of a rotation of t , followed by an outwards radial scaling. In Figure 13 above, the movement associated to the radial outwards scaling of t is illustrated by the purple arrows pointing towards the branch points labelled 14 (and 13). The movement associated to rotating t is depicted by the orange transposition arrows. Both of these movements are animated [here](#) and proved in detail in the Appendix 5.20.

We will now describe what topological classes the vanishing cycles represent in $H_1(\Sigma_*^0)$. Let:

- l denote the class in $H_1(\Sigma_*^0)$ which is represented by a curve which projects under the branched double cover to an arc connecting the twin branch points.
- $l_i, 2 \leq i \leq k - 1$ denote the class in $H_1(\Sigma_*^0)$ which is represented by a curve which projects under the branched double cover to an arc which starts at the branch point 1, goes down and around and ends up at the branch point labelled i .

We choose the orientations so that

$$\langle l_i, l_j \rangle = -1, i < j, \quad \langle l, l_i \rangle = -1$$

The projections under the branched double cover of these classes can be visualized as follows:

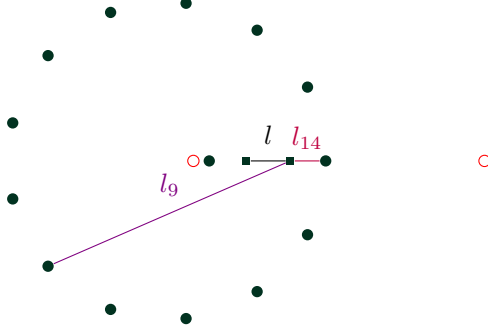


FIGURE 14. A collection of arcs in \mathbb{C}_y^x which lift to the classes l, l_9, l_{14} under the branched double cover (depicted is $k = 15$).

Proposition 3.9. *The vanishing cycles associated to the $k - 2$ critical values of type I with reference fiber Σ_*^0 and vanishing paths as in Figure 2 are given in homology by*

$$[L_j] = (-1)^j((k - 1 - j)l + l_j)$$

Proof. This is clear by our description of how the branch points move under rotation and under radial scaling. We first rotate, transposing the two twin branch points $k - 1 - j$ times. Then, the twin point closer to the branch point of type I collides with it. Unwinding this process, the projection of the vanishing cycle to the y -axis will look like in Figure 15, which is given in homology by the class $(k - 1 - j)l + l_j$. \square

For a collection of vanishing paths defining vanishing thimbles D_i , the Seifert pairing (see [GR25, Section 3.1.3]) is defined by

$$\langle D_i, D_j \rangle_{\text{Seifert}} = \begin{cases} \langle [\partial D_i], [\partial D_j] \rangle, & i < j \\ 1, & i = j \\ 0, & i > j \end{cases}$$

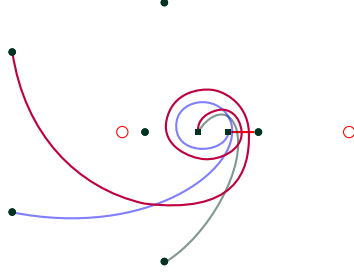


FIGURE 15. The projections under the branched double covering of the topological vanishing cycles associated to $L_{k-1}, L_{k-2}, L_{k-3}, L_{k-4}$ for $k = 7$.

Currently, the Gram matrix of the Seifert pairing for our collection of Lagrangian vanishing cycles is of the form

$$\begin{bmatrix} 1 & -2 & 3 & -4 & \dots \\ 0 & 1 & -2 & 3 & \dots \\ 0 & 0 & 1 & -2 & \dots \\ 0 & 0 & 0 & 1 & \ddots \end{bmatrix}$$

which differs from the Gram matrix of the sheaves $\langle e_2, \dots, e_{k-1} \rangle$ under the Euler pairing. To match them, we perform a series of mutations known as passing to the *left dual* (as in [AKO08, Definition 2.14]).

Explicitly, this process can be described as follows: we left mutate L_{k-2} through L_{k-1} , denoting the result by $\mathbb{L}^{(1)}L_{k-2}$. Then, we left mutate L_{k-3} through $\mathbb{L}^{(1)}L_{k-2}, L_{k-1}$, denoting this by $\mathbb{L}^{(2)}L_{k-3}$. We do this for all Lagrangians L_i . At the end of this process, we have a new sequence

$$\mathbb{L}^{(k-3)}L_2, \mathbb{L}^{(k-4)}L_3, \dots, \mathbb{L}^{(1)}L_{k-2}, L_{k-1}$$

Proposition 3.10. *The left dual to the collection $\langle L_{k-1}, \dots, L_2 \rangle$, which we denote by $\langle \tilde{L}_2, \dots, \tilde{L}_{k-1} \rangle$, is described in homology (up to a choice of orientations) by*

$$\begin{aligned} [\tilde{L}_{k-1}] &= l_{k-1} \\ [\tilde{L}_{k-2}] &= l_{k-2} - 2l_{k-1} + l \\ [\tilde{L}_i] &= l_i - 2l_{i+1} + l_{i+2}, i < k-2 \end{aligned}$$

As such, its Gram matrix matches the Gram matrix of the exceptional subcollection $\langle e_2, \dots, e_{k-1} \rangle$ on the B-side.

Proof. We prove this claim by induction. First, $[\mathbb{L}_{L_{k-1}}L_{k-2}] = [L_{k-2}] - \langle L_{k-1}, L_{k-2} \rangle [L_{k-1}] = [L_{k-2}] + 2[L_{k-1}] = (-1)(l_{k-2} - 2l_{k-1} + l)$ as claimed.

The rest of the proof is a pleasant exercise in combinatorics. First of all, left mutation on the level of homology is given by $\mathbb{L}_a b = b - \langle a, b \rangle a$, so the consecutive left mutation through a sequence of elements a_1, \dots, a_m is given by

$$\mathbb{L}_{a_1, \dots, a_m} b = b + \sum_{i_1 < i_2 < \dots < i_s} (-1)^s \langle a_{i_1}, a_{i_2} \rangle \dots \langle a_{i_s}, b \rangle a_{i_1}$$

Suppose now as an inductive hypothesis that $[\mathbb{L}^{(i)}L_{k-1-i}] = (-1)^{k-1-i}(l_{k-1-i} - 2l_{k-i} + l_{k-i+1})$ for all $i \leq m$. Thus, for $i > 1$ we have $\langle \mathbb{L}^{(i)}L_{k-1-i}, L_{k-1-(m+1)} \rangle = 0$. Moreover, $\langle L_{k-1}, L_{k-1-(m+1)} \rangle = (-1)^{m+1}(m+2)$, $\langle \mathbb{L}^{(1)}L_{k-2}, L_{k-1-(m+1)} \rangle = (-1)^{m+1}(m+3)$.

We now want to mutate $L_{k-1-(m+1)}$ past everything on its left:

$$\mathbb{L}^{(m)} L_{k-1-m}, \mathbb{L}^{(m-1)} L_{k-m}, \dots, \mathbb{L}^{(1)} L_{k-2}, L_{k-1}, L_{k-1-(m+1)}, \dots$$

By the above remark, the term of $\mathbb{L}^{(i)} L_{k-1-i}$ in $\mathbb{L}^{(m+1)} L_{k-1-(m+1)}$ will be given by the following sum:

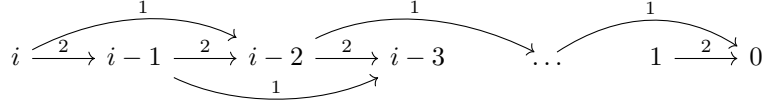
$$\sum_{i>i_1>\dots>i_s>0} (-1)^s \langle \mathbb{L}^{(i)} L_{k-1-i}, \mathbb{L}^{(i_1)} L_{k-1-i_1} \rangle \dots \langle \mathbb{L}^{(i_s)} L_{k-1-i_s}, L_{k-1-(m+1)} \rangle$$

Therefore, we must consider all possible ways to get from $\mathbb{L}^{(i)} L_{k-1-i}$ to $L_{k-1-(m+1)}$. For a composable path of maps to contribute a nonzero term to the sum above, it must traverse either L_{k-1} or $\mathbb{L}^{(1)} L_{k-2}$ penultimately.

That is, we need to consider all ways to compose morphisms starting from $\mathbb{L}^{(i)} L_{k-1-i}$ and ending at either $\mathbb{L}^{(1)} L_{k-2}$ or L_{k-1} . The coefficient of $\mathbb{L}^{(i)} L_{k-1-i}$ appearing in $\mathbb{L}^{(m+1)} L_{k-1-(m+1)}$ will then be the signed, weighted sum of all these composable paths. By the inductive hypothesis, the $\mathbb{L}^{(i)} L_{k-1-i}$ satisfy

$$\begin{aligned} \langle \mathbb{L}^{(i)} L_{k-1-i}, \mathbb{L}^{(i-1)} L_{k-1-(i-1)} \rangle &= 2, & \langle \mathbb{L}^{(i)} L_{k-1-i}, \mathbb{L}^{(i-2)} L_{k-1-(i-2)} \rangle &= 1, \\ \langle \mathbb{L}^{(i)} L_{k-1-i}, \mathbb{L}^{(j)} L_{k-1-j} \rangle &= 0, & i-j > 2 \end{aligned}$$

Hence, starting from $\mathbb{L}^{(i)} L_{k-1-i}$ we are allowed either a jump to $\mathbb{L}^{(i-1)} L_{k-i}$ weighted by 2 or a jump to $\mathbb{L}^{(i-2)} L_{k-i+1}$ weighted by 1. Consider the path algebra of the following quiver, weighing morphisms from i to $i-1$ by 2 and from i to $i-2$ by 1:



We denote the weighted sum of all possible paths from i to 0 by s_i . It is clear that these s_i satisfy the recursion

$$s_i = 2s_{i-1} - s_{i-2}, s_1 = 2, s_2 = 3$$

hence this signed sum is $s_i = i + 1$.

The relationship between this quiver and the total coefficient of $\mathbb{L}^{(i)} L_{k-1-i}$ in $\mathbb{L}^{(m+1)} L_{k-1-(m+1)}$ is the following:

- firstly, we need to consider all composable morphisms from $\mathbb{L}^{(i)} L_{k-1-i}$ to L_{k-1} , which are then concatenated by $\langle L_{k-1}, L_{k-1-(m+1)} \rangle = (-1)^{m+1}(m+2)$. These contribute $s_i(-1)^{m+1}(m+2)$
- secondly, we need to consider all composable morphisms from \tilde{L}_{k-1-i} to $\mathbb{L}^{(1)} L_{k-2}$ which at the end are concatenated with $\langle \mathbb{L}^{(1)} L_{k-2}, L_{k-1-(m+1)} \rangle = (-1)^{m+1}(m+3)$. These contribute $s_{i-1}(-1)^{m+1}(m+3)$

Adding these up, we get a contribution of

$$(-1)^i (-1)^m ((m+2)(i+1) - (m+3)i) = (-1)^{m+i} (m+2-i)$$

Therefore,

$$[\mathbb{L}^{(m+1)} L_{k-1-(m+1)}] = [L_{k-1-(m+1)}] + \sum_{i=0}^m (-1)^{m+i} (m+2-i) [\mathbb{L}^{(i)} L_{k-1-i}] =$$

$$\begin{aligned}
&= (-1)^{m+1} \left((m+1)l + l_{k-1-(m+1)} - \right. \\
&\quad \sum_{i=2}^m (m+2-i)(l_{k-1-i} - 2l_{k-i} + l_{k-i+1}) - \\
&\quad \left. (m+1)(l_{k-2} - 2l_{k-1} + l) - (m+2)l_{k-1} \right) = \\
&= (-1)^{m+1} (l_{k-1-(m+1)} - 2l_{k-1-m} + l_{k-1-(m-1)})
\end{aligned}$$

The final equality is because the l terms cancel, and moreover all the terms $l_i, i < m-1$ will telescope and cancel as well. \square

Remark 3.11. The reader should think of the relation $[\tilde{L}_{k-1-i}] = l_{k-1-i} - 2l_{k-i} + l_{k-i+1}$ as related to the local Koszul resolution

$$[\mathcal{O} \otimes \rho_{k-i+1} \rightarrow \mathcal{O}^{\oplus 2} \otimes \rho_{k-i} \rightarrow \mathcal{O} \otimes \rho_{k-1-i}] \simeq \mathcal{O}_0 \otimes \rho_{k-1-i}$$

The classes $l_i - l_{i+1}$ are represented by arcs connecting adjacent branch points. This means that \tilde{L}_i is represented by a curve that projects to an arc which joins together branch points labelled by i and $i+2$ as in Figure 16. Thinking of the branch points as representing handle attachments on the Riemann surface Σ_*^0 , the result is the same as the effect of the surgery depicted above, which in turn is the same one described in Construction 2.2.

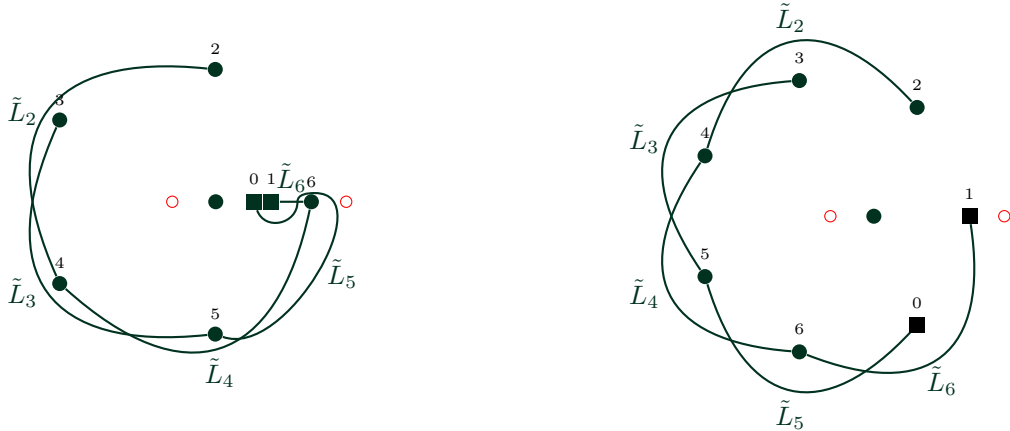


FIGURE 16. Left: the projections of the left dual Lagrangians in our reference fiber Σ_*^0 . Right: a more symmetric visualization of the same Lagrangians.

3.4.3. The vanishing cycles associated to critical values of types II and III. We now consider the vanishing cycles associated to the $k+1$ critical values near -1 and the three critical values near 0 .

When t is near the critical points around -1 , there are still $k-2$ large branch points, one close to 0 and the twin branch points are close to -1 . The only branch points that can collide here are the twin branch points (this is most easily seen by adjusting $\epsilon \rightarrow 0$ at which point the branch point equation has a double root at $y = -1$). In other words, all these $k+1$ vanishing cycles are homologous and have class l in homology.

Finally, when y is close to the origin, the branch point equation is approximated by the cubic

$$4s(1 + \epsilon) = y(y - t)^2$$

One can use computer algebra to see how the roots of this cubic vary with t .

It turns out that the vanishing cycles of type II and III are contained in Σ_*^0 which is a torus with three boundary components, which is unaffected by the $k - 2$ branch points of type I (as in 3.8). Defining a and b to be the meridian and longitude classes as depicted in Figure 17, we conclude:

Proposition 3.12. *The vanishing cycles of type II and III are given in homology by:*

- $[B_1] = [B_2] = \dots = [B_{k+1}] = l$
- $[P_{-1}] = b - l - 2a$
- $[P_0] = b$
- $[P_1] = b + l + 2a$



FIGURE 17. The twin branch points, together with the missing branch point at 0 and the one close to the origin are depicted on the left, together with the projections of representatives of the classes a, b, l . Here, the dotted lines describe branch cuts, with a and l contained inside one of the sheets and b going in between the two sheets of the branched double cover. Arcs describing the projections of the topological vanishing cycles are described on the right.

We can mutate P_{-1} past P_0 , after which it becomes $[\tilde{P}] = 2b + 2a + l$. In the mirror duality, we will identify P_0, \tilde{P}, P_1 with the sheaves $\Phi\mathcal{O}, \Phi\mathcal{T}(-H), \Phi\mathcal{O}(H)$.

3.4.4. A set of 2-cycles associated to the vanishing cycles. In the computation of the Fukaya-Seidel category, it will be important to weigh the holomorphic disk contributions by their symplectic area. In order to do that, it will be helpful to relate $H_2(M^0)$ to the vanishing cycles.

Definition 3.13. Let $\Delta_{i,j}$ be a 2-chain in Σ_*^0 which witnesses the equality $[B_i] = [B_j] \in H_1(\Sigma_*^0)$. We cap this off with vanishing thimbles, producing a 2-cycle

$$S_{i,j} := \Delta_{i,j} - D_{B_i} + D_{B_j}$$

In other words, this is a matching sphere between two critical values corresponding to the vanishing cycles B_i and B_j . Similarly, let C be a 2-chain witnessing the equality $[P_0] + [P_1] = [\tilde{P}]$. This has an associated 2-cycle

$$\bar{C} := C - D_{P_0} - D_{P_1} + D_{\tilde{P}}$$

Remark 3.14. This class is in fact homologous to the image of the generator of $H_2((\mathbb{C}^\times)^2)$ (see [AKO08, Lemma 4.9]) which will lead to a non-commutative deformation of the del Pezzo surface \mathcal{X} . We will not concern ourselves with this in this paper.

3.5. The manifold M^{in} . We describe a submanifold $M^{in} \subset M^0$ which, after applying a series of stabilizations, becomes equivalent to (M^0, \mathbf{f}_s) as a Lefschetz fibration.

Informally, it is given by restricting M^0 to a Lefschetz fibration over a smaller disk which does not see the $k-2$ critical values of type I, and furthermore restricting the fiber so that the branched double covering does not see the $k-2$ branch points of type I. Define

$$M_{r,R}^{in} := \{m \in M^0 \mid |\mathbf{f}_s(m)|^2 \leq R, r \leq |y(m)|^2 \leq 2R\} \quad (3.15)$$

for suitable values of r, R and s . We need to take s sufficiently small so that the critical values of type I are outside of the disk with radius R . Moreover, we need to have the twin branch points for $|t| \leq R$ (which are close to t) to be within radius $2R$, which again will be satisfied if s is sufficiently small. Finally, since $4sP(y) - y(y-t)^2$ is never 0 for $y=0$, and since we are constraining t to be in a compact disk, the branch points entirely avoid a small compact disk of radius r centered at the origin if r is sufficiently small.

Thus, equipping M^{in} with the restriction of the function \mathbf{f}_s , the result is a Lefschetz fibration with $k+4$ critical points and a fiber Σ_*^{in} which is a torus with three boundary components. Consider the Lagrangian vanishing cycle $L_i \subset \Sigma_*^0$ and intersect it with Σ_*^{in} , which produces an arc $L_i^o \subset \Sigma_*^{in}$. This arc intersects $\partial \Sigma_*^0$ at two points.

Proposition 3.16. *The Lefschetz fibration (M^0, \mathbf{f}_s) is equivalent to the stabilization of $(M^{in}, \mathbf{f}_s|_{M^{in}})$ along the Lagrangian arcs L_i^o in the order $i = 2, 3, \dots, k-1$.*

Proof. We describe how to iteratively go from M^{in} to M^0 by modifying step by step the domains for \mathbf{f} and y in 3.15. First, enlarge the annulus $r \leq |y|^2 \leq 2R$ to a domain so as to include the branch point labelled 2 in 13, but no other new branch points. At the same time, enlarge the disk of radius R (on which $\mathbf{f}_s : M^{in} \rightarrow \mathbb{D}_R$ is defined) to a bigger domain, so as to include the critical value corresponding to L_2 and add the vanishing path associated to it, but no other new critical points. The effect of this is to stabilize M^{in} along the Lagrangian arc L_2^o . After doing the same iteratively for the rest of the branch points respectively critical values, the claim follows. \square

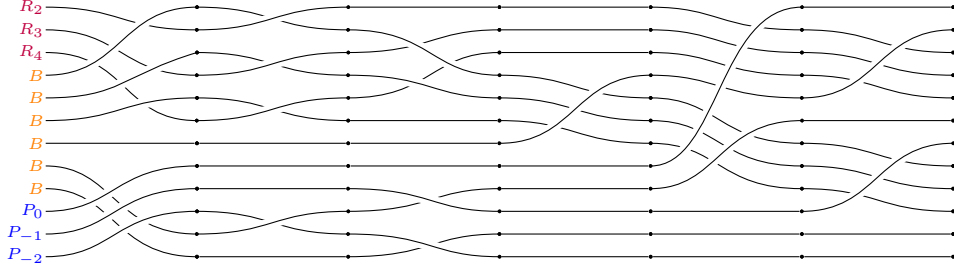
3.6. The vanishing cycles mirror to the alternative line bundle collection. In Section 1.4, we described an alternative full, strong exceptional collection on $D^b(\mathcal{X})$ which remains strong at the limit points of the moduli stack of orbifold del Pezzo surfaces. For the sake of completeness, we will explain how to mutate the collection of vanishing cycles

$$\langle L_{k-1}, \dots, L_2, P_{-1}, P_0, P_1, B_1, \dots, B_{k+1} \rangle$$

in order to get a candidate mirror collection to the collection of line bundles. However, in our proof of homological mirror symmetry, we will constrain ourselves to work with the special McKay exceptional collection and consider an open subset of the complex structure moduli on the B-side corresponding to non-exact symplectic forms on the A-side of type 0.9. As such, this subsection can be skipped without affecting the content of the main theorems of the paper.

3.6.1. A set of mutations. As a first step, we right mutate the L_i past the P 's and B 's, the result of which we denote by R_i . This changes the vanishing paths in Figure 2 so that they go up, left and around the critical points near the origin. The result on the level of homology is that $[R_i] = (l_i - (i-1)l)$.

Moreover, we mutate P_1 past P_0, P_{-1} so that it becomes $[P_{-2}] = b - 4a - 2l$. Beginning with this, we perform 6 steps, summarised in the braid diagram:

FIGURE 18. The sequence of mutations when $k = 5$, in six steps

- Step 1: move $k - 2$ of the B 's past the R_i so that they alternate. At the same time, mutate two B 's to the left of the P 's. On the level of homology, the SOD becomes

$$l, l, b - 4a - 2l, b - 2a - l, b, l_{k-1}, l, l_{k-2}, l, \dots, l_2, l$$

- Step 2: move one of the B 's over P_{-2} . At the same time, mutate $k - 2$ pairs. The result in homology is

$$l, b - 4a - l, l, b - 2a - l, b, l, l_{k-1} - l, l_{k-1}, l_{k-2} - l, l_{k-2}, \dots, l_2 - l, l_2$$

- Step 3: use the orthogonality $\langle l_i - l, l_j \rangle$ for $i < j$ to freely pass the $l_i - l$ to the left. Moreover, right mutate the two other B 's over $b - 4a - l$ and $b - 2a - l$:

$$b - 4a - l, b - 4a, b - 2a - l, b - 2a, b, l, l_{k-1} - l, l_{k-2} - l, \dots, l_2 - l, l_{k-1}, l_{k-2}, \dots, l_2$$

- Step 4: Push the $[B] = l$ that is in the middle past half of the things on the right of it by left mutating them through B :

$$b - 4a - l, b - 4a, b - 2a - l, b - 2a, b, l_{k-1}, l_{k-2}, \dots, l_2, l, l_{k-1}, l_{k-2}, \dots, l_2$$

- Step 5: Push P_0 all the way to the right, left mutating everything through it. Moreover, use the fact that $\langle b - 2a, l_i \rangle = 0$ to mutate that through as well:

$$b - 4a - l, b - 4a, b - 2a - l, l_{k-1}, l_{k-2}, \dots, l_2, b - 2a, b - l, l_{k-1}, l_{k-2}, \dots, l_2, b$$

- Step 6: Finally, push the $b - 2a - l$ and $b - l$ through:

$$b - 4a - l, b - 4a, b - 2a - l_{k-1}, b - 2a - l - l_{k-2}, \dots, b - 2a - l_2, b - 2a - l, b - 2a, b - l - l_{k-1}, b - l - l_{k-2}, \dots, b - l - l_2, b - l, b$$

It can be immediately verified that:¹¹

Proposition 3.17. *The Gram matrix (under the Seifert pairing) of the collection of vanishing thimbles whose associated vanishing cycles are given in homology by*

$$b - 4a - l, b - 4a, b - 2a - l_{k-1}, b - 2a - l - l_{k-2}, \dots, b - 2a - l_2, b - 2a - l, b - 2a, b - l - l_{k-1}, b - l - l_{k-2}, \dots, b - l - l_2, b - l, b$$

matches the Gram matrix (under the Euler pairing) of the exceptional collection of line bundles

$$\mathcal{O}(-2C + \mathbf{L}_{k+1})\mathcal{O}(-2C + \mathbf{L}_{k+1} + \mathbf{L}_k), \dots, \mathcal{O}(-\mathbf{L}_1), \mathcal{O}$$

¹¹In fact, this can also be promoted to a homological statement, at least if we work with the exact symplectic structure. Determining the weights is more difficult.

4. HOMOLOGICAL MIRROR SYMMETRY FOR X_{k+1}

In this section, we compute the directed A_∞ category (as in Definition 0.6) of vanishing thimbles associated to the vanishing paths from the previous section. We show an equivalence (in families) between the derived category of \mathcal{X} and this symplectic category, by constructing an explicit mirror map.

Recall the setup: we take the Lefschetz fibration

$$\mathbf{f}_s : M^0 \rightarrow \mathbb{C}$$

and equip it with the symplectic form as in Definition 0.9, with the non-exactness supported near the chain of spheres $S_{1,2}, \dots, S_{k,k+1}$ of Definition 3.13. To ensure the Fukaya-Seidel category is well-defined, we follow [AKO08, Section 3]: while the total space is non-exact, each fiber is an exact symplectic manifold. Moreover, $\pi_2(\Sigma^0) = \pi_2(\Sigma^0, L) = 0$ for each Lagrangian vanishing cycle L , which prevents bubbling phenomena. The fiber is a punctured curve, so $c_1(\Sigma_*^0) = 0$ hence there is a \mathbb{Z} -grading. Finally, to ensure that symplectic parallel transport and hence the Lagrangian vanishing cycles are well-defined, it is enough to show that (M^0, ω) is complete and moreover $|\nabla \mathbf{f}_s|$ is bounded from below outside of a compact subset (this is a Palais-Smale type condition, see [Sei10, Section 6]). We verify this in the appendix 5.23. The Lagrangian vanishing cycles come equipped with the unique non-trivial spin structure.

4.0.1. *B-fields and sign conventions.* To consider not just a real-valued deformation of the symplectic structure, but more generally a complex one, we will attach a B-field to M^0 . This is a closed 2-form on M^0 . We extend the objects of the Fukaya-Seidel category to be Lagrangian vanishing cycles L , coupled with a connection on the trivial line bundle on L whose curvature is $-2\pi i B$. Each holomorphic disk with Lagrangian boundary conditions appearing in the A_∞ operations will appear with the following weight:

$$(-1)^{v(u)} \exp(2\pi i \int_{D^2} u^*(B + i\omega)) \text{hol}(\partial u)$$

Furthermore, the curvature condition implies that

$$\text{hol}_\nabla(L) = \exp(-2\pi i \int_{\mathbf{D}_L} B)$$

where \mathbf{D}_L is the thimble associated to a Lagrangian vanishing cycle L . The sign $v(u)$ can be computed by using the same sign convention as in [AKO06] by picking a marked point on each Lagrangian vanishing cycle which is distinct from the intersection points. For the \tilde{L}_i , the point we pick is a lift of the midpoint as in Figure 7 in such a way so that all these lifts live on the same sheet of the covering.

The B-fields that we consider will be sums of Thom forms supported near the same -2 spheres as in the definition of the symplectic forms ω .

4.0.2. *The Lagrangian vanishing cycles.* While we have determined the vanishing cycles topologically, we need to take some care in describing them symplectically, due to the non-exactness of the symplectic form. Begin with (M^0, ω^{ex}) , with $\omega^{ex} = dx \wedge d\bar{x} + d\log y \wedge d\log \bar{y} + dz \wedge d\bar{z}$. In this situation, ω^{ex} is anti-invariant under complex conjugation, so by the same argument as in [AKO08, Section 4.2], the Lagrangian vanishing cycles are not only smoothly but also Hamiltonian isotopic to the curves which project to arcs connecting two branch points, as described in the previous Section 3. In particular, when working with ω^{ex} , all of the B_i are Hamiltonian isotopic to each other, and have two intersection points of degree 0 and 1. We want to get rid of this phenomenon, so as to achieve a strong exceptional collection. To this end, we deform slightly the symplectic form to ω^ϵ as in Definition 0.9, the effect of which is to introduce symplectic area between B_i and B_j and make them Hamiltonian displaceable from each other, but otherwise keeps the rest of the Lagrangian vanishing cycles unaffected (since this deformation is only supported near a collection of matching -2 spheres for the Lagrangian vanishing cycles B_i).

4.1. Grading and morphism spaces. The grading data for Σ_*^0 , as well as the Lagrangians and the intersection points between them, is the same one that we used in Definition 2.3. In other words, we choose the horizontal line field in the planar description of the surface Σ_* , as in Figure 19. It describes a genus $\frac{k+1}{2}$ Riemann surface with one boundary component using handle attachments. The surface Σ_*^0 should have instead two boundary components, so an extra puncture needs to be added, but we have refrained from doing so in the Figure to not cause clutter.

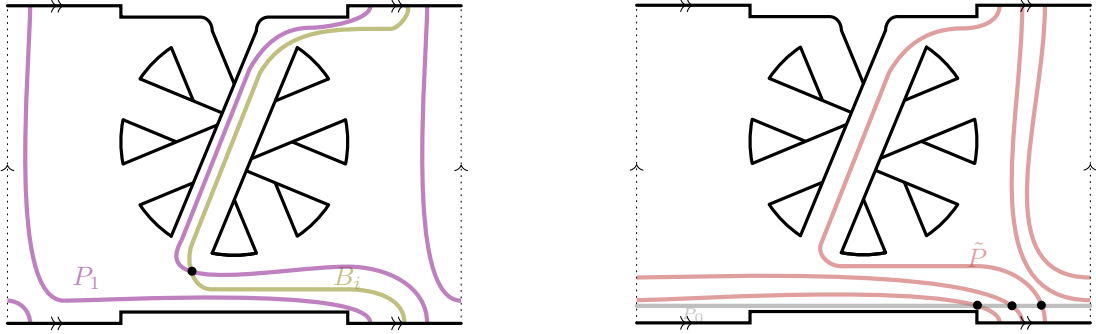


FIGURE 19. Left: description of the Lagrangians $[P_1] = b + 2a + l, [B_i] = l$. Right: depiction of the Lagrangians $[P_0] = b, [\tilde{P}] = 2b + 2a + l$. Note that we have $k - 2$ extra handle bridges (in this case $k = 5$) which are completely independent of these Lagrangians - the Lagrangians mirror to $\Phi D^b Y$ only use the special handle bridges 0 and 1

We now write down a set of generators of the morphism spaces, which can alternatively be visualized by using the branched double projection rather than the planar one above (we will do this in the following Section).

Definition 4.1. We name the intersection points in the hom-complexes as:

$$\begin{aligned}
 CF(\tilde{L}_i, \tilde{L}_{i+1}) &= \mathbb{C}p_{1,i} \oplus \mathbb{C}p_{2,i}, \quad CF(\tilde{L}_i, \tilde{L}_{i+2}) = \mathbb{C}g_i \\
 CF(P_0, \tilde{P}) &= \mathbb{C}x_1 \oplus \mathbb{C}y_1 \oplus \mathbb{C}z_1, \quad CF(\tilde{P}, P_1) = \mathbb{C}x_1 \oplus \mathbb{C}y_1 \oplus \mathbb{C}z_1, \quad CF(P_0, P_1) = \mathbb{C}x \oplus \mathbb{C}y \oplus \mathbb{C}z \\
 CF(P_j, B_i) &= \mathbb{C}r_{j,i}, \quad CF(\tilde{P}, B_i) = \mathbb{C}\tilde{r}_i \oplus \mathbb{C}\tilde{r}'_i \\
 CF(\tilde{L}_{k-1}, P_0) &= 0, \quad CF(\tilde{L}_{k-2}, P_0) = \mathbb{C}\epsilon' \\
 CF(\tilde{L}_{k-1}, \tilde{P}) &= \mathbb{C}\tilde{\epsilon}, \quad CF(\tilde{L}_{k-2}, \tilde{P}) = \mathbb{C}\tilde{\epsilon}' \oplus \mathbb{C}\tilde{x}^E \oplus \mathbb{C}\tilde{y}^E \\
 CF(\tilde{L}_{k-1}, P_1) &= \mathbb{C}\epsilon, \quad CF(\tilde{L}_{k-2}, P_1) = \mathbb{C}x_1^E \oplus \mathbb{C}y_1^E \\
 CF(\tilde{L}_{k-1}, B_i) &= \mathbb{C}\epsilon_i, \quad CF(\tilde{L}_{k-2}, B_i) = \mathbb{C}\epsilon'_i
 \end{aligned}$$

We choose the labeling so that (after removing branch cuts) $p_1, \tilde{x}^E, x_1^E, x, y_0, y_1$ are all on one sheet of the double cover and $p_2, \tilde{y}^E, y_1^E, y, x_0, x_1$ are all on the other.

Proposition 4.2. *With the grading data α^{pre} , the intersection points between P_0, \tilde{P}, P_1, B_i all have degree zero. Moreover,*

$$|p_{1,i}|^{\alpha^{pre}} = |p_{2,i}|^{\alpha^{pre}} = 1, |g_i|^{\alpha^{pre}} = 2$$

The intersection points between \tilde{L}_{k-1} and P_0, \tilde{P}, P_1, B_i all have degree 1:

$$|\tilde{\epsilon}|^{\alpha^{pre}} = |\epsilon|^{\alpha^{pre}} = |\epsilon_i|^{\alpha^{pre}} = 1$$

and similarly the intersections between \tilde{L}_{k-2} and P_0, \tilde{P}, P_1, B_i have degree 2:

$$|\epsilon'|^{\alpha^{pre}} = |\tilde{\epsilon}'|^{\alpha^{pre}} = |\tilde{x}^E|^{\alpha^{pre}} = |\tilde{y}^E|^{\alpha^{pre}} = |x_1^E|^{\alpha^{pre}} = |y_1^E|^{\alpha^{pre}} = |\epsilon_i'|^{\alpha^{pre}} = 2$$

Proof. Combined with the data of the grading 2.3 and Figure 19, the result follows by using Seidel's formula 2.4. \square

Just as on the B-side, we can shift the phase functions of the Lagrangians \tilde{L}_i by $[k-i]$. We call this modified grading data α , with which the collection becomes strong:

Corollary 4.3. *With the modified grading data α , the morphism spaces for the Lagrangian vanishing cycles $\tilde{L}_i, P_0, \tilde{P}, P_1, B_i$ are concentrated degree 0. Therefore, the only nontrivial A_∞ operation is μ^2 .*

4.2. The mirror to the algebra of the McKay quiver. We start by describing the algebra of the Lagrangians $\tilde{L}_2, \dots, \tilde{L}_{k-1}$.

Proposition 4.4. *The A_∞ algebra of the Lagrangians $\tilde{L}_2, \dots, \tilde{L}_{k-2}$ is equivalent to the dg algebra of the orbifold skyscrapers e_2, \dots, e_{k-1} .*

Proof. Recall the Floer cycles involved in the computation:

$$CF^0(\tilde{L}_i, \tilde{L}_{i+1}) = \mathbb{C}p_{1,i} \oplus \mathbb{C}p_{2,i}, \quad CF^0(\tilde{L}_i, \tilde{L}_{i+2}) = \mathbb{C}g_i$$

This enumeration of the disks was done in Lemma 2.6. However, in this case there are constants associated to the symplectic area that need to be accounted for. The two disks produce two compositions $\mu^2(p_{1,i}, p_{1,i+1}) = \vartheta_{1,i}g_i, \mu^2(p_{2,i}, p_{2,i+1}) = \vartheta_{2,i}g_i$. After a rescaling $p_{1,i}^{resc} := -\frac{\vartheta_{2,i}}{\vartheta_{1,i}}p_{1,i}$, we can arrange that

$$\mu^2(p_{1,i}, p_{1,i+1}) = -\mu^2(p_{2,i}, p_{2,i+1})$$

The resulting dg algebra is clearly the same as the McKay quiver algebra described in Section 1. \square

4.3. The mirror to the derived category of Y . We now move on to compute the algebra of the rest of the Lagrangians, namely P_0, \tilde{P}, P_1 and B_0, \dots, B_k . Here, \tilde{P} is the result of right mutating P_{-1} through P_0 and it satisfies $[\tilde{P}] = 2b + 2a + l$. In computing the compositions involving B_i , the non-exactness of ω will play a part, and hence it will be convenient to define some Novikov parameters.

Definition 4.5. We define Novikov parameters $q_{i,j} := \exp(2\pi i[B + i\omega](S_{i,j}))$. We also define $q_C := \exp(2\pi i[B + i\omega](T^2))$.

We will mostly ignore the non-commutative direction and set $q_C = 1$. The first relations we compute are exactly analogous to [AKO06, Proposition 4.7], except that our fiber is non-compact so there is no analogue of q_F . These relations are mirror to the $D^b(\mathbb{P}^2)$ component on the B-side.

Proposition 4.6. *For the compositions $CF(\tilde{P}, P_1) \otimes CF(P_0, \tilde{P}) \rightarrow CF(P_0, P_1)$, there exists constants α such that*

$$\begin{aligned} \mu^2(y_1, x_0) &= \alpha_{x,y}z, & \mu^2(x_1, y_0) &= \alpha_{y,x}z \\ \mu^2(z_1, x_0) &= \alpha_{x,z}y, & \mu^2(x_1, z_0) &= \alpha_{z,x}y \\ \mu^2(z_1, y_0) &= \alpha_{y,z}x, & \mu^2(y_1, z_0) &= \alpha_{z,y}x \\ \mu^2(x_1, x_0) &= \mu^2(y_1, y_0) = \mu^2(z_1, z_0) = 0 \end{aligned}$$

These constants satisfy

$$\frac{\alpha_{x,y}\alpha_{y,z}\alpha_{z,x}}{\alpha_{y,x}\alpha_{z,y}\alpha_{x,z}} = -q_C$$

Proof. One computes the various holomorphic disks again by projecting them along the branched double cover, as in Figure 20. There are three enclosed regions, each admitting two lifts. Let us denote the holomorphic triangles $u_{x,y}, u_{y,x}, u_{x,z}, u_{z,x}, u_{y,z}, u_{z,y}$. These disks form a 2-chain

$$u_{x,y} + u_{y,z} + u_{z,x} - u_{y,x} - u_{z,y} - u_{x,z}$$

whose boundary is exactly $P_0 + P_1 - \tilde{P}$ hence it can be capped off with the vanishing thimbles $\mathbf{D}_{P_0}, \mathbf{D}_{\tilde{P}}, \mathbf{D}_{P_1}$ to produce a cycle $[\tilde{C}] \in H_2(M^0)$. In fact, by an argument identical to the one in [AKO08, Lemma 4.9], this cycle is homologous to the image of the torus generating $H_2((\mathbb{C}^\times)^2)$. ¹²

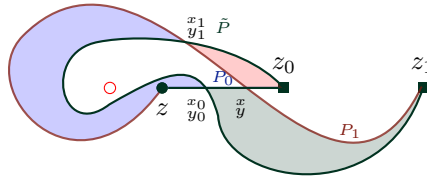


FIGURE 20. Holomorphic disks mirror to the algebra of \mathbb{P}^2

The minus sign is due to the fact that the 2-chain described above is exactly $P_0 \cup \tilde{P} \cup P_1$ which passes through each of the three marked points exactly once. \square

We compute the compositions with B_i next and illustrate the projections of the B_i as concentric dashed circles going around two branched points. The cycle $\Delta_{i,j}$ is given by a lift of the annulus between two concentric circles.

Remark 4.7. We will use the shorthand notation $A \rightarrow B \rightarrow C$ to denote a composition $CF(B, C) \otimes CF(A, B) \rightarrow CF(A, C)$.

Proposition 4.8. *For the compositions of type $P_0 \rightarrow P_1 \rightarrow B_i$ there are constants β such that:*

$$\mu^2(r_{1,i}, x) = \beta_{x,i} r_{0,i}, \quad \mu^2(r_{1,i}, y) = \beta_{y,i} r_{0,i}, \quad \mu^2(r_{1,i}, z) = 0$$

For the compositions of type $P_0 \rightarrow \tilde{P} \rightarrow B_i$, there are constants γ such that:

$$\begin{aligned} \mu^2(\tilde{r}_i, x_0) &= 0, & \mu^2(\tilde{r}_i, y_0) &= 0, & \mu^2(\tilde{r}_i, z_0) &= \gamma_{z,i} r_{0,i} \\ \mu^2(\tilde{r}'_i, x_0) &= \gamma_{x,i} r_{0,i}, & \mu^2(\tilde{r}'_i, y_0) &= \gamma_{y,i} r_{0,i}, & \mu^2(\tilde{r}'_i, z_0) &= 0 \end{aligned}$$

For the compositions of type $\tilde{P} \rightarrow P_1 \rightarrow B_i$ there are constants η such that:

$$\mu^2(r_{1,i}, x_1) = \eta_{x,i} \tilde{r}_i, \quad \mu^2(r_{1,i}, y_1) = \eta_{y,i} \tilde{r}_i, \quad \mu^2(r_{1,i}, z_1) = \eta_z \tilde{r}'_i$$

¹²The idea is that the function \mathbf{f} is a proper positive real-valued function on the relative cycle \mathbb{R}_+^2 , and the only point this relative cycle meets \tilde{C} is a transverse intersection with \mathbf{D}_{P_0} at the critical point associated to P_0 , which is real by the results in the Appendix.

These satisfy:

$$\frac{\frac{\beta_{x,i}}{\beta_{y,i}}}{\frac{\beta_{x,j}}{\beta_{y,j}}} = -\frac{\frac{\eta_{y,i}}{\eta_{x,i}}}{\frac{\eta_{y,j}}{\eta_{x,j}}} = -\frac{\frac{\gamma_{y,i}}{\gamma_{x,i}}}{\frac{\gamma_{y,j}}{\gamma_{x,j}}} = q_{i,j}$$

Proof. We study first the case of the composition $P_0 \rightarrow P_1 \rightarrow B_i$ which involves the constants β . We examine again the projection under the branched double cover.

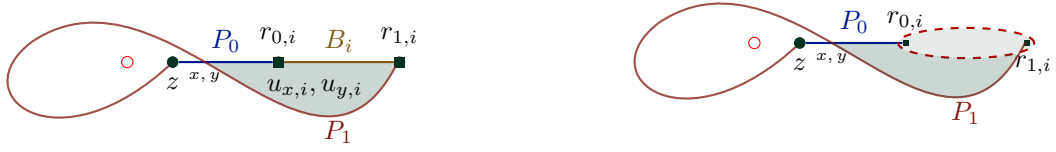


FIGURE 21. Left: Lagrangians and disks for the exact symplectic form ω^{ex} , with all B_i Hamiltonian isotopic to the same curve. Right: the Lagrangian B_i 's get perturbed off of each other once we deform ω^{ex} to ω , no longer projecting to an edge between the two twin branch points.

For each i , there are two holomorphic triangles corresponding to $\mu^2(r_{1,i}, x)$ and $\mu^2(r_{1,i}, y)$. It is also clear from the picture that there are no holomorphic triangles with boundary on P_1, P_2, B_i with z as input. We can create a 2-chain $u_{x,i} - u_{y,i}$ whose boundary consists of a piece of P_0 , a piece of P_1 and the whole of B_i . The 2-chain $u_{x,j} - u_{y,j}$ has exactly the same boundary, except that B_i is replaced by B_j . It then follows that

$$(u_{x,i} - u_{y,i}) - (u_{x,j} - u_{y,j}) = \Delta_{i,j}$$

Recall that this is the 2-chain which, when capped off with the vanishing thimbles $\mathbf{D}_{B_i}, \mathbf{D}_{B_j}$, becomes a -2 sphere $S_{i,j}$. The cross-ratio is given by

$$\frac{\frac{\beta_{x,i}}{\beta_{y,i}}}{\frac{\beta_{x,j}}{\beta_{y,j}}} = \frac{\exp(2\pi i(B + i\omega)(\Delta_{i,j}))}{\exp(-2\pi i \text{hol}(\partial\Delta_{i,j}))} = \exp(2\pi i[B + i\omega](S_{i,j})) = q_{i,j}$$

since $\exp(-2\pi i \text{hol}(\partial\Delta_{i,j})) = \exp(-2\pi i \int_{\mathbf{D}_{B_i} + \mathbf{D}_{B_j}} B)$.

In an exactly analogous way, we can compute the compositions $P_0 \rightarrow \tilde{P} \rightarrow B_i$ and $\tilde{P} \rightarrow P_1 \rightarrow B_i$:



FIGURE 22. Left: projections of triangles contributing to compositions $P_0 \rightarrow \tilde{P} \rightarrow B_i$. Right: the same, but for $\tilde{P} \rightarrow P_1 \rightarrow B_i$.

For the compositions of type $P_0 \rightarrow \tilde{P} \rightarrow B_i$, there is only one disk involving z_0 and \tilde{r}_i which is the unique lift of the really small triangle to the left of z_0 (this is a constant disk when working with ω^{ex}), giving $\mu^2(\tilde{r}_i, z_0) = \gamma_{z,i} r_{0,i}$. Moreover, the only disks involving x_0 (resp. y_0) and $r_{0,i}$ have a third insertion at \tilde{r}'_i , which gives $\mu^2(\tilde{r}'_i, x_0) = \gamma_{x,i} r_{0,i}$, $\mu^2(\tilde{r}'_i, y_0) = \gamma_{y,i} r_{0,i}$.

For the compositions of type $\tilde{P} \rightarrow P \rightarrow B_i$, the only contribution from z_1 is from the unique lift of the triangle below z_1 : $\mu^2(r_{1,i}, z_1) = \eta_{z,i} \tilde{r}'_i$. Similarly, there are two other disks which project inside the shaded region, contributing to $\mu^2(r_{1,i}, x_1) = \eta_{x,i} \tilde{r}_i$, $\mu^2(r_{1,i}, y_1) = \eta_{y,i} \tilde{r}_i$.

Finally, the argument for the other cross-ratios is either by arguing in the same way as before, or using the associativity of μ^2 :

$$\mu^2(r_{1,i}, \mu^2(y_1, z_0)) = \alpha_{z,y} \beta_{x,i} r_{0,i} = \mu^2(\mu^2(r_{1,i}, y_1), z_0) = \eta_{y,i} \gamma_{z,i} r_{0,i} \implies \alpha_{z,y} \beta_{x,i} = \eta_{y,i} \gamma_{z,i}$$

Similarly,

$$\alpha_{y,z} \beta_{x,i} = \eta_{z,i} \gamma_{y,i}, \quad \alpha_{z,x} \beta_{y,i} = \eta_{x,i} \gamma_{z,i}, \quad \alpha_{x,z} \beta_{y,i} = \eta_{z,i} \gamma_{x,i}$$

so that

$$\frac{\alpha_{z,y} \beta_{x,i}}{\alpha_{z,x} \beta_{y,i}} = \frac{\eta_{y,i}}{\eta_{x,i}}, \quad \frac{\alpha_{y,z} \beta_{x,i}}{\alpha_{x,z} \beta_{y,i}} = \frac{\gamma_{y,i}}{\gamma_{x,i}}$$

□

We notice that all of the disks appearing in this computation stay within $M^{in} \subset M^0$. Moreover, we should interpret the compositions $\tilde{P} \rightarrow P_1 \rightarrow B_i$ in the same way as on the B-side: the kernel of $\mu^2(r_{1,i}, -)$ is given by

$$\mu^2(r_{1,i}, \eta_{y,i} x_1 - \eta_{x,i} y_1) = 0$$

which can be used to define $k+1$ points $[\eta_{y,i} : -\eta_{x,i} : 0] \in \mathbb{P}^2$. These constants are nonzero, so we can identify the $k+1$ points using the cross-ratio property as $\{-\frac{\eta_{y,1}}{\eta_{x,1}}, -\frac{\eta_{y,1}}{\eta_{x,1}} q_{1,2}, \dots, -\frac{\eta_{y,1}}{\eta_{x,1}} q_{1,k+1}\} \subset \mathbb{C}^\times$.

Corollary 4.9. *There is an equivalence of categories*

$$D^b(Y) \simeq D^b \mathcal{F}uk^\rightarrow(\mathbf{f}_*|_{M^{in}}; (B + i\omega)|_{M^{in}})$$

with ω as in 0.9 and where Y is the complex surface obtained by blowing up \mathbb{P}^2 at the $k+1$ collinear points

$$\{-1, -q_{1,2}, -q_{1,3}, \dots, -q_{1,k+1}\} \subset \mathbb{C}^\times \subset \{z=0\}$$

Proof. By either rescaling the coordinates x, y, z on \mathbb{P}^2 or the generators of the Floer complexes, we can get rid of the $\frac{\eta_{y,1}}{\eta_{x,1}}$ scalar. Thus, both categories are controlled by a quiver algebra with the same relations. □

Remark 4.10. The category $D^b\mathcal{F}\mathcal{U}k^{\rightarrow}(\mathbf{f}_s|_{M^{in}}; (B+i\omega)|_{M^{in}})$ fully faithfully embeds inside $D^b\mathcal{F}\mathcal{U}k^{\rightarrow}(\mathbf{f}_s; B+i\omega)$, since all of the holomorphic disks between the Lagrangian vanishing cycles P_0, \tilde{P}, P_1, B_i in M^0 stay within M^{in} . This is an analogue of the fully faithfulness of the functor Φ on the B-side. Moreover, the general fiber of M^{in} uses the handles corresponding to the branch points labelled 0 and 1, which in turn correspond to the special representations of the group G . This should be compared to the fact that, locally, the functor $\Phi : D^b(\text{Tot } \mathcal{O}(-k)) \rightarrow D^b[\mathbb{C}^2/G]$ hits the sheaves $\mathcal{O} \otimes \rho_0, \mathcal{O} \otimes \rho_1$ associated to the special representations.

4.4. The gluing morphisms and their composition law. We have shown that the algebra of the Lagrangians $\langle \tilde{L}_2, \dots, \tilde{L}_{k-1} \rangle$ matches the algebra of the orbifold skyscrapers $\langle e_2, \dots, e_{k-1} \rangle$. Moreover, we have shown that the algebra of $\langle P_0, \tilde{P}, P_1, B_1, \dots, B_{k+1} \rangle$, depending on the cohomology class of the symplectic form ω , corresponds to the algebra of $D^b(Y) = \langle D^b(\mathbb{P}^2), \mathcal{O}_{B_1}, \dots, \mathcal{O}_{B_{k+1}} \rangle$ for a complex structure on Y determined by the composition law in the Fukaya category.

The last piece that remains is verifying that these two subcategories are glued in the same way. We do this in this section.

4.4.1. Compositions involving only \tilde{L}_{k-1} .

Proposition 4.11. *The compositions of type $\tilde{L}_{k-1} \rightarrow M \rightarrow N$ where $M, N \in \{P_0, \tilde{P}, P_1, B_i\}$ are given by:*

$$\begin{aligned} \mu^2(x_1, \tilde{\epsilon}) &= \mu^2(y_1, \tilde{\epsilon}) = 0, \mu^2(z_1, \tilde{\epsilon}) = \epsilon \text{ for } \tilde{L}_{k-1} \rightarrow \tilde{P} \rightarrow P_1 \\ \mu^2(\tilde{r}_i, \tilde{\epsilon}) &= 0, \mu^2(\tilde{r}'_i, \tilde{\epsilon}) = \alpha_{\tilde{\epsilon}, \tilde{r}'_i} \epsilon_i \text{ for } \tilde{L}_{k-1} \rightarrow \tilde{P} \rightarrow B_i \\ \mu^2(r_{1,i}, \epsilon) &= \alpha_{\epsilon, r_{1,i}} \epsilon_i \text{ for } \tilde{L}_{k-1} \rightarrow P_1 \rightarrow B_i \end{aligned}$$

for some non-zero constants α .

Proof. The proof is immediate, examining the configuration of the projections of the Lagrangians in the branched double cover. All the relevant holomorphic disks project to either a point (hence they are constant) or very small triangles near the right twin branch point. (In fact, if we were to work with ω^{ex} , all contributions would be from constant disks).

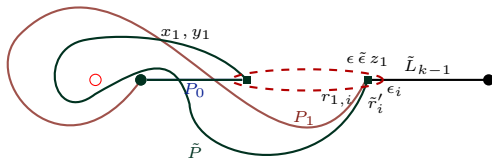


FIGURE 23. Projections of the Lagrangian vanishing cycles $\tilde{L}_{k-1}, P_0, \tilde{P}, P_1, B_i$ under the branched double cover.

4.4.2. Compositions involving both \tilde{L}_{k-2} and \tilde{L}_{k-1} .

Proposition 4.12. *There are nonzero constants such that*

$$\begin{aligned} \mu^2(\tilde{\epsilon}, p_{1,k-2}) &= \alpha_{p_1, \tilde{\epsilon}} \tilde{x}^E, & \mu^2(\tilde{\epsilon}, p_{2,k-2}) &= \alpha_{p_2, \tilde{\epsilon}} \tilde{y}^E & \text{for } \tilde{L}_{k-2} \rightarrow \tilde{L}_{k-1} \rightarrow \tilde{P} \\ \mu^2(\epsilon, p_{1,k-2}) &= \alpha_{p_1, \epsilon} x_1^E, & \mu^2(\epsilon, p_{2,k-2}) &= \alpha_{p_2, \epsilon} y_1^E & \text{for } \tilde{L}_{k-2} \rightarrow \tilde{L}_{k-1} \rightarrow P_1 \\ \mu^2(\epsilon_i, p_{1,k-2}) &= \lambda_{1,i} \epsilon'_i, & \mu^2(\epsilon_i, p_{2,k-2}) &= \lambda_{2,i} \epsilon'_i & \text{for } \tilde{L}_{k-2} \rightarrow \tilde{L}_{k-1} \rightarrow B_i \end{aligned}$$

These constants satisfy

$$\frac{\frac{\lambda_{1,i}}{\lambda_{2,i}}}{\frac{\lambda_{1,j}}{\lambda_{2,j}}} = q_{i,j}$$

Proof. The proof follows along the same lines as before: the disks contributing to the first two lines of compositions are displayed below

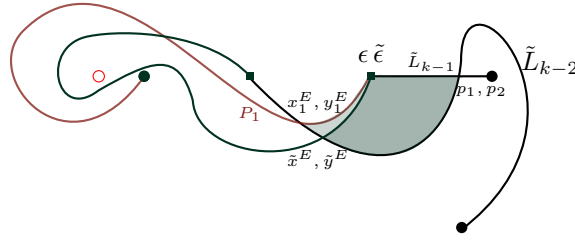


FIGURE 24. Holomorphic disks contributing to the compositions of type $\tilde{L}_{k-2} \rightarrow \tilde{L}_{k-1} \rightarrow \tilde{P}$ and $\tilde{L}_{k-2} \rightarrow \tilde{L}_{k-1} \rightarrow P_1$.

The argument for $\mu^2(p_1, \epsilon_i), \mu^2(p_2, \epsilon_i)$ is the same as for the $\beta_{x,i}, \beta_{y,i}$ and we omit it. \square

4.4.3. Compositions involving only \tilde{L}_{k-2} .

We compute finally the compositions of type $\tilde{L}_{k-2} \rightarrow M \rightarrow N$ where $M, N \in \{P_0, \tilde{P}, P_1, B_i\}$.

A lot of this has been implicitly done already: most of the maps in $CF(\tilde{L}_{k-2}, M)$ can be factorized into a map in $CF(\tilde{L}_{k-2}, \tilde{L}_{k-1})$ followed by a map $CF(\tilde{L}_{k-1}, M)$. For these types of maps, determining the composition reduces, by associativity, to the computations in the previous two sections. The only morphisms that do not factorize are $\epsilon' \in CF(\tilde{L}_{k-2}, P_0)$ and $\tilde{\epsilon}' \in CF(\tilde{L}_{k-2}, \tilde{P})$.

Proposition 4.13. *There are nonzero constants such that*

$$\begin{aligned} \mu^2(x_1, \tilde{\epsilon}') &= \alpha_{\epsilon, x_1} y_1^E, & \mu^2(y_1, \tilde{\epsilon}') &= \alpha_{\epsilon, y_1} x_1^E & \text{for } \tilde{L}_{k-2} \rightarrow \tilde{P} \rightarrow P_1 \\ \mu^2(\tilde{r}_i, \tilde{\epsilon}') &= \alpha_{\epsilon, \tilde{r}_i} \epsilon'_i, & \mu^2(\tilde{r}_i, \tilde{\epsilon}') &= 0 & \text{for } \tilde{L}_{k-2} \rightarrow \tilde{P} \rightarrow B_i \\ \mu^2(r_{0,i}, \epsilon') &= \alpha_{\epsilon, r_{0,i}} \epsilon'_i & & & \text{for } \tilde{L}_{k-2} \rightarrow P_0 \rightarrow B_i \\ \mu^2(x, \epsilon') &= \alpha_{\epsilon, x} x_1^E, & \mu^2(y, \epsilon') &= \alpha_{\epsilon, y} y_1^E, & \mu^2(z, \epsilon') &= 0 & \text{for } \tilde{L}_{k-2} \rightarrow P_0 \rightarrow P_1 \\ \mu^2(x_0, \epsilon') &= \alpha_{\epsilon, x_0} \tilde{y}^E, & \mu^2(y_0, \epsilon') &= \alpha_{\epsilon, y_0} \tilde{x}^E, & \mu^2(z_0, \epsilon') &= \tilde{\epsilon}' & \text{for } \tilde{L}_{k-2} \rightarrow P_0 \rightarrow \tilde{P} \end{aligned}$$

Proof. The proof follows exactly the same strategy as the previous propositions. We note that the intersection point $\tilde{\epsilon}'$ happens at the left twin branch point. \square

Remark 4.14. The fact that $\mu^2(\epsilon', x_0)$ is a multiple of \tilde{y}^E and not of \tilde{x}^E (and similarly for y_0, x_1, y_1) is due to the fact that they are on different sheets of the branched covering. On the B-side, this is related to the fact that, as in 1.9, $\iota^*x_0 = (0, \iota^*y), \iota^*x_1 = (\iota^*y, 0)^T$.

Corollary 4.15. *The endomorphism algebra of the exceptional collection of Lagrangian vanishing cycles*

$$\langle \tilde{L}_2, \dots, \tilde{L}_{k-1}, P_0, \tilde{P}, P_1, B_1, \dots, B_{k+1} \rangle$$

is generated by the elements $x_0, y_0, z_0, x_1, y_1, z_1, r_{1,i}, 1 \leq i \leq k+1$ as well as $p_{1,j}, p_{2,j}, 2 \leq j \leq k-2$ and $\epsilon', \tilde{\epsilon}$. When $q_C = 1$, they satisfy the relations

$$\begin{aligned} \mu^2(p_{1,i+1}, p_{1,i}) &= \frac{\vartheta_{1,i}}{\vartheta_{2,i}} \mu^2(p_{2,i+1}, p_{2,i}), \quad \mu^2(p_{1,i+1}, p_{2,i}) = \mu^2(p_{2,i+1}, p_{1,i}) = 0, \quad \mu^2(\epsilon', p_{1,k-3}) = \mu^2(\epsilon', p_{2,k-3}) = 0 \\ \mu^2(y_1, x_0) &= \frac{\alpha_{x,y}}{\alpha_{y,x}} \mu^2(x_1, y_0), \quad \mu^2(z_1, x_0) = \frac{\alpha_{z,x}}{\alpha_{x,z}} \mu^2(x_1, z_0), \quad \mu^2(z_1, y_0) = \frac{\alpha_{z,y}}{\alpha_{y,z}} \mu^2(y_1, z_0) \\ &\quad \frac{\alpha_{x,y} \alpha_{y,z} \alpha_{z,x}}{\alpha_{y,x} \alpha_{z,y} \alpha_{x,z}} = -1 \\ \mu^2(x_1, x_0) &= \mu^2(y_1, y_0) = \mu^2(z_1, z_0) = 0 \\ \mu^2(r_{1,i}, \eta_{y,i} x_1 - \eta_{x,i} y_1) &= 0 \\ &\quad \frac{\frac{\eta_{y,i}}{\eta_{x,i}}}{\frac{\eta_{y,j}}{\eta_{x,j}}} = q_{i,j} \\ \mu^2(x_1, \tilde{\epsilon}) &= \mu^2(y_1, \tilde{\epsilon}) = 0 \\ \mu^2(x_0, \epsilon') &= \frac{\alpha_{\epsilon,x_0}}{\alpha_{p_2,\tilde{\epsilon}}} \mu^2(\tilde{\epsilon}, p_{2,k-2}), \quad \mu^2(y_0, \epsilon') = \frac{\alpha_{\epsilon,y_0}}{\alpha_{p_1,\tilde{\epsilon}}} \mu^2(\tilde{\epsilon}, p_{1,k-2}) \end{aligned}$$

We are now finally ready to complete our theorem:

Theorem 4.16. *There is an equivalence of categories*

$$D^b(\mathfrak{X}) \simeq \mathcal{F}uk^\rightarrow(\mathbf{f}_s; B + i\omega)$$

where \mathfrak{X} is the orbifold del Pezzo surface obtained by blowing up the points

$$pt_1 = [1 : -1 : 0], pt_2 = [1 : -q_{1,2} : 0], \dots, pt_{k+1} = [1 : -q_{1,k+1} : 0]$$

on \mathbb{P}^2 and contracting the strict transform of $\{z = 0\}$.

Proof. The equivalence of categories follows from the previous Corollary 4.15, as well as the description of the algebra on the B-side as in Proposition 1.9 and a suitable rescaling of the generators. An explicit choice of rescaling is the following:

$$\begin{aligned} p_{1,i}^{resc} &:= -\frac{\vartheta_{2,i}}{\vartheta_{1,i}} p_{1,i}, \quad 2 \leq i \leq k-3, \quad p_{1,k-2}^{resc} := \frac{\alpha_{p_1,\tilde{\epsilon}}}{\alpha_{\epsilon,y_0}} \frac{\alpha_{\epsilon,x_0}}{\alpha_{p_2,\tilde{\epsilon}}} p_{1,k-2} \\ \tilde{\epsilon}^{resc} &:= \frac{\alpha_{p_2,\tilde{\epsilon}}}{\alpha_{\epsilon,x_0}} \tilde{\epsilon}, \quad x_1^{resc} := \frac{\eta_{x,1}}{\eta_{y,1}} x_1, \quad y_1^{resc} := -\frac{\alpha_{y,x}}{\alpha_{x,y}} \frac{\eta_{y,1}}{\eta_{x,1}} y_1, \quad z_1^{resc} := \frac{\alpha_{y,z}}{\alpha_{z,y}} \frac{\alpha_{x,y}}{\alpha_{y,x}} \frac{\eta_{x,1}}{\eta_{y,1}} z_1 \end{aligned}$$

with the other generators remaining unchanged. \square

Remark 4.17. Under a change of coordinates, any hypersurface in the family X_{k+1} can be written as $\mathbb{V}(p_{k+1}(x, y) + zw) \subset \mathbb{P}(1, 1, 1, k)$. Moreover, by a linear change of coordinates, one can ensure that $p_{k+1}(x, y)$ defines $k+1$ points on \mathbb{P}^1 , none of which are 0 or ∞ . Hence, any surface in the family X_{k+1} is isomorphic to one described in Theorem 4.16.

APPENDIX

5.5. Lemmata on the critical points and the dynamics of the branch points.

Proposition (Proof of Proposition 3.5). *As $s \rightarrow 0$ (setting $P(y) = (1+y)^{k+1} + \epsilon$ for a small ϵ), the critical values become distributed as follows:*

- I. $k-2$ of the critical values are distributed near the roots of $t^{k-2} - (\frac{k-2}{k})^{k-2} \frac{1}{s} = 0$.
- II. 3 of them will be arbitrarily close to 0
- III. Another $k+1$ critical points are equidistributed near -1 .

Moreover, all of the critical points are non-degenerate and when s is real, only two of the critical points are in \mathbb{R}_+^2 , one of which is of type II and the other of type III.

Proof. We write

$$\mathbf{f} = \frac{P(y)}{xy} + sx + g(y)$$

We consider the equations on the open torus. In fact, by the non-degeneracy of P (for generic \mathbf{q}_i), there will not be any critical points on the toric boundary of V so that suffices.

We have the system

$$\mathbf{f} = t, \partial_x \mathbf{f} = 0, \partial_y \mathbf{f} = 0$$

with t denoting the critical value, the first two of which imply that

$$2P = xy(t-g), P = sx^2y$$

and hence that $2sx = t-g$. In particular,

$$P - \frac{1}{4s}y(g-t)^2 = 0$$

The equation $\partial_y \mathbf{f}$ tells us that

$$g'(y)xy^2 - P + yP' = 0 \implies P = yP' + xy^2g'(y)$$

We now set $g = y$. We see from $P - yP' = xy^2$ together with $x^2 = \frac{P}{sy}$ that the critical points satisfy the polynomial in y :

$$(P - yP')^2 = \frac{1}{s}Py^3 \tag{5.18}$$

In particular, restricting to small y satisfying $\frac{1}{s} \gg |y^{2k+2}|$, the roots of this are close to the roots of Py^3 , hence there are three roots close to $y = 0$ and $k+1$ roots close to $-\mathbf{q}_1, \dots, -\mathbf{q}_{k+1}$. We will now assume that the \mathbf{q}_i are close to 1 so that $P = (1+y)^{k+1} + \epsilon$ for some small ϵ . The other $k-2$ roots are equidistributed with $|y^{k-2} - \frac{1}{s}| \approx 0$.

It remains to show that the associated critical values t have a similar distribution to the solutions of Equation 5.18. First,

$$t = 2sx + y = 2s \frac{P - yP'}{y^2} + y$$

Thus, when y is close to $-\mathbf{q}_i$ then also t is close to $-\mathbf{q}_i$.

Secondly, notice that since $P = (1+y)^{k+1} + \epsilon$,

$$xy^2 = P - yP' = P \frac{1-ky}{1+y} + \epsilon(k+1) \frac{y}{y+1} = sx^2y(-k + \frac{k+1}{y+1}) + \epsilon(k+1)(1 - \frac{1}{y+1})$$

hence after dividing by xy we get

$$y = sx(-k + \frac{k+1}{y+1}) + \frac{1}{xy}(k+1)\epsilon(1 - \frac{1}{y+1}) \tag{5.19}$$

Thus, when $|y^{k-2} - \frac{1}{s}| \approx 0$ and so $|y|$ is very big, then $|y + ksx| \approx 0$ and thus t is close to $\frac{k-2}{k}y$.

Finally, when y is close to 0 then since $\frac{1}{xy} = \frac{sx}{P}$, from Equation 5.19 we conclude that $|y - sx| \approx 0$ thus $t = 2sx + y$ is very close to $3y$.

For non-degeneracy, we appeal to Kouchnirenko's formula [Kou76] which in our example states that the sums of the multiplicities of the critical points of \mathbf{f}_s on $(\mathbb{C}^\times)^2$ is equal to twice the volume of the Newton polytope of \mathbf{f}_s :

$$\sum \mu_p = 2!\text{vol}(\text{Newt}(\mathbf{f}_s))$$

By Pick's formula, $2\text{vol}(\text{Newt}(\mathbf{f})) = 2i + b - 2 = (k+1) + (k+2+1) - 2 = 2k+2$. Since there are $2k+2$ critical points, they must all have multiplicity 1 i.e. they are non-degenerate. Note that we need the Laurent polynomial \mathbf{f}_s to be Newton non-degenerate to apply Kouchnirenko's formula, which in turn requires $P(y)$ to have distinct roots. Otherwise, we might have a degenerate critical point at infinity.

Finally, we find which of the critical points are real. The polynomial in equation 5.18 takes negative values for $y = 0$ and also for $y \gg 0$. (strictly speaking, we are only considering $y \in \mathbb{C}^\times$ but for the purpose of understanding the behaviour of this polynomial, we can take $y = 0$.) Moreover, it is positive for y in a bounded interval $I \subset \mathbb{R}_+$, provided $\frac{1}{s} > \sup_I \frac{(P(y) - P'(y))^2}{P(y)}$. There are thus at least two real roots, but also by Descartes' rule of signs, there can be at most two, so we conclude there are exactly two. In fact, one of these is very close to 0 and the other is very big, since they must be outside of the compact interval I . \square

Proposition 5.20. *Suppose $\frac{1}{s} \gg |t| \gg 0$ and t is moving in a straight line radially outwards to a critical value at large radius. The result of this on the level of the branch points is the following: the twin branch points (labelled 0 and 1 in Figure 13) are moving radially outward towards one of the equidistributed branch points labelled $2, 3, \dots, k-1$, without changing their relative position. This continues until the twin branch point with the larger absolute value collides with it.*

Proof. We summarize the proof in three steps:

- We approximate and replace our polynomial by a simpler one in the form $y_0^k - (y_0 - t_0)^2$
- We notice the new polynomial has a \mathbb{Z}_{k-2} -equivariant property so that we can restrict to only studying the case when t is real.
- We use a Sturm sequence argument to show that when t is real and increases towards the critical value, the two twin branch points will live on the real line (or arbitrarily close to it), moving towards to a far away branch point which is also arbitrarily close to being real. The smaller of the twin branch points remains less than the bigger one, whereas the bigger of the twins hits the far away branch point as we move t radially to the critical point.

Consider again the branch point equation: $(1+y)^{k+1} + \epsilon = P = \frac{1}{4s}y(y-t)^2$. Divide everything by r^{k+1} where $r^{k-2} = \frac{1}{4s}$, resulting in:

$$\left(\frac{y}{r} + \frac{1}{r}\right)^{k+1} + \frac{\epsilon}{r^{k+1}} = \frac{y}{r}\left(\frac{y}{r} - \frac{t}{r}\right)^2$$

Denote $y_0 := \frac{y}{r}, t_0 := \frac{t}{r}$. The roots of this polynomial are arbitrarily closely approximated by the roots of

$$y_0^{k+1} = y_0(y_0 - t_0)^2$$

since we can take s as small as we want. Hence, we will have a root very close to 0, and $k-2$ other roots close to the roots of

$$y_0^k = (y_0 - t_0)^2 \tag{5.21}$$

We notice the following property of this polynomial: if (y_0, t_0) is a solution, then $(\zeta_{k-2}y_0, \zeta_{k-2}t_0)$ is also a solution, where $\zeta_{k-2}^{k-2} = 1$. We will show that for a given range of real t_0 , the twin branch points (or their infinitesimal approximations) are collinear. By a Sturm sequence argument we will show that 5.21 has three real roots, two of them corresponding to the 'twin' branch points and one corresponding to one

of the equidistributed branch points. We will show that, as t_0 increases, the bigger twin branch point will hit the far away real one. By the ζ_{k-2} property, the real case suffices, as it will imply the case when t_0 is in any of the rays $\zeta_{k-2}\mathbb{R}_+$.

So, as our first step, fix t_0 real and let $h = y_0^k - (y_0 - t_0)^2$. We will show this has three real roots. Firstly, $h'(y_0) = ky_0^{k-1} - 2(y_0 - t_0) > 0$ for $y_0 \in (0, t_0]$ so it is strictly increasing. Moreover, $h(0) < 0, h(t_0) > 0$ so there is exactly one real root here and it happens just before t_0 . This is the stable root - the one that does not collide with another branch point as we increase t_0 .

Now let's write the Sturm sequence for h :

$$h_0 = h, h_1 = h' = ky_0^{k-1} - 2y_0 + 2t_0, h_2 = \frac{k-2}{k}y_0^2 - 2t_0\frac{k-1}{k}y_0 + t_0^2$$

We continue the Sturm sequence by finding the remainder $h_3 = Ay_0 + B$ in the division

$$h_1 = qh_2 - h_3$$

Since the roots of h_2 are $t_0, \frac{k}{k-2}t_0$, then

$$A = -\frac{h_1(t_0 \frac{k}{k-2}) - h_1(t_0)}{t_0 \frac{2}{k-2}} = -\frac{k-2}{k} \left(t_0^{k-2}k((\frac{k}{k-2})^{k-1} - 1) - 2\frac{k}{k-2} + 2 \right)$$

which can also be written as

$$-\left(t_0^{k-2}k(\frac{\lambda^{k-1} - 1}{\lambda - 1}) - 2 \right), \lambda = \frac{k}{k-2}$$

and

$$B = -\frac{t_0 \frac{k}{k-2}h_1(t_0) - t_0 h_1(t_0 \frac{k}{k-2})}{\frac{2}{k-2}t_0} = -2t_0 + \frac{k^2}{2}((\frac{k}{k-2})^{k-2} - 1)(t_0)^{k-1}$$

We have that

$$h_0(0) = -t_0^2 < 0, h_1(0) = 2t_0 > 0, h_2(0) = t_0^2 > 0$$

Moreover,

$$h_3(0) = B$$

which is negative for $(1/t_0)^{k-2} > (\frac{k}{k-2})^{k-2} - 1$ and positive if the opposite holds. The double point occurs when there is equality: we denote this by t_{double} , at which $h_3(0) = 0$. In particular, for

$$\frac{1}{t_0} > \frac{k}{k-2}(\frac{k^2}{4})^{1/k-2}$$

the inequality $h_3(0) < 0$ holds. It moreover implies that $A > 0, B < 0$.

By Descartes rule of signs, the number of real roots of $y_0^k - (y_0 - t_0)^2$ is either 3 or 1. For $t_0 \in (0, t_{\text{double}})$ we can observe the Sturm sequence:

$$h_0(0) < 0, h_1(0) > 0, h_2(0) > 0, h_3(0) < 0, h_4 = ?$$

By Sturm's theorem, the number of real roots is equal to the number of sign changes in the above sequence, which is at least 2. We conclude it is equal to 3 for $t_0 \in (0, t_{\text{double}})$. Thus, we see that there are always three real roots with multiplicity in this range, and the double root occurs when the two bigger real roots (namely, the bigger of the two twin branch points and the far away real branch point) join together, as claimed. \square

Proposition 5.22. *Starting at a value of t such that $\frac{1}{s} \gg |t| \gg 0$, and then rotating it along the path $t_\theta = te^{-i\theta}, \theta \in [0, \frac{2\pi}{k-2}]$, the two twin branch points will interchange position, with their phase difference changing by approximately $\pi + \frac{2\pi}{k-2}$. Hence, the monodromy around such a circle will interchange the twin branch points k times.*

Proof. Consider again the infinitesimal approximation $h = y_0^k - (y_0 - t_0)^2$. We showed that when t_0 is on the ray $\mathbb{R}_{\geq 0}\zeta_{k-2}$, there are exactly three roots of this polynomial on this ray: the twin branch points and one farther away. As such, we can consider the ratios y_0/t_0 where y_0 is one of these three roots - this is a real quantity.

Centering at $y = t_0$, there are Puiseux expansions for the roots closest to t_0 (the 'twin branch points'), namely

$$y_0 = t_0 \pm t_0^{k/2} + \frac{k}{2}t_0^{k-1} + \dots$$

For $t_0 < 1$ real, the ratios are $1 \pm t_0^{\frac{k-2}{2}} + O(t_0^{k-1})$ - one slightly above 1 and one slightly below. As we rotate t_0 by $-\frac{2\pi}{k-2}$, the twin branch points will flip because of the square root producing the \pm sign ambiguity: the one that had $y_0/t_0 > 1$ will now have $y_0/t_0 < 1$ and vice versa.

The outcome is that for each $1/(k-2)$ rotation, the two twin branch points switch, in fact in a specified manner: the initially bigger branch point goes over the smaller one. \square

5.6. The Palais-Smale condition.

Proposition 5.23. *The symplectic manifold (M^0, ω) is complete and the gradient of \mathbf{f}_s is bounded from below outside of a compact subset, for distinct values of \mathbf{q}_i and $s > 0$ real.*

Proof. When the \mathbf{q}_i are distinct, we can realize M^0 as a smooth hypersurface $\{zx = P(y)\} \subset \mathbb{C}^2 \times \mathbb{C}^\times$. The fact that M^0 is complete is due to the fact that (M^0, ω^{ex}) is complete, since it is just a hypersurface in $\mathbb{C}^2 \times \mathbb{C}^\times$ with a complete metric, and ω coincides with ω^{ex} outside of a compact subset. We verify the Palais-Smale condition by brute force: we need to show that $|\nabla \mathbf{f}_s|^2$ is bounded from below outside of a compact subset, so we will again use the metric induced by ω^{ex} . We have that

$$\nabla^{M^0} \mathbf{f}_s = \nabla \mathbf{f}_s - \frac{\langle \nabla \mathbf{f}_s, \nabla g \rangle}{|\nabla g|^2} \nabla g$$

where ∇ denotes the gradient in the ambient $\mathbb{C}^2 \times \mathbb{C}^\times$ and $g = xz - P(y)$ is the function defining M^0 . As such,

$$|\nabla^{M^0} \mathbf{f}_s|^2 = |\nabla \mathbf{f}_s|^2 - \frac{\langle \nabla \mathbf{f}_s, \nabla g \rangle}{|\nabla g|^2}$$

which is given explicitly as the non-negative quantity

$$|s|^2 + \frac{1}{|y|^2} + |y - \frac{z}{y}|^2 - \frac{|s\bar{z} + \frac{\bar{x}}{y} - |y|^2(1 - \frac{z}{y^2})\overline{P'(y)}|^2}{|x|^2 + |z|^2 + |yP'(y)|^2} \geq 0$$

In particular, for $s = 0$ we have that

$$\frac{1}{|y|^2} + |y - \frac{z}{y}|^2 - \frac{|\frac{\bar{x}}{y} - |y|^2(1 - \frac{z}{y^2})\overline{P'(y)}|^2}{|x|^2 + |z|^2 + |yP'(y)|^2} \geq 0 \tag{5.24}$$

We want to show the gradient 5.6 (for $s \neq 0$) is bounded from below outside of a compact set, so we may take $x, z \gg 0$, in other words we look at $M^0 \setminus (M^0 \cap \mathbb{D} \times \mathbb{D} \times A)$ where A is a compact annulus. Since

$xz = P(y)$, this implies that also $y \gg 0$. We compute:

$$\begin{aligned}
 & |s|^2 + \frac{1}{|y|^2} + |y - \frac{z}{y}|^2 - \frac{|s\bar{z} + \frac{\bar{x}}{y} - |y|^2(1 - \frac{z}{y^2})\overline{P'(y)}|^2}{|x|^2 + |z|^2 + |yP'(y)|^2} \geq \\
 & |s|^2 + \left(\frac{1}{|y|^2} + |y - \frac{z}{y}|^2 - \frac{|\frac{\bar{x}}{y} - |y|^2(1 - \frac{z}{y^2})\overline{P'(y)}|^2}{|x|^2 + |z|^2 + |yP'(y)|^2} \right) + \left(\frac{|\frac{\bar{x}}{y} - |y|^2(1 - \frac{z}{y^2})\overline{P'(y)}|^2}{|x|^2 + |z|^2 + |yP'(y)|^2} - \frac{|s\bar{z} + \frac{\bar{x}}{y} - |y|^2(1 - \frac{z}{y^2})\overline{P'(y)}|^2}{|x|^2 + |z|^2 + |yP'(y)|^2} \right) \geq \\
 & |s|^2 + \underbrace{\left(\frac{|\frac{\bar{x}}{y} - |y|^2(1 - \frac{z}{y^2})\overline{P'(y)}|^2 - |s\bar{z} + \frac{\bar{x}}{y} - |y|^2(1 - \frac{z}{y^2})\overline{P'(y)}|^2}{|x|^2 + |z|^2 + |yP'(y)|^2} \right)}_{\text{bounded in norm by } \frac{1}{2}|s|^2} \geq \frac{1}{2}|s|^2 \quad (5.25)
 \end{aligned}$$

The last inequality is due to the fact that, for $|x|, |y|, |z| \gg 0$, we have by the reverse triangle inequality:

$$\left| \frac{|\frac{\bar{x}}{y} - |y|^2(1 - \frac{z}{y^2})\overline{P'(y)}|^2 - |s\bar{z} + \frac{\bar{x}}{y} - |y|^2(1 - \frac{z}{y^2})\overline{P'(y)}|^2}{|x|^2 + |z|^2 + |yP'(y)|^2} \right|^2 \leq |s|^2 \frac{|z|^2}{|x|^2 + |z|^2 + |yP'(y)|^2}$$

and finally

$$\frac{1}{|\frac{x}{z}|^2 + 1 + |\frac{yP'(y)}{z}|^2} \leq \frac{1}{2} \iff \left| \frac{yP'(y)}{z} \right|^2 + \left| \frac{x}{z} \right|^2 \geq 1$$

Since $xz = P$, then $|\frac{yP'(y)}{z}|^2 = |x|^2 |\frac{yP'(y)}{P(y)}|^2$ which for $|x|, |y| \gg 0$ is asymptotically given by $|x|^2 \gg 0$ because $yP'(y)$ and $P(y)$ are both monic polynomials of degree $k+1$. We can conclude that the gradient is bounded from below, \square

5.7. Special representations and modular arithmetic. Consider the special I -series $I(n, q)$ (which is defined in [GR23, Definition 2.5]) and its subset $I' := I \setminus \{n\} = \{i_1 = q, i_2, \dots, i_{r+1} = 0\}$.

Proposition 5.26. *The map*

$$\begin{aligned}
 I' & \rightarrow \{0, 1, \dots, n-1\} \\
 a & \mapsto -aq^{-1} \pmod{n}
 \end{aligned}$$

is order-preserving.

Proof. Start with $i_1 = q$. This is sent to $n-1$. By definition of the recursion for the I -series,

$$i_2 = b_1 i_1 - i_0 = b_1 q - n$$

implies that i_2 is sent to $n-b_1$. If i_j is sent to $n-P_j$, $0 \leq P_j < n$, then by the definition of the I -series, the P_j satisfy the recursion

$$P_i = b_i P_{i-1} - P_{i-2}$$

with $P_0 = 1, P_1 = b_1$. This is exactly the sequence in [CLS11, Proposition 10.2.2], which shows that the P_i form an increasing sequence of integers with $0 \leq P_i \leq d$, which proves the claim. \square

REFERENCES

[Akh+15] Mohammad Akhtar et al. “Mirror symmetry and the classification of orbifold del Pezzo surfaces”. en. In: *Proceedings of the American Mathematical Society* 144.2 (Sept. 2015), pp. 513–527. ISSN: 0002-9939, 1088-6826. DOI: [10.1090/proc/12876](https://doi.org/10.1090/proc/12876). URL: <https://www.ams.org/proc/2016-144-02/S0002-9939-2015-12876-6/>.

[AKO06] Denis Auroux, Ludmil Katzarkov, and Dmitri Orlov. “Mirror symmetry for Del Pezzo surfaces: Vanishing cycles and coherent sheaves”. In: *Inventiones mathematicae* 166.3 (Oct. 2006). arXiv:math/0506166, pp. 537–582. ISSN: 0020-9910, 1432-1297. DOI: [10.1007/s00222-006-0003-4](https://doi.org/10.1007/s00222-006-0003-4). URL: [http://arxiv.org/abs/math/0506166](https://arxiv.org/abs/math/0506166).

[AKO08] Denis Auroux, Ludmil Katzarkov, and Dmitri Orlov. “Mirror symmetry for weighted projective planes and their noncommutative deformations”. en. In: *Annals of Mathematics* 167.3 (May 2008), pp. 867–943. ISSN: 0003-486X. DOI: [10.4007/annals.2008.167.867](https://doi.org/10.4007/annals.2008.167.867). URL: <http://annals.math.princeton.edu/2008/167-3/p04>.

[Art62] Michael Artin. “Some Numerical Criteria for Contractability of Curves on Algebraic Surfaces”. In: *American Journal of Mathematics* 84.3 (July 1962), p. 485. ISSN: 00029327. DOI: [10.2307/2372985](https://doi.org/10.2307/2372985). URL: <https://www.jstor.org/stable/2372985?origin=crossref>.

[BD11] Igor Burban and Yuriy Drozd. “Tilting on non-commutative rational projective curves”. en. In: *Mathematische Annalen* 351.3 (Nov. 2011), pp. 665–709. ISSN: 1432-1807. DOI: [10.1007/s00208-010-0585-4](https://doi.org/10.1007/s00208-010-0585-4). URL: <https://doi.org/10.1007/s00208-010-0585-4>.

[CG21] Alessio Corti and Giulia Gugliatti. “Hyperelliptic integrals and mirrors of the Johnson–Kollar del Pezzo surfaces”. en. In: *Transactions of the American Mathematical Society* 374.12 (Sept. 2021), pp. 8603–8637. ISSN: 0002-9947, 1088-6850. DOI: [10.1090/tran/8465](https://doi.org/10.1090/tran/8465). URL: <https://www.ams.org/tran/2021-374-12/S0002-9947-2021-08465-2/>.

[CLS11] David A. Cox, John B. Little, and Henry K. Schenck. *Toric varieties*. eng. Graduate studies in mathematics 124. Providence (R.I.): American mathematical society, 2011. ISBN: 9780821848197.

[CP20] Daniel Cavey and Thomas Prince. “Del Pezzo surfaces with a single $\mathbb{P}^1/\mathbb{P}^1$ singularity”. en. In: *Journal of the Mathematical Society of Japan* 72.2 (Apr. 2020). ISSN: 0025-5645. DOI: [10.2969/jmsj/79337933](https://doi.org/10.2969/jmsj/79337933). URL: <https://projecteuclid.org/journals/journal-of-the-mathematical-society-of-japan/volume-72/issue-2/Del-Pezzo-surfaces-with-a-single-1k11-singularity/10.2969/jmsj/79337933.full>.

[Cro25] Calum Crossley. *A categorical flop in dimension one*. arXiv:2505.06940. July 2025. DOI: [10.48550/arXiv.2505.06940](https://doi.org/10.48550/arXiv.2505.06940). URL: [http://arxiv.org/abs/2505.06940](https://arxiv.org/abs/2505.06940).

[Eva11] Jonathan David Evans. “Symplectic mapping class groups of some Stein and rational surfaces”. en. In: *Journal of Symplectic Geometry* 9.1 (2011), pp. 45–82. ISSN: 15275256, 15402347. DOI: [10.4310/JSG.2011.v9.n1.a4](https://doi.org/10.4310/JSG.2011.v9.n1.a4). URL: <https://link.intlpress.com/JDetail/1806597718216699905>.

[GP17] Emmanuel Giroux and John Pardon. “Existence of Lefschetz fibrations on Stein and Weinstein domains”. en. In: *Geometry & Topology* 21.2 (Mar. 2017), pp. 963–997. ISSN: 1364-0380, 1465-3060. DOI: [10.2140/gt.2017.21.963](https://doi.org/10.2140/gt.2017.21.963). URL: [http://msp.org/gt/2017/21-2/p06.xhtml](https://msp.org/gt/2017/21-2/p06.xhtml).

[GPS20] Sheel Ganatra, John Pardon, and Vivek Shende. “Covariantly functorial wrapped Floer theory on Liouville sectors”. en. In: *Publications mathématiques de l’IHÉS* 131.1 (June 2020), pp. 73–200. ISSN: 1618-1913. DOI: [10.1007/s10240-019-00112-x](https://doi.org/10.1007/s10240-019-00112-x). URL: <https://doi.org/10.1007/s10240-019-00112-x>.

[GPS23] Sheel Ganatra, John Pardon, and Vivek Shende. “Sectorial descent for wrapped Fukaya categories”. en. In: *Journal of the American Mathematical Society* (Oct. 2023). ISSN: 0894-0347,

1088-6834. DOI: [10.1090/jams/1035](https://doi.org/10.1090/jams/1035). URL: <https://www.ams.org/jams/0000-000-00/S0894-0347-2023-01035-5/>.

[GR23] Giulia Gugliatti and Franco Rota. “Full exceptional collections for anticanonical log del Pezzo surfaces”. In: *International Mathematics Research Notices* 2023.21 (Nov. 2023). arXiv:2205.00553 [math], pp. 18803–18855. ISSN: 1073-7928, 1687-0247. DOI: [10.1093/imrn/rnad228](https://doi.org/10.1093/imrn/rnad228). URL: [http://arxiv.org/abs/2205.00553](https://arxiv.org/abs/2205.00553).

[GR25] Giulia Gugliatti and Franco Rota. *On the mirrors of low-degree del Pezzo surfaces*. arXiv:2506.21758 [math]. June 2025. DOI: [10.48550/arXiv.2506.21758](https://doi.org/10.48550/arXiv.2506.21758). URL: [http://arxiv.org/abs/2506.21758](https://arxiv.org/abs/2506.21758).

[Hab25] Matthew Habermann. “Homological mirror symmetry for nodal stacky curves”. en. In: *Mathematical Research Letters* 32.1 (2025), pp. 177–237. ISSN: 10732780, 1945001X. DOI: [10.4310/MRL.250708030801](https://doi.org/10.4310/MRL.250708030801). URL: <https://link.intlpress.com/JDetail/1942299799422287874>.

[HK23] Paul Hacking and Ailsa Keating. “Homological mirror symmetry for log Calabi-Yau surfaces”. In: *Geometry & Topology* 26.8 (Mar. 2023). arXiv:2005.05010 [math], pp. 3747–3833. ISSN: 1364-0380, 1465-3060. DOI: [10.2140/gt.2022.26.3747](https://doi.org/10.2140/gt.2022.26.3747). URL: [http://arxiv.org/abs/2005.05010](https://arxiv.org/abs/2005.05010).

[HKK17] F. Haiden, L. Katzarkov, and M. Kontsevich. “Flat surfaces and stability structures”. en. In: *Publications mathématiques de l’IHÉS* 126.1 (Nov. 2017), pp. 247–318. ISSN: 1618-1913. DOI: [10.1007/s10240-017-0095-y](https://doi.org/10.1007/s10240-017-0095-y). URL: <https://doi.org/10.1007/s10240-017-0095-y>.

[Huy06] D. Huybrechts. *Fourier-Mukai Transforms in Algebraic Geometry*. en. 1st ed. Oxford University PressOxford, Apr. 2006. ISBN: 9780199296866 9780191711329. DOI: [10.1093/acprof:oso/9780199296866.001.0001](https://doi.org/10.1093/acprof:oso/9780199296866.001.0001). URL: <https://academic.oup.com/book/11573>.

[Ish02] A. Ishii. “On the McKay correspondence for a finite small subgroup of $GL(2, \mathbb{C})$ ”. In: *Journal für die reine und angewandte Mathematik (Crelles Journal)* 2002.549 (Jan. 2002). ISSN: 0075-4102, 1435-5345. DOI: [10.1515/crll.2002.064](https://doi.org/10.1515/crll.2002.064). URL: <https://www.degruyter.com/document/doi/10.1515/crll.2002.064/html>.

[Ito02] Yukari Ito. “Special McKay correspondence”. In: *Séminaires et Congrès* (Nov. 2002). arXiv:math/0111314. DOI: [10.48550/arXiv.math/0111314](https://doi.org/10.48550/arXiv.math/0111314). URL: [http://arxiv.org/abs/math/0111314](https://arxiv.org/abs/math/0111314).

[IU15] Akira Ishii and Kazushi Ueda. “The special McKay correspondence and exceptional collections”. In: *Tohoku Mathematical Journal* 67.4 (Dec. 2015). ISSN: 0040-8735. DOI: [10.2748/tmj/1450798075](https://doi.org/10.2748/tmj/1450798075). URL: <https://projecteuclid.org/journals/tohoku-mathematical-journal/volume-67/issue-4/The-special-McKay-correspondence-and-exceptional-collections/10.2748/tmj/1450798075.full>.

[JK01] Jennifer M. Johnson and János Kollár. “Kähler-Einstein metrics on log del Pezzo surfaces in weighted projective 3-spaces”. en. In: *Annales de l’Institut Fourier* 51.1 (2001), pp. 69–79. ISSN: 1777-5310. DOI: [10.5802/aif.1815](https://doi.org/10.5802/aif.1815). URL: <https://aif.centre-mersenne.org/articles/10.5802/aif.1815/>.

[Kea18] Ailsa Keating. “Homological mirror symmetry for hypersurface cusp singularities”. en. In: *Selecta Mathematica* 24.2 (Apr. 2018), pp. 1411–1452. ISSN: 1420-9020. DOI: [10.1007/s00029-017-0334-6](https://doi.org/10.1007/s00029-017-0334-6). URL: <https://doi.org/10.1007/s00029-017-0334-6>.

[KL12] Alexander Kuznetsov and Valery A. Lunts. “Categorical resolutions of irrational singularities”. In: (2012). DOI: [10.48550/ARXIV.1212.6170](https://doi.org/10.48550/ARXIV.1212.6170). URL: <https://arxiv.org/abs/1212.6170>.

[Kou76] A. G. Kouchnirenko. “Polyèdres de Newton et nombres de Milnor.” und. In: *Inventiones mathematicae* 32 (1976), pp. 1–32. ISSN: 0020-9910; 1432-1297/e. URL: <https://eudml.org/doc/142365>.

[Laz00] L. Lazzarini. “Existence of a somewhere injective pseudo-holomorphic disc.” en. In: *Geometric and Functional Analysis* 10.4 (Nov. 2000), pp. 829–862. ISSN: 1016-443X. DOI: [10.1007/PL00001640](https://doi.org/10.1007/PL00001640). URL: <http://link.springer.com/10.1007/PL00001640>.

[LO10] Valery Lunts and Dmitri Orlov. “Uniqueness of enhancement for triangulated categories”. en. In: *Journal of the American Mathematical Society* 23.3 (Feb. 2010), pp. 853–908. ISSN: 0894-0347, 1088-6834. DOI: [10.1090/S0894-0347-10-00664-8](https://doi.org/10.1090/S0894-0347-10-00664-8). URL: <https://www.ams.org/jams/2010-23-03/S0894-0347-10-00664-8/>.

[LP17] Yankı Lekili and Alexander Polishchuk. “Arithmetic mirror symmetry for genus 1 curves with n marked points”. en. In: *Selecta Mathematica* 23.3 (July 2017), pp. 1851–1907. ISSN: 1022-1824, 1420-9020. DOI: [10.1007/s00029-016-0286-2](https://doi.org/10.1007/s00029-016-0286-2). URL: <http://link.springer.com/10.1007/s00029-016-0286-2>.

[LP18] Yankı Lekili and Alexander Polishchuk. “Auslander orders over nodal stacky curves and partially wrapped Fukaya categories”. In: *Journal of Topology* 11.3 (Sept. 2018). arXiv:1705.06023 [math], pp. 615–644. ISSN: 1753-8416, 1753-8424. DOI: [10.1112/topo.12064](https://doi.org/10.1112/topo.12064). URL: <http://arxiv.org/abs/1705.06023>.

[OP18] Alessandro Oneto and Andrea Petracci. “On the quantum periods of del Pezzo surfaces with $\frac{1}{3}(1,1)$ singularities”. In: *Advances in Geometry* 18.3 (July 2018). arXiv:1507.08589 [math], pp. 303–336. ISSN: 1615-7168, 1615-715X. DOI: [10.1515/advgeom-2017-0048](https://doi.org/10.1515/advgeom-2017-0048). URL: <http://arxiv.org/abs/1507.08589>.

[Sei08] Paul Seidel. *Fukaya Categories and Picard–Lefschetz Theory*. en. ISBN: 9783037190630 9783037195635 ISSN: 2943-4963, 2943-4971 Publisher: European Mathematical Society - EMS - Publishing House GmbH. June 2008. DOI: [10.4171/063](https://doi.org/10.4171/063). URL: <https://ems.press/books/zlam/2>.

[Sei10] Paul Seidel. “SUSPENDING LEFSCHETZ FIBRATIONS, WITH AN APPLICATION TO LOCAL MIRROR SYMMETRY”. en. In: *Communications in Mathematical Physics* 297.2 (July 2010), pp. 515–528. ISSN: 1432-0916. DOI: [10.1007/s00220-009-0944-8](https://doi.org/10.1007/s00220-009-0944-8). URL: <https://doi.org/10.1007/s00220-009-0944-8>.

[Syl19] Zachary Sylvan. “On partially wrapped Fukaya categories”. en. In: *Journal of Topology* 12.2 (June 2019), pp. 372–441. ISSN: 1753-8416, 1753-8424. DOI: [10.1112/topo.12088](https://doi.org/10.1112/topo.12088). URL: <https://onlinelibrary.wiley.com/doi/10.1112/topo.12088>.

[Wum88] Jürgen Wunram. “Reflexive modules on quotient surface singularities”. en. In: *Mathematische Annalen* 279.4 (Dec. 1988), pp. 583–598. ISSN: 1432-1807. DOI: [10.1007/BF01458530](https://doi.org/10.1007/BF01458530). URL: <https://doi.org/10.1007/BF01458530>.